INVESTIGATION OF SUITABLE METHODS TO PROTECT MAIN ROADS ADJACENT TO WATER BODIES

Joseph Logeswaran

(218088 B)

Master of Science by Research

Department of Civil Engineering

University of Moratuwa

Sri Lanka

October 2024

Declaration

I hereby declare that the research thesis entitled “Investigation of suitable methodsto protect main roads adjacent to water bodies” submitted by me in partial fulfillment ofthe requirements for MSc. (Research), is my original work and that it has not previously formed on the basis of any other academic qualification at any institution.

Also, I hereby grant to University of Moratuwa the non-exclusive right to reproduce and distribute my dissertation, in whole or in part in print, electronic or other medium. I retain the right to use this content in whole or part in future works (such as articles or books).

…………………………………………

Joseph Logeswaran

Department of Civil Engineering

University of Moratuwa

31st October 2024

The above candidate has carried out research for the Master of Science by Research (Part Time) thesis under my supervision.

…………………………………

Prof. S.A.S. Kulathilaka

Senior professor

Department of Civil Engineering

University of Moratuwa

Date: 06.11.2024

Abstract

Main roads adjacent to water bodies often face significant stability challenges due to erosion caused by, heavy rainfall, increased water flow along riverbanks, the sudden drawdown of water levels after flooding, sand mining and various other human activities within river catchments. These conditions can lead to failures in the river banks disrupting the functioning of the road.

This thesis presents four such problematic locations, identifying the root cause of the problem and presenting appropriate different rectification measures adopted. Common features and different aspects at the four locations are elaborated. The locations all in the Western Province are; Kelani River bank along the low-level road, the right side of the Halwathura Phalakotasa stream bank along the Ingiriya-Halwathura-Ekgaloya road, Halkotiyawatta stream bank on Seelarathana Mawatha, and Diyawanna Lake bank on Denzil Kobbekaduwa Mawatha.

A comprehensive literature review was done on various techniques involving both hard and flexible solutions, including reinforcing techniques and integrating natural vegetation developed in different parts of the world over the last decade. Novel approaches appropriate for Sri Lanka were proposed based on the findings of the literature review. At each location, different alternatives were closely evaluated considering cost, constructability and sustainability to decide on the best to be adopted. Stabilization techniques evaluated are; (1) Gabionwall with rock packing at the toe, (2) vegetated live bamboo crib wall construction with Gabion at the toe, and (3) vegetated flapped soil bag with live stake retaining structure with a Gabion at the toe. The proposals were implemented at three locations and the performance is being monitored. The satisfactory performance over few years serves as an encouragement to adopt sustainable techniques in infrastructure development in Sri Lanka.

Keywords: Bamboo, Bio-slope engineering, Gabion wall, Slope stability, and Stream bank erosion

Delegation

I delegate this thesis to my beloved family members who are the pillar of my strength and existence.

Acknowledgement

I would like to express my sincere gratitude to my supervisor, Prof. S.A.S. Kulathilaka, for his invaluable guidance, unwavering support, and constructive criticism throughout the MSc (Research) program and during this research study. His expertise, dedication, and willingness to invest time have been instrumental in shaping this study. I am also sincerely thankful to the progress review panel members, Prof. U.P. Nawagamuwa and Dr. T.M.N. Wijayaratna, for their valuable time and proper guidance.

I extend my heartfelt thanks to the Geotechnical Engineering Unit of the Department of Civil Engineering, University of Moratuwa, for organizing the MSc (Research) program. This program has been immensely beneficial for addressing emerging expressway infrastructure development projects in Sri Lanka related to the geotechnical area.

I am grateful to the Director General of the Road Development Authority for approving my participation in this part-time study opportunity. Additionally, I would like to acknowledge the technical staff of the Department of Civil Engineering, University of Moratuwa, for their invaluable assistance in conducting laboratory tests on soil samples.

Furthermore, I extend my thanks to all who have supported me, whether directly or indirectly, throughout this research study. Your encouragement and assistance have been deeply appreciated and have contributed significantly to the successful completion of this work.

CONTENTS

LIST OF FIGURES

LIST OF TABLES

LIST OF SYMBOLS & ABBREVIATIONS

A	Sectional area of sheet pile (cm^2/m)
B	Gabion wall width of the base (m)
C	Cohesion (kPa)
C_w	Design adhesion (kPa)
D	Depth of embedment of sheet pile wall (m)
e	Eccentricity (m)
e_0	Initial Void ratio
f_b	Allowable bending stress in mild steel (N/mm^2)
fy	Ultimate stress of pre stress anchor bar (N/mm^2)
G_S	Specific gravity of soil
H	Retaining wall height (m)
I	Moment of inertia (cm^4/m)
K_a	Active earth pressure coefficient
λ_{ah}	Coefficient of active lateral pressure
M_{max}	Maximum bending moment on sheet pile wall (kNm/m)
M_o	Overturning moment on retaining wall (kNm/m)
M_r	Resisting moment on retaining wall (kNm/m)
P_a	Total active force on retaining wall (kN/m)
P_{AN}	Active horizontal earth pressure (kN/m)
Po^1	Effective overburden pressure
q/p	Surcharge load (kPa)
$q_{allowable}$	Allocable bearing capacity below the retaining wall (kPa)
$qult$	Ultimate bearing capacity below the retaining wall (kPa)
q_u	Unconfined compression strength of soil
T	Anchor force (kN/m)
V_{max}	Allowable Shear force in steel sheet pile (kN/m)
Wg	Weight of the retaining wall (kN)
Ws	Weight of the soil (kN)
Z	Section modulus of Steel sheet pile wall (cm^3/m)

α	Wall inclination angle (degree)
β	Fill slope angle above wall (degree)
θ	Inclination angle to Vertical plane, (degree)
δ	Angle of wall friction (degree)
δ_b	Angle of base friction (degree)
ϕ	Angle of internal friction of soil (degree)
P_A	Active soil earth pressure (kPa)
$б_V$	Vertical soil stress (kPa)
$б'$	Effective stress (kPa)
U	Pore water pressure
P_p	Passive soil Side resistance (kPa)
γ_d	Dry unit weight of soil (kN/m^3)
γ_s	Saturated unit weight of soil (kN/m^3)
γ_{bulk}	Bulk Density of Soil (kN/m^3)
bv_{max}	Maximum stress at bottom of the retaining wall (kPa)
τ	Shear stress or mobilized shear stress (kPa)
τ_f	Average shear strength of soil (kPa)
ζam	Allowable stress of the retaining wall (kPa)
ASTM	American Society for Testing and Materials
FOS	Factor of safety
FEM	Finite element method
LEA	limit equilibrium approach
M	Mobilization factor
M-PM	Morgenstern-Price method
MSE	Mechanically stabilized earth wall system
N_{Field}	Field SPT blow counts
N'_{70}	Corrected SPT blow counts by energy method
RDA	Road Development Authority
SLOPE/W	limit equilibrium approach software for slope stability analysis
SPT	Standard penetration test
ULS	Ultimate Limit State

LIST OF APPENDICES

CHAPTER 1

1.1 Background

Development activities are inherently interdisciplinary, and slope instability is a common challenge worldwide. In Sri Lanka, road embankment failures and riverbank erosion are particularly prevalent. Main roads adjacent to water bodies frequently face significant stability issues due to factors such as heavy rainfall, increased water flow along riverbanks, sudden drawdown of water levels after flooding, sand mining, and various human activities within river catchments. These conditions often lead to riverbank failures, disrupting road functionality.

This research study examines four problematic locations in the road network in Sri Lanka, identifies the root causes of the issues, and presents various rectification measures. The common features and unique aspects of each location are elaborated upon. The locations are; the left side of the Kelani River bank along the low-level road (AB010) at the 26th-kilometer post (location 1); the right side of the Halwathura Phalakotasa stream bank along the Ingiriya-Halwathura-Ekgaloya road (B068) at the 4th-kilometer post (location 2); the right side of the Halkotiyawatta stream bank on Seelarathana Mawatha at the 1st-kilometer post (location 3); and the right side of the Diyawanna Lake bank on Denzil Kobbekaduwa Mawatha at the 1st-kilometer post (location 4). Figure 1.1 depicts a map of the Western Province of Sri Lanka, highlighting these four problematic locations.

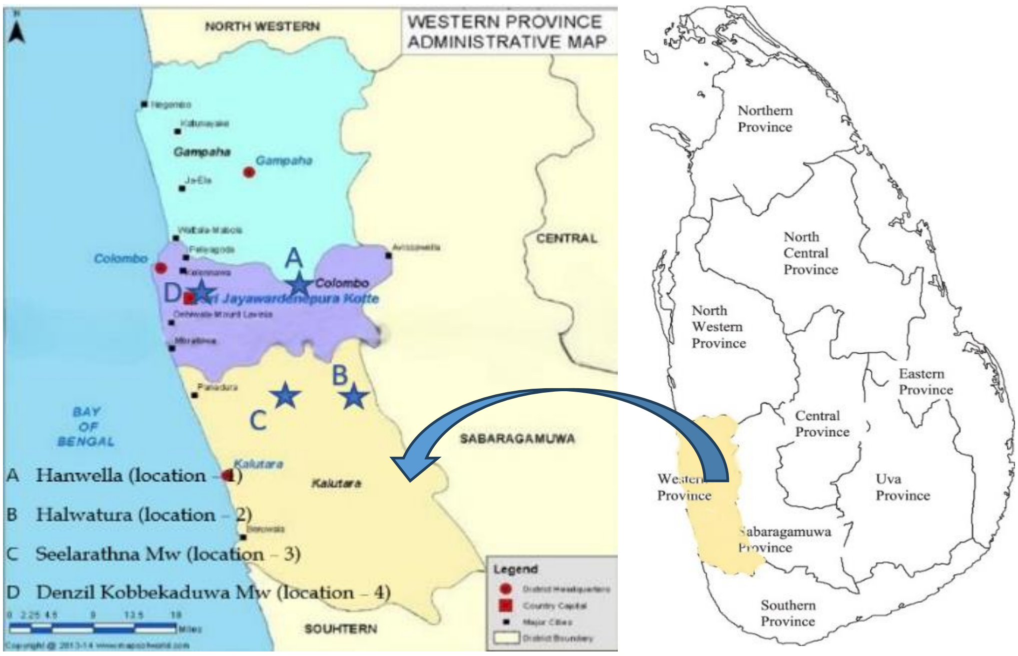

Figure 1.1 A map showing all problematic locations

All selected bank locations are bordered by various water bodies, each experiencing distinct hydraulic conditions and water forces. These factors significantly contribute to observed instabilities, impacting the overall stability of the adjacent road network managed by the Road Development Authority (RDA). Addressing these issues is crucial for ensuring the resilience and safety of transportation infrastructure.

While global researchers have developed numerous techniques involving both hard and flexible solutions, such as reinforcing techniques and integrating natural vegetation, (Acharya 2020, Brunet 2007, Guillermo 2016, Tardio 2020, Jotisankasa 2019), Sri Lanka lacks innovative studies that lead to cost-effective and environmentally friendly methods. In this study, an initial comprehensive literature survey was conducted to identify novel approaches applicable to such circumstances. Different solutions were proposed for each site, considering factors such as cost, constructability, and sustainability.

By analyzing these four locations and proposing tailored solutions, this study aims to contribute to the development of effective and sustainable methods for managing slope instability and erosion challenges in Sri Lanka's Road infrastructure.

1.2 Objective and Scope of the Study

The objective and Scope of the study is:

1. Review different methods of stabilization of roads adjacent to water bodies published in the literature.
2. Establish the basic reasons for instability at four identified locations and study the applicability of different possible alternatives.
3. Establish the most appropriate hard and flexible solutions taking into consideration the use of Bio-Engineering techniques, develop a design, and prescribe the appropriate construction sequence.
4. Proceed with the construction, monitor the performance, and maintain.
5. Create guidelines for future projects.

1.3 Organization of the Thesis Study

The thesis is divided into five chapters, each serving as an individual part of the study. The chapters are further divided into sub-sections based on the requirements of the study. A brief outline of the thesis is presented below:

Chapter 1 describes the background of the study, identifies the four unstable road segments adjacent to water bodies, outlines the techniques developed by researchers, and states the objective and scope of the study.

Chapter 2 reviews the destabilization process and various methods of stabilizing roads adjacent to water bodies as published in the literature, and identifies novel approaches that can be adopted for this study.

Chapter 3 explains the research methodology, detailing the study and investigations conducted to establish the subsoil profile and the results obtained. This data is essential to assess the current state of stability, determine the reasons for instability, and evaluate the applicability of different possible alternatives at the four identified locations. Additionally, it outlines the development of the design and the establishment of the implementation process, giving due consideration to the construction sequence.

Chapter 4 provides a comprehensive summary of the solutions adopted for the four identified locations, detailing the implementation process and the performance outcomes of these solutions. This chapter evaluates the effectiveness of each solution, discusses any challenges encountered during implementation, and presents a comparative analysis of the results

Chapter 5 concludes that the rectification solutions for the selected four locations, which include both conventional hard engineering solutions and bio-engineering solutions coupled with hard engineering techniques, have proven to be satisfactory. The success of these solutions is encouraging for future applications.

CHAPTER 2

2.0 LITERATURE REVIEW

2.1 Modes of slope failure

Many different types of slopes are encountered in the road network of Sri Lanka ranging from; natural slopes in hilly terrains, natural slopes modified by excavations, embankment slopes constructed to increase the road elevation and slopes adjacent to water bodies. These slopes would be formed of; parent rock, rocks at different levels of weathering, residual soils and colluvial soils. The parent rock is metamorphic in most parts of the island and there are significant changes in the mineralogical structure. These rocks may have one or more systems of joints. Due to this inherited state of the parent rock and weathering under tropical conditions of high temperatures and heavy rainfall the weathered product would also be highly variable. As such, sloping grounds encountered in the road network are of highly nonuniform conditions with abrupt changes. There are layers of contrasting shear strength and permeability characteristics. The groundwater table can be deep during periods of dry weather and near surface levels could be unsaturated with quite high matric suctions. With the infiltration of water due to rainfall, matric suction will be reduced or completely lost and positive pore water pressure may develop. The shear strength τ_f, will decrease and the factor of safety will reduce.

The water level in the water bodies adjacent to the roads could be low during periods of dry weather and the near surface ground would possess some matric suctions. The rise of water level in the water body would saturate these zones. There could be events of flooding also. If the floods recede rapidly instability may occur in sloping ground due to prevailing undissipated pore water pressures. Water currents of high velocity during times of flooding could also induce erosional failures in these sloping grounds.

Sand mining in the riverbed lowers the stream bottom, which would lead to bank erosion. Excessive stream sand mining is a threat to bridges, river banks and nearby structures. The 'rapid' drawdown of water levels after a flood, would also adversely affect the river bank stability.

2.2 The Factor of Safety (FOS)

The safety margin of a slope is often quantified by the factor of safety. It is commonly defined as the ratio between Maximum shear stress can sustain, τ_f, of the soil along a possible slip surface and the corresponding shear stress mobilized for equilibrium, τ_{mob},

The Factor of safety can be evaluated by considering the static equilibrium of the mass of soil. Methods that can be used are; limit equilibrium, limit analysis and finite element. The most widely used is the limit equilibrium approach.

With the variable ground conditions methods of slices in the limit equilibrium approach would be appropriate to assess the stability of these sloping grounds. Out of the many different methods of slices, methods such as the Spencer Method that can handle both circular and non-circular modes of failure would be more appropriate under variable ground conditions. The Bishop's method would be appropriate if the failure surface is likely to be circular. The most appropriate technique must be used and appropriate types of trial failure surfaces should be used with the assistance of modern software (such as GEOSLOPE) to identify the most critical circumstance.

The assessment of the factor of safety of slopes can be effectively and reliably carried out using the Finite Element (FE) method in combination with an elastic–perfectly plastic (Mohr–Coulomb) stress–strain model. The primary advantage of employing finite element analysis is that it does not require the prior assumption of a particular failure mechanism when evaluating the factor of safety. However, due to the complexity of the method and the additional data it demands FE method is not used very widely in general stability analysis.

This research has mainly used the limit equilibrium approach with the help of GEOSLOPE Software. As the development and presence of the pore water pressure is the reason for instability, effective stress analysis is adopted in all analyses with the prevailing critical pore water pressures.

Table 2.1 shows the minimum FOS specified by codes and guidelines.

Table 2.1 FOS for BS code and Guidelines for slope design (Jabatan Kerja Raya MALAYSIA, Jan.2010)

REFERENCE	**FACTOR OF SAFETY**	**CIRCUMSTANCE**
BS6031: 1981	1.3 to 1.4	For the initial slide
	1.2	For a slide where the slip surface is already present
	1.5	For permanent loading condition
	1.15 to 1.2	For transient load such as earthquake
JKR Road Work	1.2	For soft ground embankments and slopes without reinforcement
	1.5	For reinforced slope
	1.0 to 1.4	For new slope depending on risk
	1.0 to 1.2	For existing slope depending on risk

Based on these guidelines a target factor of safety of 1.2 was adopted in the rectification designs.

2.3 River Bank Erosion and Associated Failures

In Sri Lanka, embankment failure and erosion along riverbanks have been significant problems in the past and are likely to become more critical in the future as the population increases, leading to more intensive and potentially destructive land use. Soil erodibility, which results in soil loss, increased overland runoff, larger amounts of sediment transported by rivers, lower quality drinking water supplies, heightened flooding hazards, reduced economic returns, and greater hardships for both rural and urban dwellers, is a major concern. In many parts of the world, surface runoff and erosion significantly contribute to land degradation by causing water and soil fertility losses, as well as intensifying flooding risks and surface water pollution.

Topsoil erosion on natural slopes can easily occur during rainfalls when there is no vegetation cover, as vegetation naturally holds the soil in place. Therefore, slopes need stabilization through various holding structures. However, two-fold mechanisms may be involved in topsoil erosion.

a) Impact of raindrops: Rain drop energy causes the top soil to loosen and crater After a long period in which rainfall exceeds infiltration capacity, this loosened layer is exposed crustless sheet erosion.
b) Surface runoff caries it downwards: The loosened soil mass is further pushed by surplus of surface run off inducing failure surface.

Rainfall intensity that exceeds the soil's infiltration rate and water-holding capacity results in runoff, which indicates an increase in runoff extent. The formation of a seal at the soil surface is a major cause of decreased rainfall infiltration into soils in arid and semi-arid regions. This surface seal is typically a thin layer characterized by higher bulk density and lower saturated hydraulic conductivity compared to the underlying soil. Rill and interrill erosion are the two types of soil erosion processes. Runoff from a soil surface can concentrate during these processes into tiny, erodable channels called gullies or rills, destroying infrastructure and earth embankments. Arifuzzaman (2011) divides the most frequent reasons for embankment and riverbank failure into two main categories based on earlier research;

I. Natural forces include rainfall impact, wave action, sudden drawdown, wind action, etc

Several key natural forces are responsible for embankment erosion or damage. The slope erosion caused by rain runoff is significant due to the impinging action of the rainfall, with its velocity and force increasing exponentially towards the toe of the embankment. Toe erosion occurs due to runoff and wave action. The main features of rainfall impact are:

i. Holes and the initiation of piping action can significantly affect the embankment crest and may lead to collapses. This process, in combination with other factors, is illustrated in Figure 2.1 (Drave, 2012) below.

Figure 2.1 Failure of road Embankment

ii. Surface runoff due to rainfall leads to sheet erosion and the creation of gullies and rills on poorly protected embankment shoulders, slopes, and toes, as shown in Figure 2.2 below (Drave, 2012).

Figure 2.2 Failure of River Bank

iii. Flooding: Monsoon/ periodic floods, storm/cyclone-induced floods

iv. The riverside's high head of water causes piping to cross the embankment, which could eventually cause the polder system to rupture and collapse.

Monsoon flooding quite frequently causes rather severe erosion of embankments by undermining due to the action of currents, vortices, and waves. It is a a full-embankment process that starts with undermining-related damage to the shoulders and crest, then gradually overtopping results in total washdown.

Highly near-the-sea embankments incur damage from tidal waves. In order to shield coastal areas from wave action, earthen embankments must have sufficient setbacks. Erosion is caused by a heavy hydraulic load that is applied to the slopes and toes over time. Recurrent cyclonic storms in the coastal zone work against the water's surface, pushing it towards the shore with massive hydraulic loads.

This process is illustrated in Figure 2.3, as described by Islam and Arifuzzaman (2010). The developed waves eventually hit the embankment toe and slopes. The high hydraulic loads imposed on the embankment cause erosion, and in cases of overtopping, the physical structure of the embankment is destroyed.

(a) (b)

Figure 2.3 Photographs 'a' and 'b' depict embankment damage brought on by wave action

Combined with vortex motion in rivers and estuaries, turbulent water currents generally undercut banks through erosion, which can ultimately lead to the collapse of the embankment if adequate protection is not taken. At the mouth of a branch river or canal, and particularly around sluice gates, turbulent water currents erode the banks and, consequently, the embankments. Figure 2.4 shows the failure of an embankment slope due to turbulent water currents (Wikimedia Commons, 2010). The formation of continuous borrow-pits in a river or by the seaside tends to undercut the embankment toes and slopes due to full inundation during the monsoon. These borrow-pits, together with the associated low-lying areas, if flooded, may cause a flow of water that runs very close to the embankment toes and slopes, rapidly eroding the surfaces in some places.

Figure 2.4 Photograph illustrating how turbulent water currents can cause embankments to break.

II. Human interference (such as; Applying heavy vehicle loads adjacent to embankments, unplanned forestation of embankment slopes, excavation in the river to extract sand for construction).

Heavy vehicle loads applied adjacent to embankments and riverbanks can significantly contribute to their failure. The concentrated pressure exerted by these vehicles can cause soil compaction, increasing pore water pressure and reducing soil stability. This process leads to the deformation and weakening of the embankment structure. Additionally, the vibrations from heavy traffic can exacerbate existing weaknesses, triggering subsidence or even landslides. In riverbank areas, such loads can disrupt the natural balance, leading to erosion and increased sedimentation in water bodies. These changes compromise the integrity of both embankments and riverbanks, posing risks to infrastructure, safety, and the environment.

Forestation, if undertaken without proper planning and management techniques, can destroy undergrowth grass cover and thus prove ineffective for erosion protection. Conversely, trees on the embankment slopes may be overturned or uprooted during cyclones. In these situations, forestation weakens the embankment without making a significant contribution to stability.

Due to improper design and construction techniques, many embankments are built with insufficient setbacks, increasing their exposure to wave and current action. This is often due to the high cost of acquiring land. Sometimes, even the setback area itself becomes eroded. Additionally, poor construction supervision can lead to lower-quality earthworks, including the use of incorrect soil materials, inadequate or no clod breaking, insufficient compaction, and failure to lay topsoil layers. Scouring holes and rills often form shortly after construction is completed. Therefore, proper supervision and the correct selection of embankment materials are essential to improving embankment stability.

2.3.1 Erosion Mechanics

To effectively prevent and control erosion, it is essential to comprehend the physics of the erosion process. Particle movement and particle detachment are the two processes that make up erosion. Inertial or cohesive forces between particles balance the drag or tractive forces applied by the flowing stream. Erosion is caused by drag or tractive forces, which are influenced by particle form, roughness, discharge, and velocity. On the other hand, erosion is resisted by resistive elements such inertial, frictional, and cohesive forces, which are dependent on soil structure, characteristics, and physicochemical interactions. Erosion protection essentially entails two steps: 1) decreasing drag or tractive forces by dissipating water energy in a protected area or reducing the velocity of water flow over the surface, and 2) increasing resistance to erosion by reinforcing the surface with a suitable cover or strengthening interparticle bond strength.

2.3.2 Key Factors of Erosion

i) Erosion due to Rainfall

Four main elements affect rainfall erosion: soil type, terrain, vegetation cover, and meteorological conditions. The intensity and duration of precipitation are the main meteorological factors influencing rainfall erosion. According to Wischmeier and Smith, is the most significant single indicator of the propensity for rainfall to cause erosion. The mechanism of topsoil erosion is illustrated in Figure 2.5.

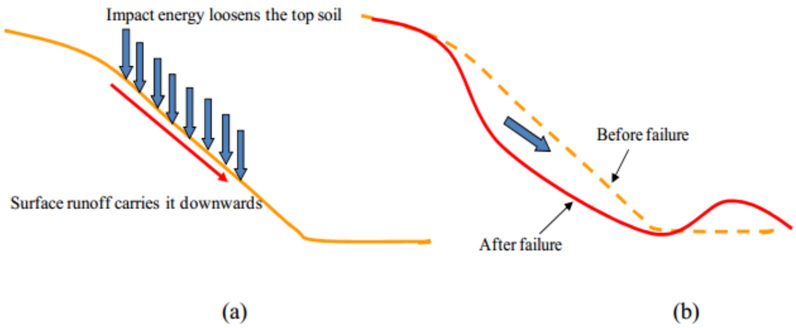

Figure 2.5 Mechanism of topsoil erosion: (a) raindrop impact on the slope and (b) after rainfall-induced slope failure Wischmeier and Smith, 1978.

ii) Erosion due to Wind

In general, the same controlling factors influence wind erosion as those affecting rainfall erosion. Climatic factors, such as the quantity and supply of precipitation, temperature, and moisture, affect soil moisture. Only moderately dry soils can be eroded by wind. Among the characteristics of wind, velocity, duration, direction, and degree of turbulence are the most important. Wind can only lift and transport very fine, dry soil particles in suspension, mainly those smaller than 0.1 mm, such as fine silt-sized materials.

2.4 Methods of Stabilization to Protect Riverbank Slope Failure

To protect riverbank slopes from failure, it is essential to undertake strengthening works. Slope stabilization typically involves several key principles. These include changing the slope geometry, enhancing surface and subsurface drainage, and replacing less stable soils with extra capable materials. Support can be provided through various retaining structures, such as gravity retaining walls, reinforced soil walls, interlocking sheet pile walls, and contiguous bored pile walls. Flexible solutions using reinforcing techniques and natural vegetation are also common. Additionally, perpendicular piles, ground anchors, soil nails, rock anchors, or geosynthetic reinforcements can be used to bolster the slope. The choice of stabilization method depends on several factors, including appropriateness, sustainability, accessibility, and the convenience of equipment, skills, and resources. Careful consideration of these aspects ensures the most effective and sustainable solution for preventing riverbank slope failures.

These techniques can be used separately or in combination. Remedial measures generally adopted fall into three categories (Broms and Wong,1985):

I. By modifying geometry

This method is generally straightforward and inexpensive. It allows for easy variation in slope geometry, ranging from a sharp slope to a milder slope, which can enhance slope stability. The method involves cutting the slope and removing any external load from the top. Additionally, a wall can be constructed either at the top of the slope or at the toe of the slope to provide support. But this approach can only be used if there is enough room.

II. By improvement of drainage

One factor contributing to slope catastrophe is the saturation and increase in pore water pressure in the subsoil. Providing a drainage system can reduce the buildup of pore water pressure and decrease the saturation of the subsoil. This method can be very effective, but its performance depends on proper maintenance. Surface drains are relatively easy to maintain, while subsoil drains are more challenging. Consequently, this approach is frequently combined with other approaches to guarantee overall effectiveness.

III. By use of earth retaining structures

Although generally more expensive, the flexibility of this method in constrained sites makes it the most usually accepted solution. The belief behind this method is that the retaining structure resists the downward forces of the soil mass. Retaining structures include gravity-type retaining walls integrated with various bio-engineering techniques, cantilever walls, adjoining bored piles, caissons, and steel sheet piles with rock anchors. In cases where the driving forces possibly too big to resist, ground anchors or other tie-back systems can be used in conjunction with the retaining structures.

2.5 Earth Retaining Structures for Protecting Riverbank Slopes

Earth retaining structures support masses of soil that are unstable on their own, retaining large heights of soil at steep angles and rehabilitating failed slopes. Over the past two to three decades, various retaining structures have evolved, based on different stabilization principles. These structures can be fundamentally categorized into externally stabilized and internally stabilized structures. Internally stabilized structures include reinforced earth techniques, where reinforcement strips or grids are integrated into the soil, and soil nailing, where reinforcements are inserted into the existing natural soil. These methods rely on internal reinforcements to provide stability. Externally stabilized structures, on the other hand, involve constructing large structures to provide stability. These structures may achieve stability through their weight (gravity structures), their embedment and flexure (embedded structures), or a combination of both.

Today, gravity retaining structures are made from a wide variety of materials. Traditionally, they were constructed from rubble masonry or mass concrete. However, in recent decades, more flexible forms have emerged, such as gabion walls combined with vegetation, bamboo crib walls, crib walls, and interlocking modular block works. These newer forms are gaining popularity due to their ease of construction and their ability to handle differential settlements and lateral movements more effectively than traditional masonry or mass concrete walls. Additionally, these permeable structures prevent the growth of high pore water pressures in the earth fill behind the wall, enhancing overall stability and performance.

2.5.1 Use of Gabion Retaining Walls

A Gabion Retaining System has the ability to stabilize a slope in a cost effective method. In most cases, gabion walls are analyzed as gravity retaining walls, meaning they use their mass to provide lateral earth pressure resistance. Gabions walls are a flexible form of gravity retaining structures that are capable of withstanding significant differential settlements. Furthermore, they are effectively permeable structures and prevent the growth of high pore water pressures in the earth fill behind the wall.

Individual gabion boxes are made up of protected steel (galvanized steel of minimum diameter 2.7mm and minimum tensile strength 350 N/mm^2) and provided with a PVC coating at least 0.5mm thick in more aggressive environments. Some special features of gabion walls are;

1. They can be erected quickly and are effective as soon as erected.
2. It ensures good drainage. To stop fines from the backfill from migrating into the gabion's coarse-grained rock fill, a geotextile filter needs to be installed behind the wall's back face.
3. They are flexible and capable of withstanding high differential settlements. Good founding soil is not essential. Easy to construct river bank protection.
4. They require minimum lateral space. If excessive movements are observed another unit can be added on front.
5. Only mesh needs to be transported to the site fill material and labor can be found locally
6. No special plants are required for the construction

Two most popular supplies of gabions are Maccaferri gabions and Bakaert gabions. Rock used to fill the gabion basket should be of sizes greater than the mesh size and smaller than 200mm (BS 8002). They should be packed to a porosity less than 0.4 and their weathering rate must be comparable with the design life of the structure.

2.5.2 Use of Crib Wall to Protect Slope Failure

A crib retaining wall is a structure made up of separate parts that come together to create a number of cells that resemble boxes and are used to hold infill, which is integrated into the structure. As shown in Figures 2.6 and 2.7, a crib cell is a box-like structure made of headers and stretchers that is used to hold in-fill (Acharya et al., 2018). Wood or concrete can be used to make cot components. Live cuttings are inserted between two crib cells in the current project, which uses bamboo as the crib element. For this reason, these walls are also known as vegetative crib walls, live-reinforced crib walls, or living crib walls. Crib walls are often referred to as a unique type of gravity-retaining construction that use fill material that is placed on the site and secured within a built framework to supply the majority of the mass required to prevent the slope from tipping over. Crib retaining walls are typically built to stabilise the base of a slope that has collapsed, according to Morgan & Rickson. Consequently, it is anticipated that crib walls will function as a type of retaining wall to guard against embankments or slopes.

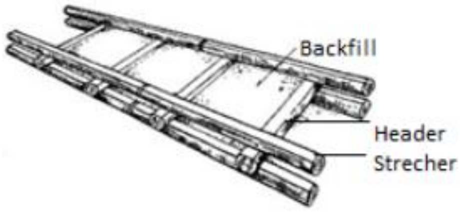

Figure 2.6 A commonly built crib

Figure 2.7 A wooden crib wall example

a) Materials and construction techniques

There are essentially four methods for building cot walls (Figure 2.8). Crib walls can reach up to 25 meters in height, depending on the type of crib pieces and the material utilised (Brandl, 1987). In Acharya's (2020) study, bamboo cribs were constructed using schema type 2, which is appropriate for walls with low ceiling heights.

Ten bamboo crib walls, ranging in height from 1.5 to 2.0 meters, totalling around 150 running meters, were built between May 2003 and June 2004 on three research locations on a hillside in Lalitpur, Nepal. Their actions were thoroughly observed.

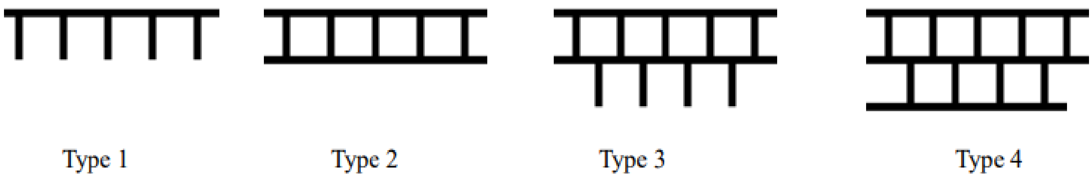

Figure 2.8 Different constructions of cribs – plan view

The crib walls were constructed from field-cut bamboo that was obtained from the surrounding area. Two variations of bamboo, Tama Bans and Taru Bans, were used. The freshly cut bamboo, brought to the site, was around 8 to10 meters in length, with an average diameter of about 8 cm. Typically, the diameter of round timbers used for constructing wooden crib walls is in the range of 20–25 cm. Due to the smaller diameter of the bamboo used in this study (about 8 cm), many layers were needed to achieve the desired wall height. For the header or stretcher elements, bamboo bundles each consisting of three bamboos fastened together with wire were used in order to increase stability.

To create a type 2 crib cell, the bamboo was first cut to the appropriate lengths and assembled on the spot. After that, a rammer was used to compact the infill. The cuttings were placed horizontally, spaced 15 to 20 centimeters apart, filled with soil, sprayed with water, and then compacted once more using a rammer. Layer by layer, this technique was carried out until the desired wall height was attained. Phaledo (Erythrina arborescens/Roxb.), Kalki (Callistemon citrinus/Crimson bottlebrush), Lakuri (Fraxinus floribunda/Himalayan Ash), Chutro (Berberis aristata/Indian Barberry), Amliso (Thysanolaena latifolia/Broom grass), Khareto (Phyllanthus parvifolius), and Kanda Phul (Lantana camara) were the principal branches/rooted plants utilised in the current study.

In Figure 2.9, a bamboo crib wall covered in vegetation is being built. The construction turns into a retaining wall when it is filled. The previously described local species of chopped branches, when collected from a nearby region, offer immediate mechanical support before taking root in the soil and stabilizing the slope. In addition, the branches' exposed portions will sprout leaves, resulting in an aesthetically beautiful and low-maintenance vegetative cover on the slope. Although the bamboo gives the building instant rigidity and shelter, as it decomposes and the live cuttings develop and proliferate, its significance progressively decreases. The root mass that is created will eventually stabilize the slope by uniting the parent soils and fill.

Figure 2.9 Stages of bamboo crib wall construction

2.5.2.1 Design of Crib wall

A crib wall is a kind of gravity retaining wall that is constructed with transverse and longitudinal elements to create a grid of rectangular cells that are then filled with infill. Its construction eliminates the risk of hydrostatic pressure building up behind the wall by using interlocking precast concrete components and filling them with free-draining material and earth backfill. A cot wall's components might be made of wood, bamboo, steel or concrete. Sand or aggregate, or other granular material, is placed inside the interconnecting spaces. One of the following mechanisms may cause the wall to fail:

a. Wall sliding and overturning
b. Foundation overstress
c. Moving and toppling crib components

The earth pressure force on the wall should be estimated using an appropriate method based on the prevailing geometry.

2.5.3 Bioengineered Retaining Wall to Protect Slope Failure

Various bio-engineering techniques have been developed and used in practice to prevent erosion and enhance slope stability for geotechnical structures, embankments, and stream banks (Gray and Sotir, 1996). These methods typically combine different vegetation covers, such as vetiver grass, live stakes, and erosion control blankets, with retaining structures like gabion walls, geotextile bags, or soil bags. This approach has gained significant attention due to its cost-effectiveness, environmental and ecological benefits, sustainability, and aesthetics. To improve friction resistance between soil bag interfaces, a flapped soil-bag was developed in Thailand (PTTGC, 2007). The connection between adjacent bags is enhanced by friction forces on the flaps due to the weight of overlying and adjacent bags. Made of high-density polyethylene (HDPE) with UV-resistant additives, the bags are designed to last 15 years. Jotisankasa et al. (2017) conducted full-scale pullout friction tests on these bags filled with uniform sand, finding a friction angle of 57.4 degrees, nearly three times that of non-flapped soil bags.

In a study by Jotisankasa et al. (2019), a bio-engineering technique using flapped soil bags and a gabion toe wall was implemented in 2015 along a stream bank in Lablae district, Uttaradit province, Northern Thailand. The site, 10 m long, 5 m high, with a 45° gradient, was monitored for crest movement, live stake survival rate, and root growth over 1.5 years. This study aims to assess the performance of this bio-engineering technique for stream bank stabilization.

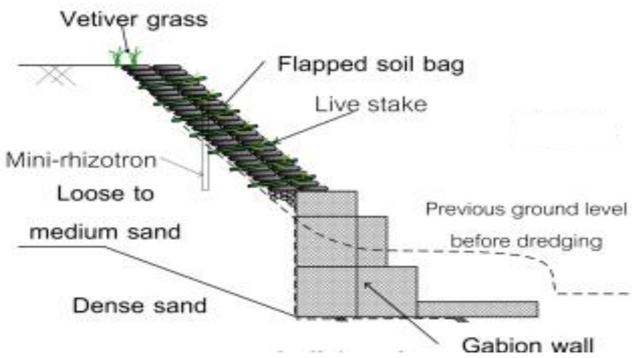

Figure 2.10 Schematic cross-section of the bio-stabilization

The flapped soil bag dimensions are shown in Figure 2.11. Friction forces between bags are enhanced by the weight of overlying and adjacent bags. Live stakes (0.8 to 1 meter long and 18-25 cm in diameter) of various species were placed horizontally between each flapped soil bag at 0.5-meter intervals (Figure 2.12). Species used included Bougainvillea, Erythrina subumbrans, Salix tetrasperma, and Spondias pinnata. The lower end of the live stake was cut sharply and positioned to touch the soil behind the bags, allowing roots to grow out and act as living soil nails.

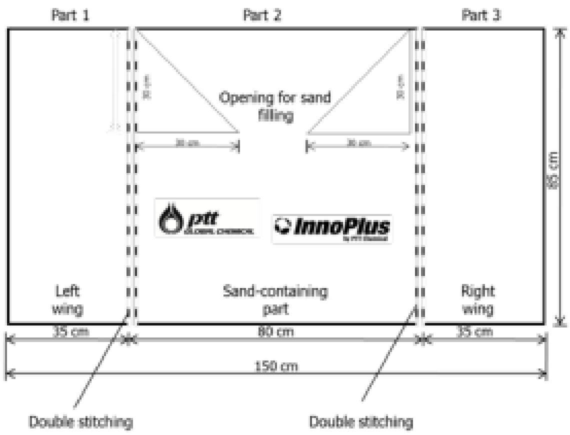

Figure 2.11 Flapped plastic sack used in this study

Figure 2.12 Placement of flapped soil bag with live stake

Figure 2.13 shows the stabilization at different stages: before construction (Jan 2015), immediately after construction (June 2016), 8 months later (Feb 2016), 1 year and 4 months later (Oct 2016), and 2 years and 5 months later (Nov 2017). Eight months after construction, the aesthetic value of the bio-engineered wall had clearly improved, with vegetation almost fully covering the flapped bags, protecting them from UV rays. After one year, local species began to dominate the vegetation on the bags, and biodiversity was evident after two years (Nov 2017). Overall, the ecological restoration of the stream bank showed significant long-term improvement.

Figure 2.13 Appearance of the vegetation cover of the failed sections over time

Based on this research study, a similar sustainable solution was adopted at failed location 3, using flapped soil-bags with a gabion toe wall to stabilize a 0.9-meter high stream bank with a 40-degree gradient. By horizontally placing live stakes of various species along the connections between adjacent soil bags (1 meter long and 20 centimeters in diameter) at a spacing of 0.5 meters, the anchoring effect is expected to improve similarly. This approach was anticipated to provide a cost-effective and environmentally friendly method for stream bank stabilization, promoting vegetation growth and enhancing the overall stability of the structure over time. The use of locally available materials and the integration of live plantings contribute to the sustainability and effectiveness of this solution, making it a viable option for similar applications in other regions.

2.5.4 Embedded Retaining Wall (Flexible Wall) to Prevent Slope Failure

This study explored the use of steel sheet pile walls as a solution to space constraints between the Kelani River and low-level road, and the need for minimal disturbance in urban areas. Steel sheet piles offer versatility in cross-sectional variety, rapid construction, resistance to buckling during installation, reusability, high stiffness, relatively low weight, and the ability to extend their length through welding or bolting. Given the challenging soil conditions at this location, including weak subsoil and bedrock constraints that limit embedment depth, it is crucial to anchor the sheet piles. In areas with weak peaty clay layers, sheet piles must be anchored to the bedrock to ensure stability and effectiveness. This approach addresses the specific conditions of the site, providing a robust solution to protect the slope from failure. The sheet pile wall may be designed conventionally using either the fixed earth support or free earth support method.

2.5.5 Indigenous method (Grass) to Protect Slope Failure

Considering this kind of secure work, there are no hard and fast rules. Historically, chailla grass has been utilized. A split bamboo woven net holds the chailla grass straw in place on the slope's surface after it has been applied at a specific thickness. Pegs secure this bamboo net to the incline. It is called aar bandh, although technically it is termed soft protection. In order to prevent it from collapsing during the dry season, it must be constructed each year at the start of the monsoon and taken down at its conclusion. When the wave height consistently exceeds 0.6 meters, it is unable to endure the force of erosive waves (CIDA,2002).

In my study, vetiver grass was used for erosion control on embankment slopes above the gabion wall protection at the toe. Many countries, including Australia, China, India, Malaysia, and Zimbabwe, utilize vetiver for various erosion protection purposes. Vetiver grass (Vetiveria zizanioides) forms a dense, deeply rooted clump that acts as a vegetative barrier, slowing runoff and retaining sediment on site.

Vetiver is used in over 100 countries worldwide (Truong, 2000) and is a highly adaptable plant, producing good growth in annual rainfall ranging from 200 mm to 5,000 mm (Rahman et al., 1996). It can tolerate temperatures from 0°C to 50°C and produces very well in extremely acidic soils with pH values from 3.0 to 10.5. Additionally, vetiver is highly tolerant to heavy metals such as Al, Mn, As, Cd, Cr, Ni, Pb, Hg, Se, and Zn (Truong and Baker, 1998). Vetiver has a relative yield of 100% on soils with an ECse value of 7.8 dS/m, but the yield reduces to 90% in soils with an ECse of 10 dS/m and to 50% (Truong et al., 2002) in soils with an ECse of 20 dS/m. Hengchaovanich (1998) reported that the tensile strengths of vetiver roots exceed 75 MPa, while Verhagen et al. (2008) stated that the lifespan of vetiver hedges can exceed 100 years.

2.5.6 Sand bags and Sand-Cement mixed bags to Protect Slope Failure

This method is comparatively low-cost and temporary for protection. Gunny or polyethylene bags, each with a capacity of about 1.25 cubic feet and filled with low FM sand, are arranged in a rip-rap pattern across the terrain. Polyethylene bags are preferable to gunny bags due to their greater durability. This approach is ideal for emergency repairs and situations requiring minimal time and expense. Sandbags' inadequate performance against a cyclonic storm surge is depicted in Figure 2.14 (Islam and Arifuzzaman, 2010). The failure may be due to the absence of proper connections between the individual polythene sand bags. Often, the bags were simply placed adjacently without any mechanical linkage, leading to shifting and displacement under external forces like heavy rainfall and water flow. Sand-filled polythene bags, especially those not mixed with cement, might lack sufficient weight and compaction, making them more susceptible to movement by water forces. Effective drainage is crucial in slope protection; inadequate drainage can lead to water accumulation behind the rip-rap, increasing hydrostatic pressure and causing the bags to shift or collapse.

Figure 2.14 Cyclonic Storm Surge Protection: The Poor Performance of Sand Bags

Lessons learned include the necessity of connecting individual bags for stability, achievable through tying techniques, mesh netting, or other fastening methods to ensure the bags act as a unified structure. Mixing sand with cement in the polythene bags can increase their weight and compaction, providing better resistance to displacement. Additionally, ensuring proper filling and compaction of the bags can enhance their stability. Incorporating a well-designed drainage system is essential to manage water flow and reduce pressure behind the rip-rap, involving both surface and subsurface mechanisms to mitigate water-induced failures effectively.

In this research, the use of gunny or flapped soil bags combined with vegetation as a bioengineered solution for stabilizing failed stream bank slopes was explored. This method leverages the benefits of natural vegetation to enhance the structural integrity of the gunny bags, offering an effective alternative for slope stabilization.

2.5.7 Cement-Concrete blocks with Geotextile to Protect Slope Failure

Cement-concrete blocks combined with geotextile have recently been used for slope protection. However, this approach is expensive and not ecologically friendly. Cement-concrete (CC) block-based protected embankment slope failure at Keraniganj is depicted in Figure 2.15 (Source: Prothom Alo, dated 04.04.2011). This failure's causes could include the absence of any interlocking arrangements between individual units to keep them as one unit or washing away due to high tidal surge in the absence of poor drainage arrangements and the geotextile used in the construction was not anchored adequately. Lessons learned from this failure include ensuring that individual blocks are interconnected for overall stability, achievable through interlocking designs or additional fastening materials. The geotextile must be securely anchored to perform its reinforcing role effectively, requiring proper tensioning and fixing at regular intervals. Additionally, incorporating a well-designed drainage system is essential to mitigate water-induced failures, involving both surface and subsurface mechanisms to manage water flow and reduce pressure behind the wall. By addressing these issues, future slope protection projects using cement-concrete blocks and geotextile can achieve greater durability, effectiveness, and longevity.

Figure 2.15 The Keraniganj Beribadh site's CC blocks are performing poorly

In this study, the use of boulder packing combined with gabions was explored for stabilizing failed riverbank slope.

2.6 Related case studies on stabilization of a river bank by appropriate measures

2.6.1 Ghislain Brunet et al.'s case study on using vegetated gabions to stabilize stream banks (2007)

A study conducted by Brunet et al. (2007) detailed the process of choosing, designing, building, and evaluating the efficacy of biotechnologies used in a bank stabilisation project at Manchester, New Hampshire's Intervale Country Club Golf Course. The Club was founded in 1903 and is situated near the Amoskeag hydroelectric dam's storage basin on the Merrimack River. Roughly 15-20 feet of beachfront have been lost to erosion in the last 20 years. The site's soils are mostly made up of medium-to-fine sands that have very little cohesive strength. Boat traffic has contributed to increased financial instability, among other reasons. Strict adherence to local laws and the preservation of old pine trees that serve as winter roosting habitat for the endangered Bald Eagle were important factors in the solution selection process. The involvement of state and federal agencies was significant due to the presence of Bald Eagles, anadromous fish, and the project's scale. To address erosion and maintain wildlife habitat, two new biotechnologies were employed: modified gabions with live staking and container plants. These structures are designed to resist erosion from the river and ice movement each spring.

In the preliminary design, If the toe was not undercut, the natural slope angle of repose may be 1:1 or steeper and still be stable. The stability analysis was restricted to on-site visual inspections. Silty sand was the natural soil used for the analysis. Three types of applications for rock toe protection and lifts wrapped in geosynthetic fabric were identified: Where there were no trees to protect, the slopes could be graded back using a combination of the two above solutions: (1) where slopes needed to be built out to protect existing trees and provide a stable slope, involving rock toe protection and geolifts; (2) where the trees were set back far enough to use a combination of the two above solutions. The selection of materials was crucial for the project's environmental characteristics in all respects. One of the most important things was how well the art blended into the surroundings. Two new product categories were chosen: PVC-coated woven wire mesh was used to create both Green Gabion, a trapezoidal gabion, and Envirolog, a cylindrical gabion. These materials are naturally porous and flexible, with

30–40% spaces that can be filled with dirt. In addition to providing a substrate for root growth between the stones, the topsoil aids in the retention of water for vegetation. A thick layer of coconut mat (minimum 900 g/m2) was placed within the wire mesh basket to hold the topsoil in place. This coconut mat is durable and helps retain moisture for vegetation; it will last 3–5 years before biodegrading.

To evaluate the bank's stability in terms of slope and resistance to erosion, analysis was done. Using MacStars 2000 software, the Bishop simplified technique was used to analyse the slope stability for both internal and global stability. The findings showed that the safety factor for internal stability was 4.02 and for global stability was 1.55. Using willows' shear resistance, the impact of vegetation to slope stability was examined. According to published research, the ultimate shear stress of a 3-year-old willow can reach 9.1 kN/m². According to Goldsmith (1996), it was thought that the root system's reinforcement extended two meters below the surface, with each plant in a row of units having a spacing of 30 cm between them. To account for errors, a shear resistance value of 3.0 kN/m² was employed in the computations. The structure's internal stability safety factor increased to 4.55 due to the vegetation's contribution, but the global safety factor stayed at 1.55

Following vegetation establishment, there may be a 10% increase in internal stability. However, because the potential slip plane did not run through the vegetation, global stability was unaffected, hence this study was only done for informational purposes and not for design stability. Using MACRA 1 software, erosion resistance was measured both immediately following installation and again following three years of vegetation establishment. The shear resistance of the vegetated gabion revetment improved with vegetation from 336 N/m² to 450 N/m². The safety factor against erosion was 9.9. Budget constraints prevented the inclusion of wave action from boats and potential ice impact in the analysis. According to Maccaferri literature, waves reaching a height of 1.7 meters can be resisted by a gabion revetment on a 1:1.5 slope. Local navigation on the Merrimack River produces waves of about 1 meter (3 ft), which is below the threshold for stability. Ice impact analysis was not performed due to added costs and the absence of recent ice-related issues in this section of the river. Manufacturer experience implies that plants protecting the gabion's exterior face from ice impact damage; although local damage might occur, the risk is low.

A 30 cm by 2-meter rivet mattress was placed under the units to prevent scour, extending 1 meter in front to mitigate erosion (Figure 2.16).

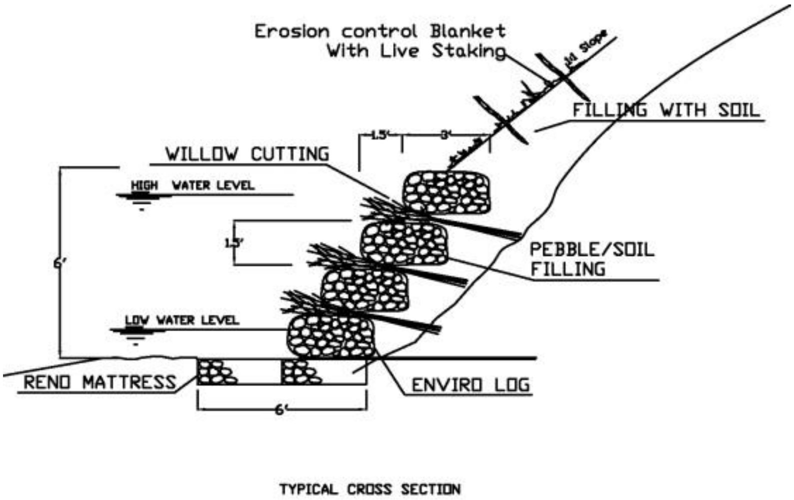

Figure 2.16 Modified Gabion with Vegetation

The project work was generally done according to specifications, but budget limitations precluded a full-time inspector. Some issues, such as the size of stones in the Reno mattresses for toe protection, could have been prevented with better oversight. After a year, some stones have emerged from the mattresses, necessitating refilling with properly sized stones. Vegetation was generally well-established after one growing season, though some areas faced establishment problems due to small or improperly placed plants. The vegetation progression during the first growing season, from spring to mid-summer, is depicted in Figure 2.17. When paired with a thick layer of coconut, the modified gabions can withstand erosion for three to five years before the coconut starts to deteriorate. To address missing areas, it is recommended to further enhance vegetation through live staking.

Figure 2.17 showing the post-construction performance

Based on this research study, I have adopted an alternative sustainable solution at failed location 3, using modified gabion with vegetation to stabilize a 2-meter high stream bank with a 10-degree gradient.

2.6.2 Guillermo Tardio et al. (2018) The Use of Bamboo for Erosion Control and Slope Stabilization

According to Tardio et al. (2018), the live bamboo crib wall is a three-dimensional construction made of live cuttings, fill material, and untreated bamboo. According to Morgan and Rickson, it serves as a gravity-retaining structure by providing the necessary mass within a built framework to prevent the slope and materials' weight from toppling it over. Bamboo can be used to build cot walls both newly cut and seasoned, though bamboo stems that have been chemically or lime-treated may cost more to build. Green bamboo that has just been chopped or air-dried is generally preferred. Twigs and large knots should be trimmed, but the bamboo does not need to be smooth. Depending on the diameter of the available bamboo stems, either single stems or bundles of three bamboo pieces can be used for the header and stretcher elements in the crib construction. The crib's construction process will be similar to that of a wooden log wall with bigger diameters. To guarantee a constant thickness of the crib layer, uniform-sized bamboo stems should be used when working with single stems. To keep the bamboo stems from breaking, bending, or tearing along their length, they should be secured or fixed using binding wires, binding materials, or nails. To build a bamboo crib wall, it requires binding wires, bamboo, and live cuttings or rooted plants that are longer than the wall's depth to allow for soil penetration behind the wall and appropriate fill material. Fill material is typically made from locally accessible slope or cut material. To encourage root formation, a layer of humus or fine, organic-rich soil should be positioned around the cuttings if the surrounding material is extremely coarse gravel, which prevents roots from growing. Boulders or large stones are not appropriate for use as fill material. Large voids inside the crib construction must be prevented by properly compacting the fill materials. Before building begins, bamboos, binding wires, and cuttings should also be put close to the site.

It is necessary to lay out the wall and construct a foundation while keeping the crib wall's intended size in mind. Depending on the height of the bamboo crib wall, the foundation trench should be between 0.3 and 0.5 meters deep, with an inward inclination of 10-15° to improve stability against sliding. To stop sliding and shield the foundation from seepage water, at least one layer of cribs needs to be positioned below ground level. Depending on the test settings and methods used, tests have indicated that the compressive strength of bamboo varies between 35 and 70 N/mm^2, which is approximately two to four times that of typical timber species. In comparison to bamboo with a high moisture level, bamboo with a low moisture content has a better compressive strength. Bamboo has an average tensile strength of about 160 N/mm^2, which is almost three times greater than most conventional construction-grade timber products.

To define technical standards for Soil Bioengineering Systems, field investigations were carried out in a case study by Tribhuvan University, Kathmandu, Nepal, and the University of Natural Resources and Life Sciences, Vienna (BOKU). In Kusunti, Kathmandu, the performance of a bamboo crib wall and a traditional gabion retaining wall were compared. To allow for a technical and financial comparison, the site was split into two sections: one was treated with a bamboo crib wall and the other with a gabion retaining wall. The gabion retaining wall was constructed with a total height of 3 meters, starting on November 11, 2006, and completed by November 23, 2006. The construction quality was supervised throughout the process. Students from Pulchowk Campus and the University of Applied Sciences Wadenswil (HsW), Switzerland, were directly involved. Figure 2.18 displays images of the site taken both before and after construction. Following project activities and site observation, the following conclusions about bamboo cot walls were made:

- While offering the same level of technical stability, vegetative crib walls are less expensive than gabion or stone masonry walls, costing only 25% of the former and 15% of the latter.
- Although vegetative crib walls have more vertical settlement compared to a gabion/masonry wall, they are better attached to the slope.
- Low soil moisture levels are guaranteed by vegetative crib walls, which also prevent cracking and improve rainfall interceptions.
- Because of the improved cohesiveness and soil reinforcement, they offer better stability.

Figure 2.18: Kusunti, Lalitpur, before and after construction photos

According to this research study, the vegetative crib wall composed of bamboo is a more appropriate, long-lasting, and ecologically friendly solution for safeguarding road embankments in Sri Lanka or resolving issues with slope stability.

2.6.3 Acharya, M. S. (2020) argues that bamboo crib walls are a sustainable method of soil bioengineering that can stabilize slopes in Nepal.

Acharya, M. S. (2020) presented experimental work on the performance of bamboo crib walls, demonstrating that they offer a cost-effective alternative for slope management. As a flexible measure, bamboo crib walls can be integrated with larger geotechnical and civil engineering solutions for extensive slope failures. In regions where vegetation can thrive, soil bioengineering techniques like bamboo crib walls can yield superior economic and ecological outcomes compared to outdated geotechnical results. The incorporation of plants into bamboo crib walls enhances their service life and overall slope stability over time. The findings indicate that locally available bamboo used for crib walls in slope stabilization can be a feasible substitute to conventional gabion walls. According to post-performance evaluations, this technology may be used in place of more conventional geotechnical slope stabilization techniques. Additionally, in the long term, it can contribute to improved air and water quality and develop into a sustainable solution for geotechnical challenges. Education and dissemination of new technologies are crucial; therefore, further testing of this technique under various conditions and broad publication of results are recommended. A research team of geotechnical and soil bioengineering specialists should continue to refine and dimension these structures. It's essential to emphasize that techniques should not be blindly replicated without considering basic engineering principles.

Key issues include thorough site investigation to determine the causes of failure and designing an appropriate system using suitable mitigation and remediation techniques. Vegetative crib techniques should be integrated into a complete soil bioengineering system, with proper site assessment and design being critical for successful implementation. According to test results and qualitative evaluations, vegetative bamboo crib walls offer a viable substitute for traditional retaining walls that could have a major positive socioeconomic impact on local communities.

2.7 Summary

Researchers worldwide have developed various techniques involving both hard and flexible solutions that incorporate natural vegetation for slope stabilization. However, in Sri Lanka, the lack of innovative studies has hindered the development of cost-effective, sustainability, and environmentally friendly methods. This study aims to address this knowledge gap by identifying novel approaches suitable for Sri Lanka.

The next chapter will present the methodology adopted in this study, including establishing subsoil conditions and assessing stability. Rectification processes were formulated, and necessary designs were developed using the Morgenstern-Price Limit Equilibrium Approach through SLOPE/W software (GeoStudio, 2018) to analyze global stability. The external stability of the rectification methods was assessed according to BS8002 (1994). Special attention was given to the construction sequence to ensure the efficacy of the solutions. By studying four case histories, each with different hydraulic flow conditions, guidelines will be established to inform similar projects in the future.

CHAPTER 3

3.0 METHODOLOGY ADOPTED

3.1 Introduction

Due to time constraints, four distinct problematic locations within the highway road network, each exhibiting unique characteristics, were selected for the study. Comprehensive geotechnical investigations were conducted at these sites to evaluate the subsoil conditions, considering the degradation processes over time caused by both natural phenomena and human activities. These investigations aimed to identify the root causes of the issues at each location.

Appropriate rectification and alternative solution processes were then formulated, and necessary designs were developed using the Limit Equilibrium Approach using the Morgenstern-Price method implemented through SLOPE/W software (GeoStudio, 2018), to assess the global stability. Additionally, the stability of the retaining structures used in rectification was assessed following BS8002 (1994). Special attention was given to the construction sequence to ensure the efficacy of the solutions.

3.2 Establishment of subsoil condition

To determine the subsoil profile relevant to the retaining slope heights at four selected locations appropriate geotechnical investigations were conducted. This investigation utilized several methodologies, including advancing boreholes with Standard Penetration Testing (SPT), Dynamic Cone Penetrometer (DCP) tests, Mackintosh Probe (MT) tests, and laboratory sampling. Subsequent laboratory tests were performed following BS 1377 Part 2 (1990) to ensure accuracy and reliability. Additionally, hand auguring methods were employed to identify subsurface layers. These extensive investigations provided a detailed understanding of the subsoil conditions at each site. All problematic locations selected in the study and locations of field investigations are presented in Figure 3.1.

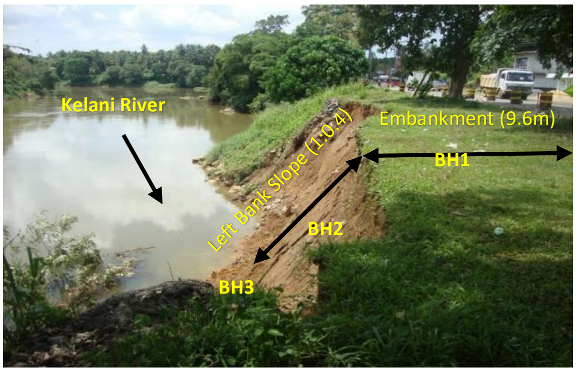

(a) Location 1

(b) Location 2

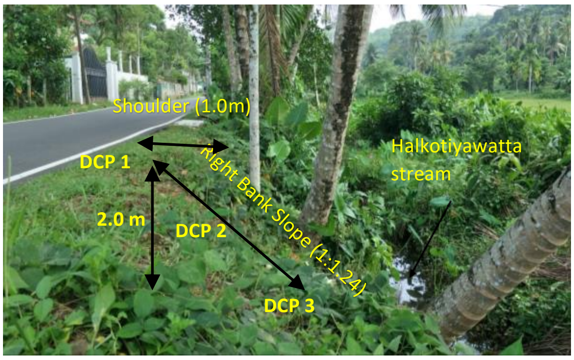

(c) Location 3

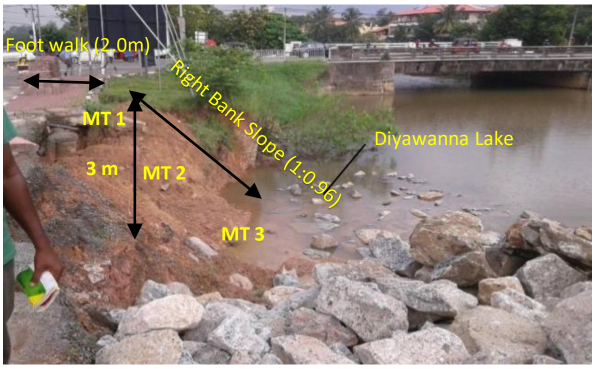

(d) Location 4

Figure 3.1 Problematic locations 1,2,3 and 4

<u>Location 1</u>

Location 01 is situated at the Low Level Road near the 26th-kilometer milestone, a crucial entry point for heavy vehicles transporting goods to the capital city of Colombo. This site has been potentially active for several years. While the slope appears relatively stable during the dry season, it experiences significant stability issues during the rainy season due to heavy water flow through the banks and a sudden drawdown of water levels in the river within a 6-hour period after the flood recedes, owing to the rapid discharge of river water. Additionally, tidal action causes the slopes of the embankment to change their original shape, becoming steeper. Another factor contributing to the scouring is sand mining in the river area. Three boreholes were drilled at the locations marked in Figure 3.1, and the subsoil profile deduced from these boreholes is presented in Figure 3.2.

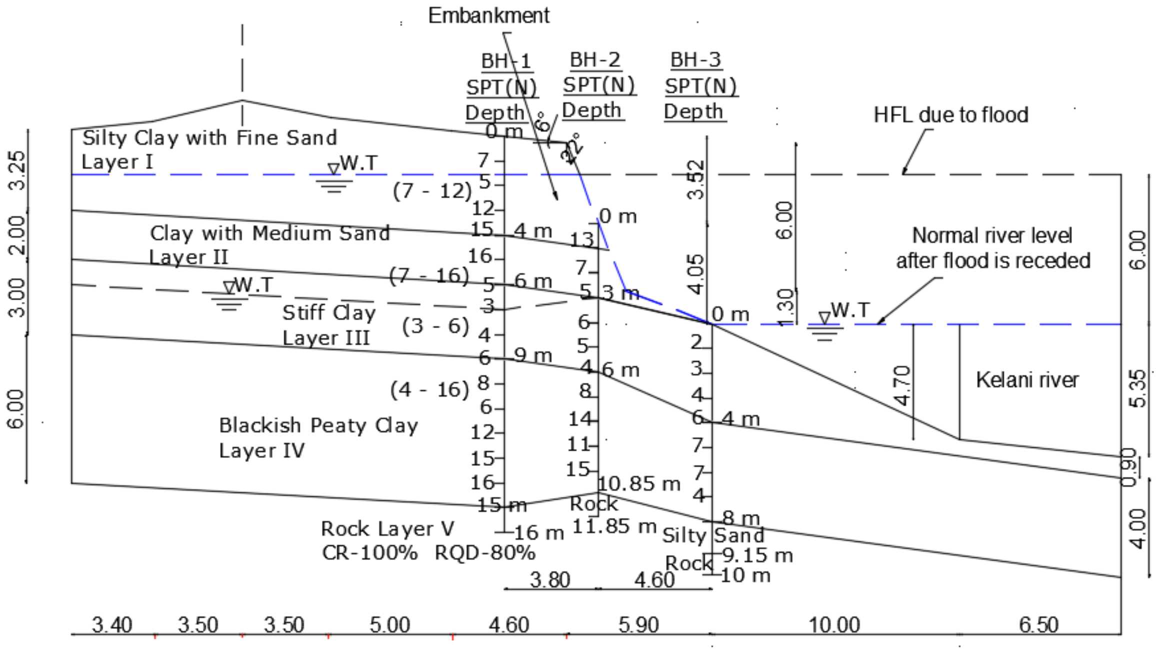

Figure 3.2 A subsoil profile at location 1

<u>Layers present in the subsurface based on the SPT</u>

Based on the SPT, the following main layers are identified in the subsurface.

Layer 1 – A top soil of Silty Clay with Fine sand layer is present in both boreholes, the thickness varies between 1 to 4m, the SPT blow count varies from 7 – 12.

Layer II – Clay with medium Sand layer is present in both boreholes. Thickness varies between 0 to2 m. The SPT blow count varies from 7 – 16.

Layer III – Stiff Clay of high plasticity is present in all three boreholes. Thickness varies between 2 to 4m and the SPT blow counts are reported in the range of 3 – 6.

Layer IV – Blackish Peaty Clay layer is present in all three boreholes. Thickness varies between 4 to 6 m and the SPT blow counts are reported in the range of 4– 16.

Layer V – Hard Rock is present in all three boreholes (CR-100% and RQD-80%).

According to the energy method and the empirical correlation between ϕ^1 ,D_r, q_u and estimated SPT N'_{70} (Bowles, 1997) the soil shear strength parameters were determined. The results from the laboratory consolidated drained direct shear test, along with the shear strength parameters determined using Bowles' correlation, are summarized in Table 3.1. This table presents the estimated soil shear strength parameters used for the study, including the drained angle of friction (ϕ^1), Drained cohesion (C') and Undrained cohesion (C_u).

Table 3.1 Geotechnical parameters of the soil layers using appropriate correlations and Experimental result

Type of soil	Layer	SPT-N (range)	Unit weight (kN/m^3)		Estimated Shear strength parameters				Shear strength parameters used for the study		
					With correlations given in Bowels (1997)		Experimental result				
			γ_{wet}	γ_{sat}	ϕ' (deg.)	C_u (kPa)	ϕ' (deg.	C' (kPa)	C_u (kPa)	ϕ' (deg.)	C' (kPa)
Silty Clay with Fine Sand	I	7-12	16	-	32	-	-	-	-	30	2
Clay with Medium Sand	II	7-16	17	-	33	-	36	5	-	32	3
Stiff Highly Plastic Clay	III	3-6	17.5	18	-	19	-	-	20	28	0
Peaty Clay	IV	4-16	-	14	-	26	-	-	25	25	0

Location 2

Location 2 is identified on the right side of the Halwathura Phalakotasa stream bank along the Ingiriya-Halwathura-Ekgaloya road (B068) at the 4th-kilometer milepost. It suffers substantial stability problems during the rainy season due to poor soil drainage. During heavy rainfall, increased runoff and a steeper slope angle result in more severe soil erosion and the ascent of the wetting front, leading to the failure of soil slopes. The groundwater level in the road section rises to the high flood level for a short period, but there is a sudden drawdown of water levels in the stream within 2 hours after the flood recedes, with adjacent paddy fields on both sides of the road. Three Dynamic Cone Penetrometer (DCP) tests were conducted at the location 2 marked in Figure 3.1, and the subsoil profile deduced from these DCP tests as well as hand auguring is presented in Figure 3.3.

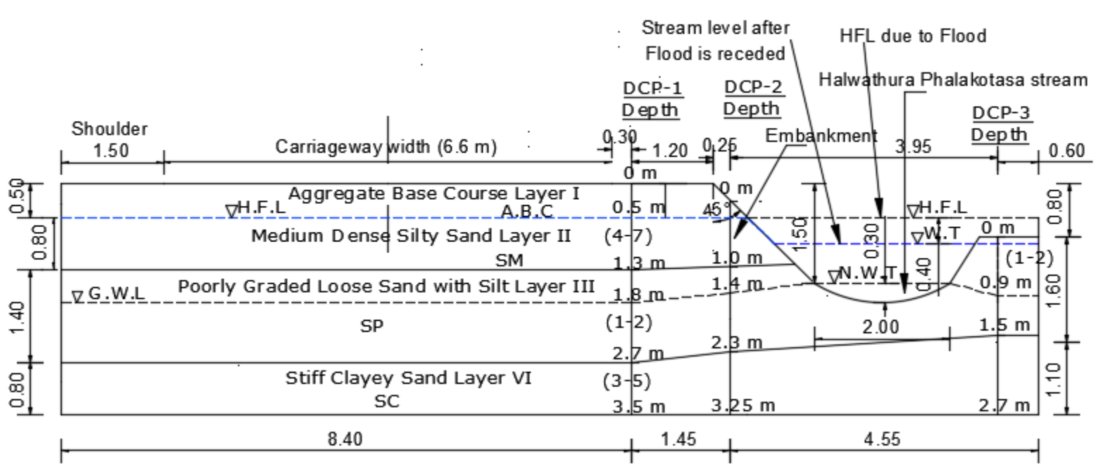

Figure 3.3 A subsoil profile at location 2

Layers Identified in the Subsurface by Hand Augering

The following layers present in the subsurface were identified by hand augering, which was conducted in addition to the DCP tests.

Layer 1 – A top layer of Asphalt concrete (50mm) plus Aggregate Base Course (ABC-500mm) is present.

Layer II – Medium Dense Silty Sand (SM) layer is present in both DCP tests and identified from USC system. Thickness varies between 0.5 to 1.3 m. The DCP blow count varies from 4 – 7 per 100mm penetration.

Layer III – Poorly Graded Loose Sand with Silt (SP) layer is present in all three DCP tests and identified from USC system. Thickness varies between 1.3 to 2.7 m and the DCP blow counts are reported in the range of 1 – 2 per 100mm penetration.

Layer IV – Stiff Clayey Sand (SC) layer is present in all three DCP tests and identified from USC system. Thickness varies between 2.7 to 3.3 m and the DCP blow counts are reported in the range of 3 – 5 per 100mm penetration.

The number of blows, N_{DCP} (Blows/100 mm), was obtained from the DCP test. The N_{SPT} was determined using the empirical correlation between N_{DCP} and N_{SPT} provided by Samuel Innocent et al. (2018). The shear strength parameters, determined using correlations by Bowles (1997) and Burt Look (2007), are charted in Table 3.2.

Table 3.2 Geotechnical parameters of the soil layers using appropriate correlations

Type of soil	Layer	N_{DCP} - n / (Blows/ 100 mm)	Empirical correlation N_{DCP} Vs N_{SPT} by Samuel Innocent et al.(2018)	Unit weight (kN/m^3)		Shear Strength Parameters Used for the Study Given by Bowles (1997) and Burt Look (2007)		
			N_{SPT}	γ_{dry}	γ_{sat}	Cu (kPa)	ϕ' (deg.)	C' (kPa)
Aggregate Base Course	I	-	-	20	-	-	34	-
Medium Dense Silty Sand (SM)	II	4-7	5-8	18	20	-	32	2
Poorly Graded Loose Sand with Silt (SP)	III	1-2	1		17	-	28	1
Stiff Clayey Sand (SC)	IV	3-5	1-2	-	18	-	25	10

Location 3

Location 3 is identified on the right side of the Halkotiyawatta stream bank on Seelarathana Mawatha at the 1st-kilometer mile post. It suffers substantial stability problems during the rainy season. This instability is attributed to the closure and filling of the existing drain on the hillside with soil. During the rainy season, rainwater flows across the road to the other side, with the left-hand side having a higher elevation than the right-hand side, causing a rise in the groundwater table. This rise in groundwater potentially renders the slope unstable and causes shoulder erosion. Three Dynamic Cone Penetrometer (DCP) tests were conducted at the location 3 marked in Figure 3.1, and the subsoil profile deduced from these DCP tests as well as hand augering is presented in Figure 3.4.

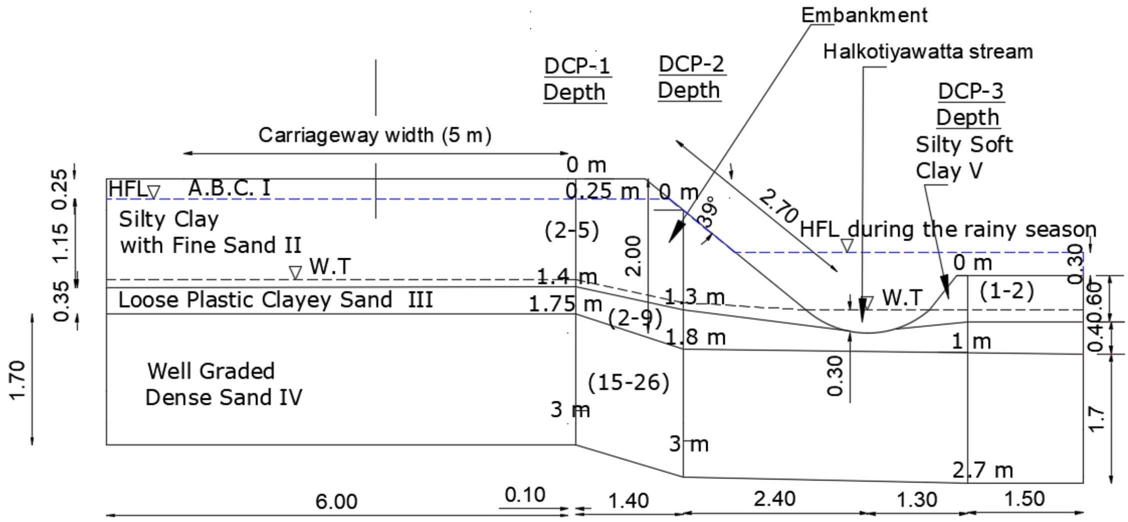

Figure 3.4 A subsoil profile at location 3

Layers Identified in the Subsurface by Hand Augering

The following layers present in the subsurface were identified by hand augering, which was conducted in addition to the DCP tests.

Layer 1 – A top layer of Asphalt concrete (50mm) plus Aggregate Base Course (ABC-200mm) is present.

Layer II – Silty Clay with Fine Sand (CL+ML) layer is present in both DCP tests and identified from USC system. Thickness varies between 0.25 to 1.4 m. The DCP blow count varies from 2 – 5 per 100mm penetration.

Layer III – Loose Plastic Clayey Sand (SC) layer is present in all three DCP tests and identified from USC system. Thickness varies between 1.3 to 1.8 m and the DCP blow counts are reported in the range of 2 – 9 per 100mm penetration.

Layer IV – Well Graded Dense Sand (SW) layer is present in all three DCP tests and identified from USC system. Thickness varies between 1.8 to 3 m and the DCP blow counts are reported in the range of 15 – 26 per 100mm penetration.

Layer V – Silty Soft Clay (CL) layer is present in third DCP test and identified from USC system. Thickness varies between 0 to 0.6 m. The DCP blow count varies from 1 – 2 per 100mm penetration.

The number of blows, N_{DCP} (Blows/100 mm), was obtained from the DCP test. The N_{SPT} was determined using the empirical correlation between N_{DCP} and N_{SPT} provided by Samuel Innocent et al. (2018). The soil strength properties, determined using correlations by Bowles (1997) and Burt Look (2007), are summarized in Table 3.3.

Table 3.3 Geotechnical parameters of the soil layers using appropriate correlations

Type of soil	Layer	N_{DCP} - n / (Blows/ 100 mm)	Empirical correlation N_{DCP} Vs N_{SPT} by Samuel Innocent et al.(2018)	Unit weight (kN/m^3)		Shear Strength Parameters Used for the Study Given by Bowles (1997) and Burt Look (2007)		
			N_{SPT}	γ_{dry}	γ_{sat}	Cu (kPa)	ϕ' (deg.)	C' (kPa)
Aggregate Base Course	I	-	-	20	-	-	34	-
Silty Clay with Fine Sand (CL+ML)	II	2-5	1-2	16	17	-	31	2
Loose Plastic Clayey Sand (SC)	III	2-9	1-3		16	-	26	5
Well Graded Dense Sand (SW)	IV	15-26	5-9	-	18	-	33	-
Silty Soft Clay (CL)	V	1-2	1	-	14	10	25	-

Location 4

Location 4 is identified on the right bank of the Diyawanna Lake on Denzil Kobbekaduwa Mawatha at the 1st-kilometer milestone. It has been potentially active for several years and suffers substantial stability problems during heavy water flow. The small opening size at the bridge near the failed section alters water velocity, causing differential movement in the bed materials and inducing toe erosion. This erosion, exacerbated by the high discharge velocity from Diyawanna Lake, leads to the collapse of overhanging slope soil under traffic load and results in channel incision and widening due to hydrological changes in the watershed. Three Mackintosh Probe (MT) tests were conducted to obtain details about the 10 meters depth at Location 4, as marked in Figure 3.1. The subsoil profile deduced from these MT tests, along with hand augering, is presented in Figure 3.5.

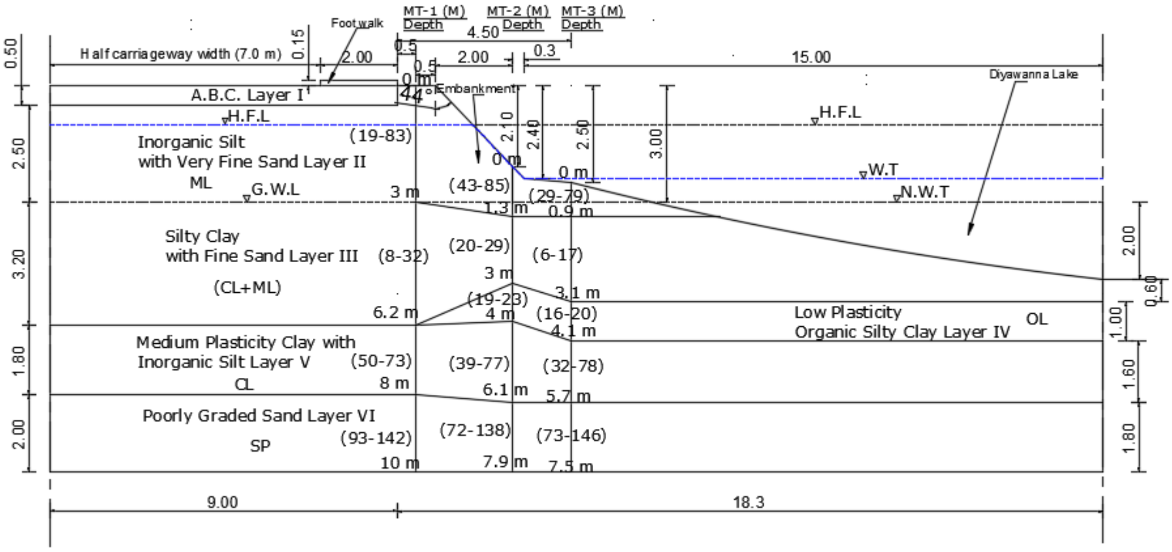

Figure 3.5 A subsoil profile at location 4

Layers Identified in the Subsurface by Hand Augering

The following layers present in the subsurface were identified by hand augering, which was conducted in addition to the Mackintosh Probe (MT) tssts.

Layer 1 – A top layer of AC overlay (50mm) plus ABC (450mm) is present.

Layer II – Inorganic Silt with Very Fine Sand (ML) layer is present in all three MT tests and identified from USC system. Thickness varies between 0.9 to 3 m. The MT blow count varies from 19 – 85 per 300mm penetration.

Layer III – Silty Clay with Fine Sand (CL+ML) layer is present in all three MT tests and identified from USC system. Thickness varies between 1.7 to 3.2 m and the MT blow counts are reported in the range of 6 – 32 per 300mm penetration.

Layer IV – Low Plasticity Organic Silty Clay (OL) layer is present in two MT tests. Thickness varies between 0 to 1 m and the MT blow counts are reported in the range of 16 – 23 per 300mm penetration.

Layer V – Medium Plasticity Clay with Inorganic Silt (CL) layer is present in all three MT tests and identified from USC system. Thickness varies between 1.6 to 2.1 m and the MT blow counts are reported in the range of 32 – 78 per 300mm penetration.

Layer VI – Poorly Graded Sand (SP) layer is present in all three MT tests. Thickness varies between 1.8 to 3 m and the MT blow counts are reported in the range of 72 – 146 per 300mm penetration.

The number of blows, M (Blows/300 mm), was obtained from the MT test. The N_{SPT} was determined using the empirical correlation between M and N_{SPT} provided by Fakher et al. (2005). The soil strength properties, determined using correlations by Bowles (1997) and Burt Look (2007), are summarized in Table 3.4.

Table 3.4 Geotechnical parameters of the soil layers using appropriate correlations

Type of soil	Layer	M / (Blows/300 mm)	Empirical correlation M Vs N_{SPT} by Fakher et al.(2005)	Unit weight (kN/m^3)		Shear Strength Parameters Used for the Study Given by Bowles (1997) and Burt Look (2007)		
			N_{SPT}	γ_{dry}	γ_{sat}	Cu (kPa)	ϕ' (deg.)	C' (kPa)
Aggregate Base Course	I	-	-	20	-	-	34	-
Inorganic Silt with Very Fine Sand (ML)	II	19-85	2-9	15	18	-	29	2
Silty Clay with Fine Sand (CL+ML)	III	6-32	1-4		17	-	28	2
Low Plasticity Organic Silty Clay (OL)	IV	16-23	2-3		14	20	20	-
Medium Plasticity Clay with Inorganic Silt (CL)	V	32-78	4-9		18	20	26	-
Poorly Graded Sand (SP)	VI	72-146	8-16	-	19	-	32	-

3.3 Assessment of stability

The factor of safety (FOS) of the bank slopes under varying water table conditions was thoroughly evaluated through Limit Equilibrium approach using SLOPE/W software at all identified problematic locations. The analysis considered both circular and non-circular failure surfaces. Stability analyses were conducted using the Morgenstern-Price method, ensuring a comprehensive assessment. This rigorous analysis was aimed to accurately identify the root cause of the slope stability issues at each specific location.

At location 1

The left bank of the Kelani River along the low-level road (AB010) at the 26th-kilometer milestone has a slope with a height of 6 meter and an inclination of 1:0.4 (Vertical: Horizontal). This slope consists of four different soil layers and a rock layer, each with distinct shear strength parameters. A surcharge load of 10 kN/m² was applied on the embankment as specified in BS 5400 and the Bridge Design Manual used by the Road Development Authority for all design purposes. The stability analysis conducted using SLOPE/W is presented in Figure 3.6, and the summary of results is shown in Table 3.5. The original slope profile, with varying water levels from low tide to high tide, was analyzed to determine the minimum factor of safety and the critical slip surface based on different scenarios.

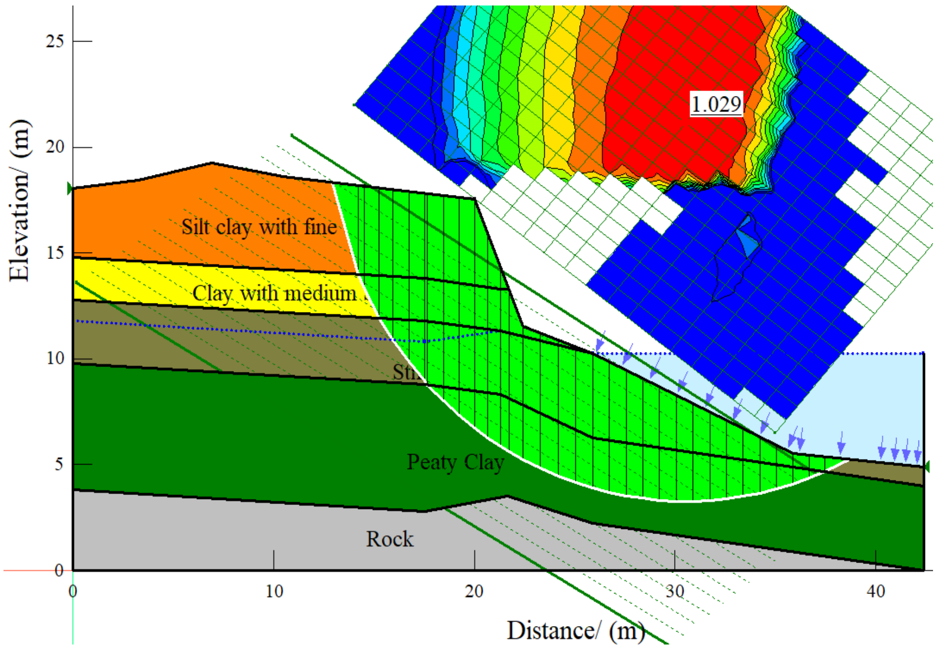

a) During the Normal River water level

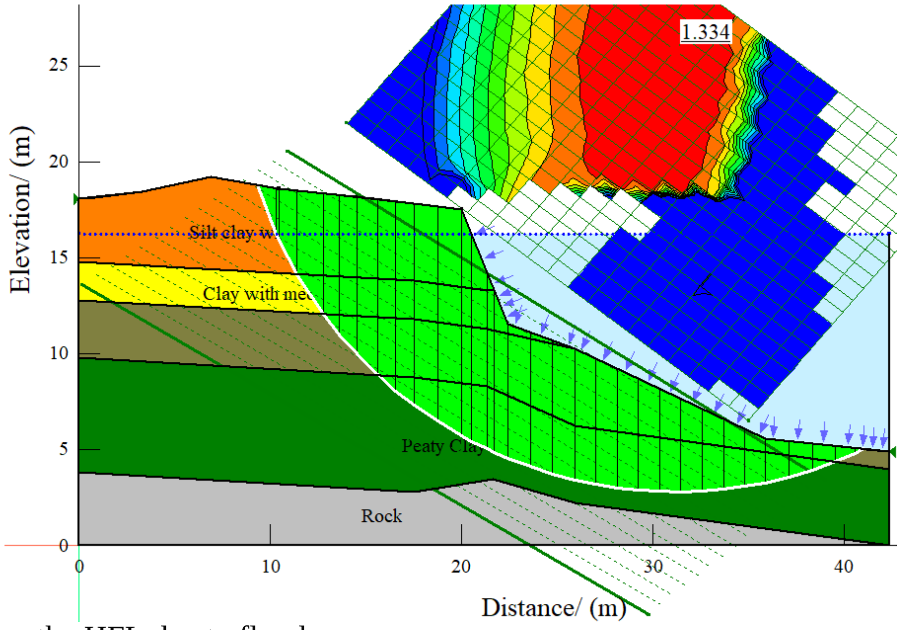

b) During the HFL due to flood

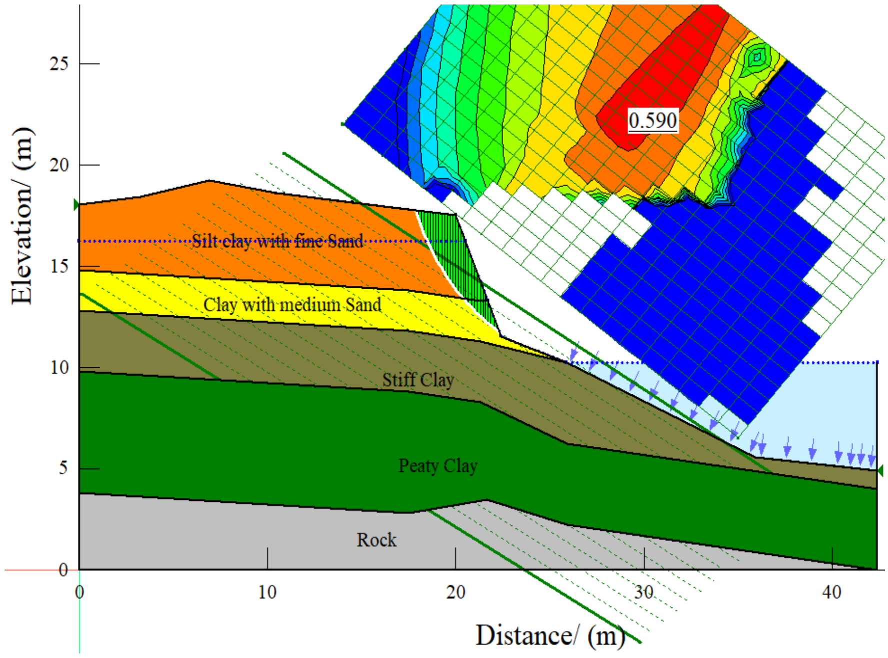

c) During the Sudden Drawdown of the water level in the River after the flood recedes

Figure 3.6 Assessment of Stability for Existing Slope Profile Under Varying Water Table Conditions

Table 3.5 Summary of Global stability for deep-seated failure of Existing Slope

Methods	Types of Failure	Minimum F.O.S.		
		Normal G.W. T	High Flood level	Sudden drawdown
Grid and Radius	Circular	1.029	1.334	0.590

Based on the analysis results at location 1 indicate that the existing slope is marginally stable, with a factor of safety (FOS) of 1.029, during low tide periods. During high flood levels, the slope is stable. However, there is a significant risk of collapse, with a factor of safety dropping to 0.59, due to the sudden drawdown of the water level in the river which would occur within a 6-hour period after the flood recedes. This instability is caused by the rapid discharge of river water flow. Additionally, erosion resulting from floods, toe scour, and mass wasting of trees has been observed, further exacerbating the slope stability concerns. However, the slope has not collapsed due to the matric suction that prevails. In this study, the soil was considered saturated in the analysis, and any matric suction present was ignored.

At location 2

The right side of the Halwathura Phalakotasa stream bank along the Ingiriya-Halwathura-Ekgaloya road (B068) at the 4th-kilometer milepost has a slope with a around height of 1.5 meter and an inclination of 1:1 (Vertical: Horizontal). This slope consists of four different soil layers, each with distinct shear strength parameters. A surcharge load of 10 kN/m² was applied to the embankment as specified in BS 5400 and the Bridge Design Manual used by the Road Development Authority for all design purposes. The stability analysis conducted using SLOPE/W is presented in Figure 3.7, and the summary of results is shown in Table 3.6. The original slope profile, with varying water levels from low tide to high tide, was analyzed to determine the minimum factor of safety for global stability concerning deep-seated failure.

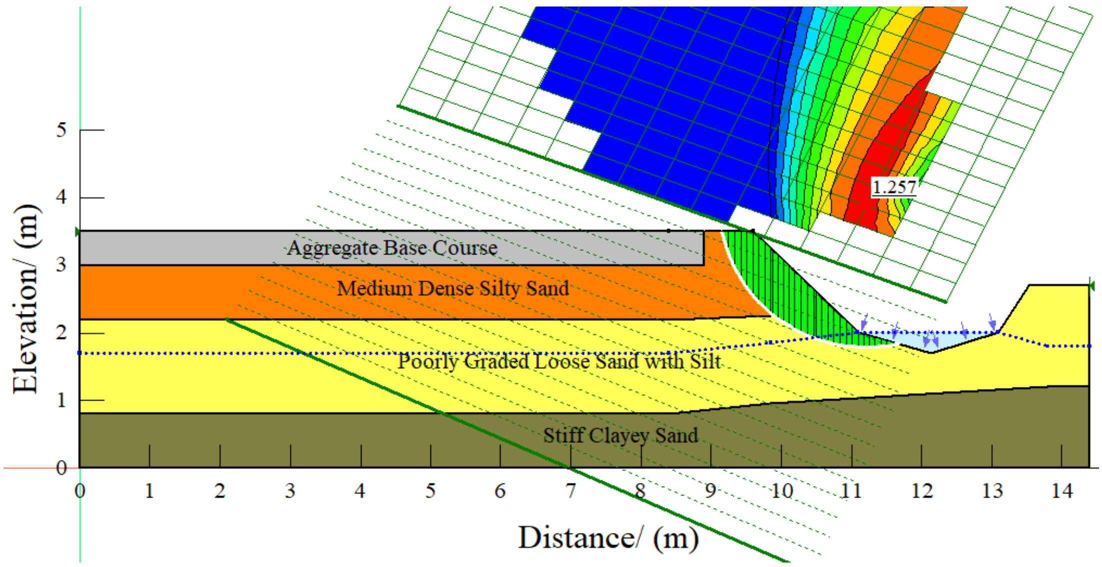

a) During the Normal Stream water level

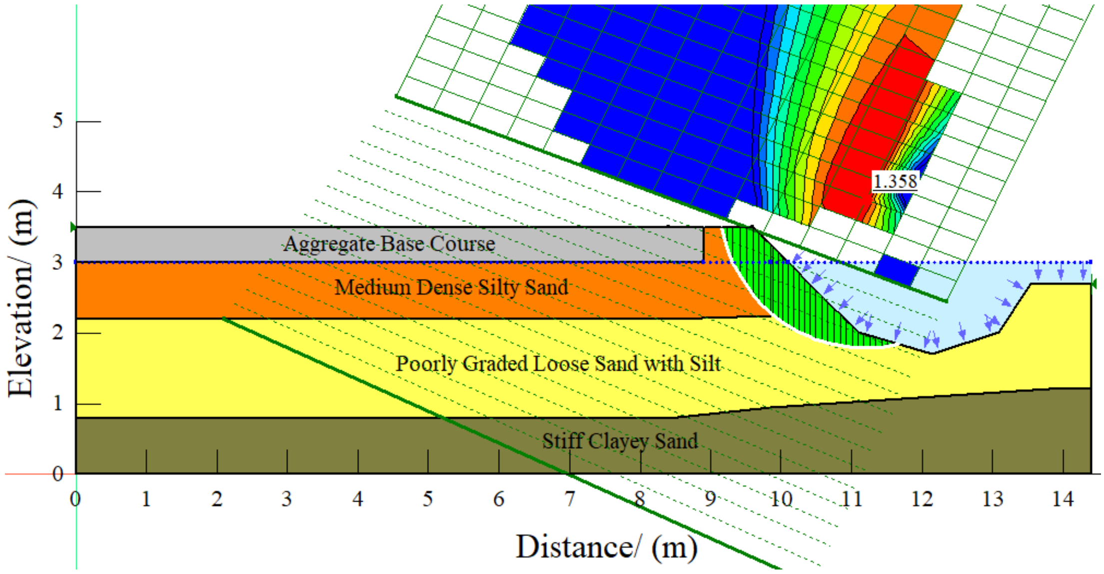

b) During the HFL due to flood

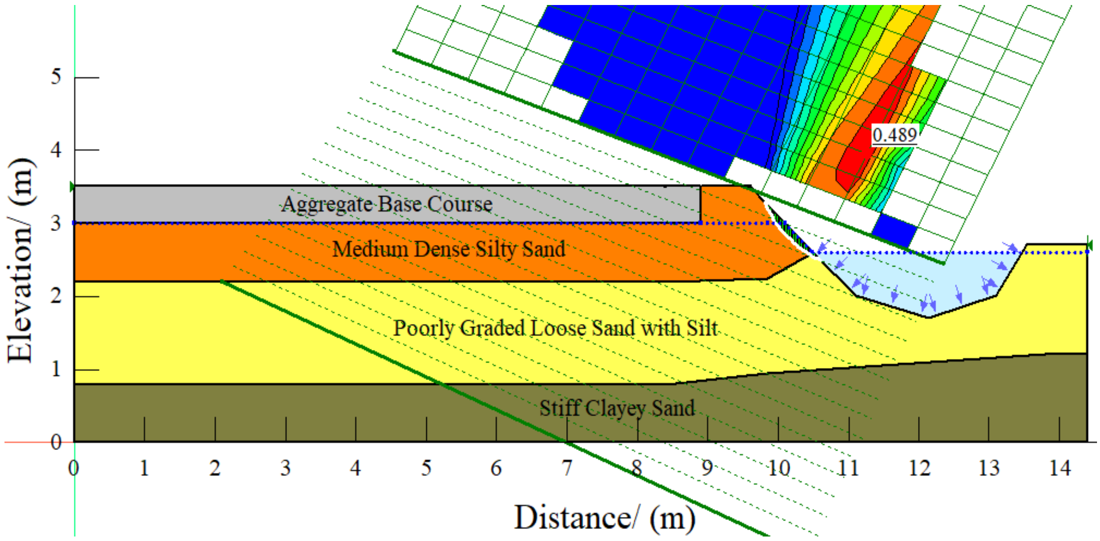

c) During the Sudden Drawdown of the water level in the Stream after the flood recedes

Figure 3.7 Assessment of Stability for Existing Slope Profile Under Varying Water Table Conditions

Table 3.6 Summary of Global stability for deep-seated failure of Existing Slope

Methods	Types of Failure	Minimum F.O.S.		
		Normal G.W. T	High Flood level	Sudden drawdown
Grid and Radius	Circular	1.257	1.358	0.489

According to the analysis results at location 2, it is evident that the current slope remains marginally stable, with a factor of safety (FOS) of 1.257, during low tide and is also secure during high flood levels. However, the slope is highly susceptible to collapse, with a factor of safety dropping to 0.489, when there is a sudden drawdown of water levels in the stream which would occur within a 2-hour period after the flood recedes. This instability is worsened during the heavily rainy season, as the groundwater level in the road section rises to the high flood level for a short period. The presence of adjacent paddy fields on both sides of the road further contributes to the instability by influencing the water table and increasing the probability of rapid changes in groundwater conditions.

At location 3

The right side of the Halkotiyawatta stream bank on Seelarathana Mawatha at the 1st-kilometer milepost has a slope with an approximate height of 2 meter and an inclination of 1:1.24 (Vertical: Horizontal). This slope comprises five different soil layers, each with distinct shear strength parameters. A surcharge load of 10 kN/m² was applied to the embankment, as specified in BS 5400 and the Bridge Design Manual used by the Road Development Authority for all design purposes. The stability analysis, conducted using SLOPE/W, is presented in Figure 3.8, with a summary of the results shown in Table 3.7. The original slope profile, with varying water levels from low tide to high tide, was analyzed to determine the minimum factor of safety for global stability concerning deep-seated failure.

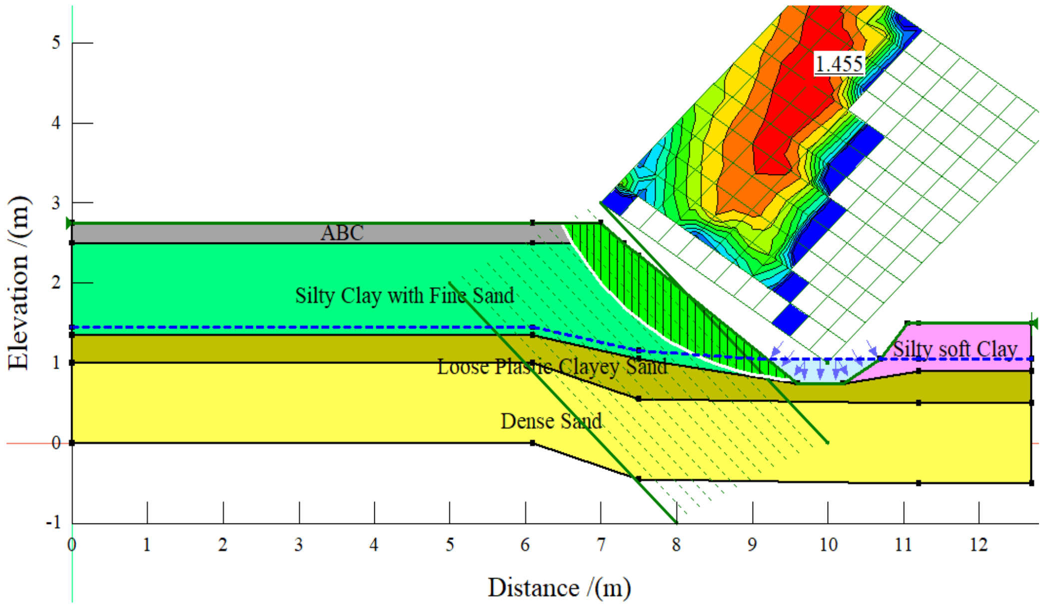

a) During Normal Ground water level

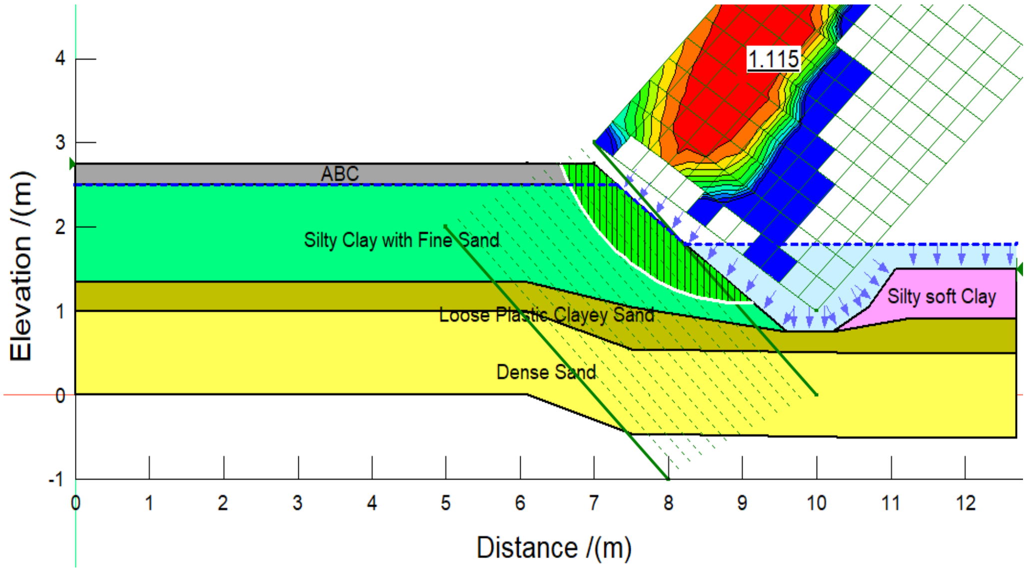

b) During High Flood Levels

Figure 3.8 Assessment of Stability for Existing Slope Profile Under Varying Water Table Conditions

Table 3.7 Summary of Global stability for deep-seated failure of Existing Slope

Methods	Types of Failure	Minimum F.O.S.	
		Normal G.W.T	High Flood level
Grid and Radius	Circular	1.455	1.115

According to the analysis results at location 3, it is evident that the existing slope is stable during low tide periods, with a factor of safety (FOS) of 1.455. However, the slope becomes only marginally stable during high flood levels, with a reduced FOS of 1.115. This instability is primarily attributed to the closure and subsequent filling of the existing drain on the hillside with soil. During the rainy season, rainwater flows across the road to the opposite side, with the left-hand side (LHS) having a higher elevation than the right-hand side (RHS). This causes a rise in the groundwater table, which could potentially render the slope unstable. The increased groundwater level and the altered drainage patterns exacerbate the risk, highlighting the need for effective drainage solutions to maintain slope stability.

At location 4

The right side of the Diyawanna Lake bank on Denzil Kobbekaduwa Mawatha at the 1st-kilometer milepost features a slope with an approximate height of 3 meter and an inclination of 1:0.96 (Vertical: Horizontal). This slope comprises six distinct soil layers, each with unique shear strength parameters. A surcharge load of 10 kN/m² was applied to the embankment, as specified in BS 5400 and the Bridge Design Manual utilized by the Road Development Authority for all design purposes. The stability analysis, conducted using SLOPE/W, is presented in Figure 3.9, with a summary of the results shown in Table 3.8. The original slope profile, with varying water levels from low tide to high tide, was analyzed to determine the minimum factor of safety for global stability concerning deep-seated failure.

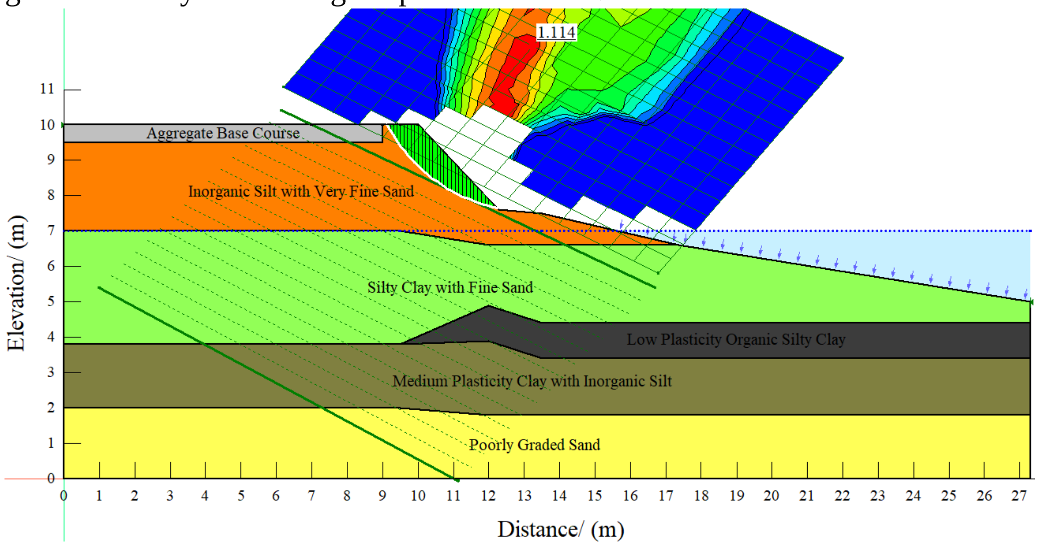

a) During the Normal Lake water level

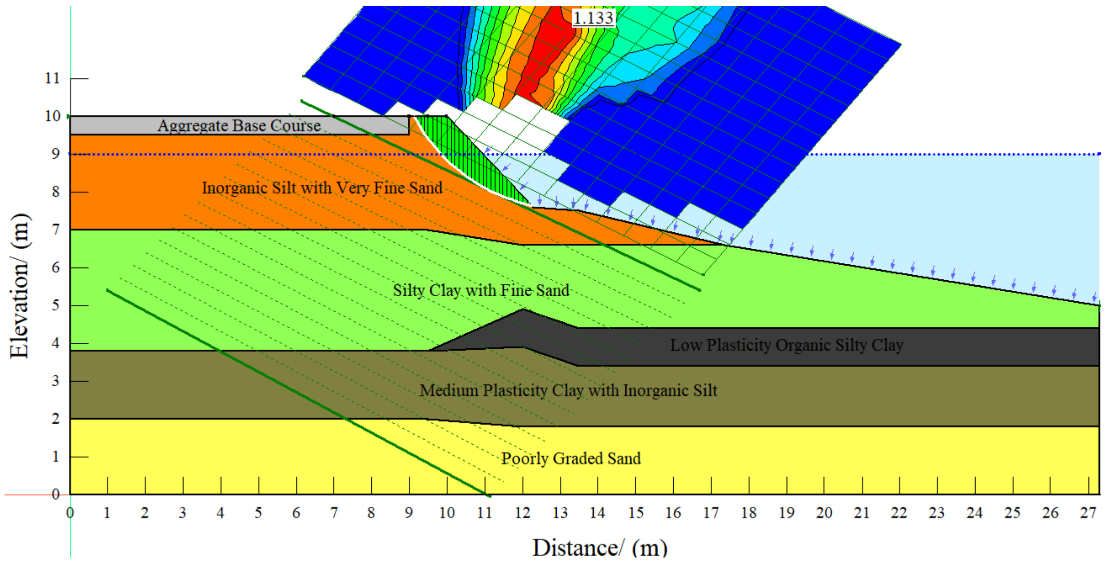

b) During the HFL due to flood

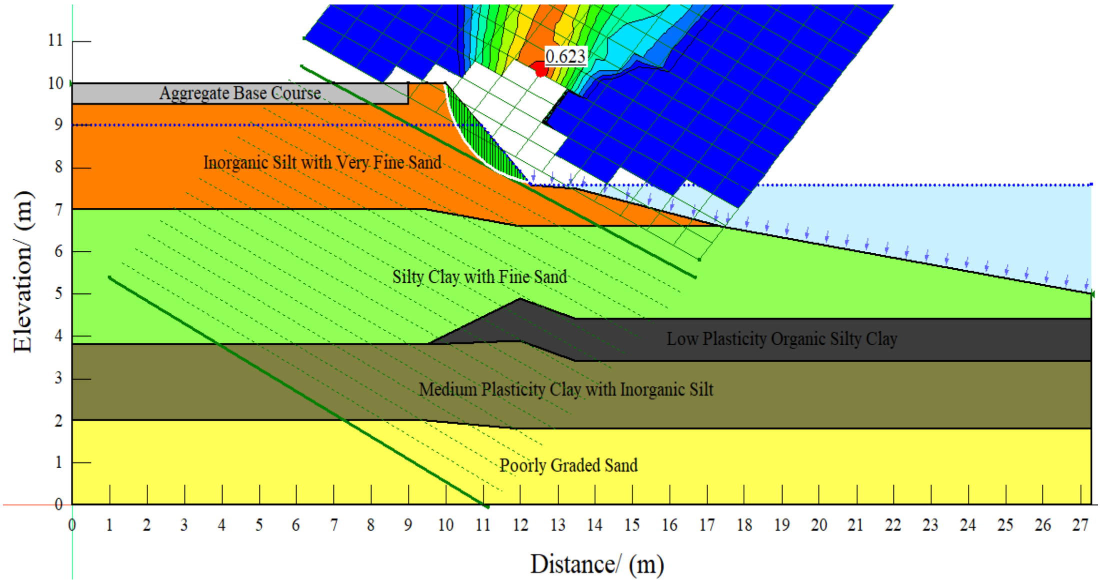

c) During the Sudden Drawdown of the water level in the Lake after the flood recedes

Figure 3.9 Assessment of Stability for Existing Slope Profile Under Varying Water Table Conditions

Table 3.8 Summary of Global stability for deep-seated failure of Existing Slope

Methods	Types of Failure	Minimum F.O.S.		
		Normal G.W.T	High Flood level	Sudden drawdown
Grid and Radius	Circular	1.114	1.133	0.623

Based on the analysis results at location 4, it is evident that the current slope remains marginally stable during both low tide (FOS = 1.114) and high flood levels (FOS = 1.133). But the slope has not collapsed due to the matric suction that prevails. In this study, the soil was considered saturated in the analysis, and any matric suction present was ignored. However, the slope is susceptible to sudden collapse (FOS = 0.623) when there is a rapid drawdown of water levels in the lake which would occur within a day after the flood recedes. This instability is exacerbated by the inadequate bridge opening near the embankment, which delays effective drainage. Consequently, the channel has experienced incision and widening due to hydrological alterations in the watershed. Furthermore, the erosion at the slope toe has occurred due to the high velocity of discharge from Diyawanna Lake.

3.4 Establishment of the most appropriate technique for stabilization and development of a design

3.4.1 Establishment of the most appropriate technique at Location 1

This study assessed the feasibility of two alternate rectification measures to retain the 6m height at location 1;

a) Gabion wall with Boulder packing
b) Anchored Sheet pile wall

For the design, to be conservative, the proposed gabion wall is assumed to have a vertical back that conforms to the geometry outlined in Kerisel and Absi's (1990) charts as specified in BS 8002:1994. The gabion basket is filled with rubble material assumed to have a shear strength friction angle of 45°, a rubble specific gravity of 2.7 at a porosity of 0.4.

The stability analysis, ensured that the resisting moment exceeds the overturning moment by an appropriate safety margin, the resultant force lies within the middle third of the wall's base, and the maximum bearing pressure remains within allowable limits. Additional stability measures were needed for the gabion wall to achieve acceptable sliding safety factors. One alternative is to position the gabion wall with a 6-degree batter towards the retained slope without increasing its cross-section.

Geotextile filter fabric is crucial for gabion gravity retaining walls, as the stone fill's void ratio allows for free drainage of retained soils. The filter fabric, placed between the gabion wall and backfill soil, prevents soil loss during drainage and drawdown. Without it, gabion walls risk losing retained soils and grade elevation. Properly placed and compacted backfill material is vital for long-term performance. Poor compaction can cause structural settlement, lateral wall movement, and insufficient shear strength. Backfill material should be compacted to a minimum of 95% Standard Proctor density in lifts not exceeding 225 millimeters, complying with local standards.

The high SPT N value, ranging between 6 to 16, observed in the Peary Clay layer IV from the borehole, indicates significant shear strength. Generally, Peaty Clays are expected to have lower SPT N values due to their cohesive nature. The SPT N value averaging 15 in clay is relatively high and indicates firm to stiff clay.

This unusual characteristic for clay can be attributed to various factors such as over consolidation, mineral composition, environmental conditions, depth, and testing procedures.

Figure 3.10 and Figure 3.11 show the idealized proposed section of the gabion wall and the diagrams for active earth pressure and other forces acting on the gabion wall for low water level at the back case, considering drained conditions. Similarly, Figure A2.1 and Figure A3.1 show the diagrams for all forces acting on the gabion wall for the high water level at the back and sudden drawdown cases, are given in Appendix A, Section: A.2 and Section: A.3.

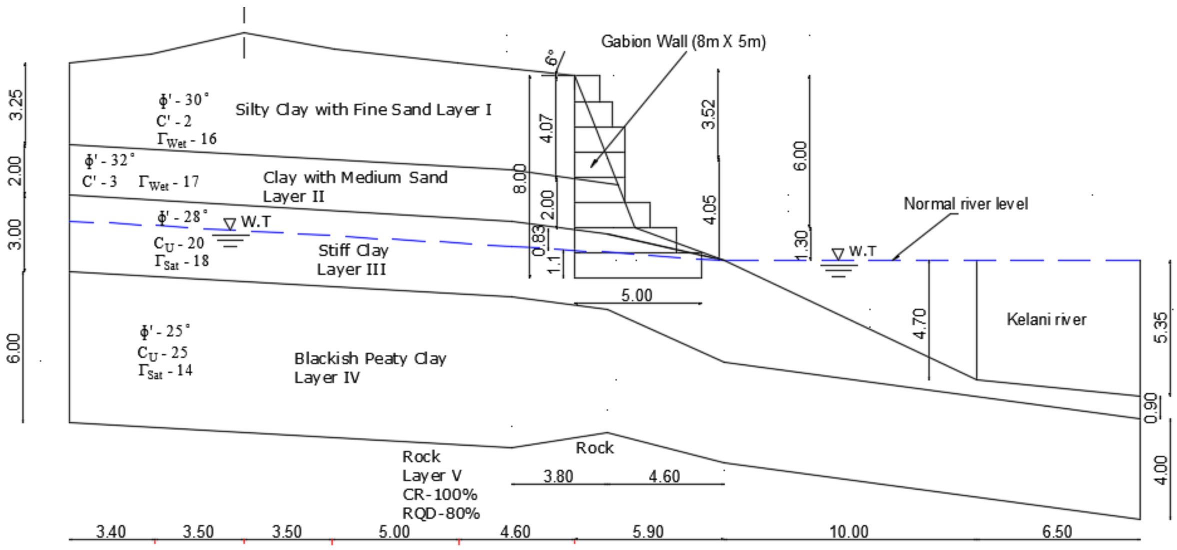

Figure 3.10 Idealized proposed section of the gabion wall

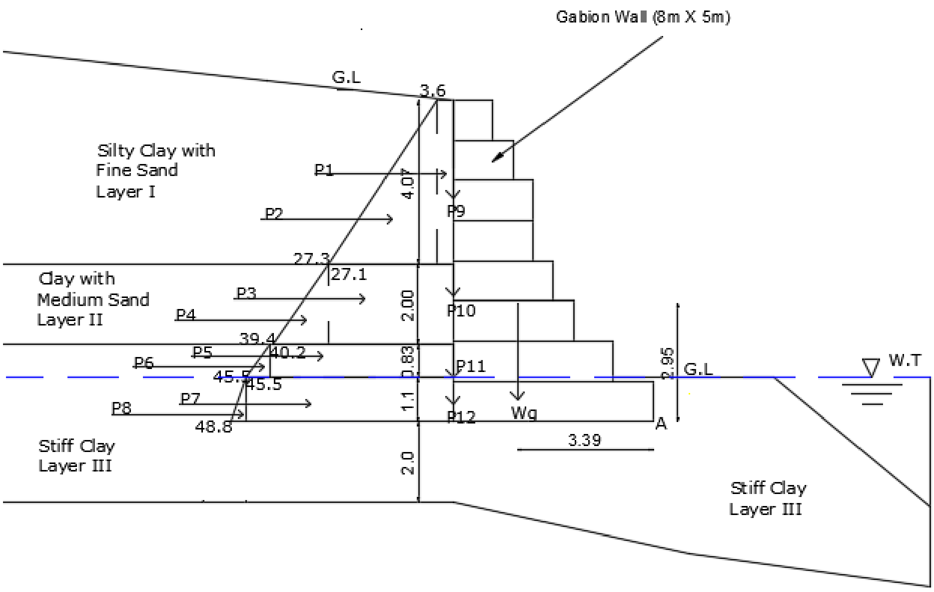

Figure 3.11 Active earth pressure and forces acting on the gabion wall

Weight of the Gabion wall, $W_g = 333.69\ kN/m$

The stability calculations using drained shear strength parameters for different water table conditions, such as low water level at the back, high water level at the back, high groundwater level on the retained side, and low water level in the river as sudden drawdown cases, are given in Appendix A, Section: A.1, Section: A.2 and Section: A.3. The Summary of results for external and internal stability of the Gabion wall under different water table conditions is presented below in Table 3.9.

Table 3.9 Summary of results for external and internal stability of the Gabion wall

Stability criteria	Low water level at the back	High water level at the back	Sudden Drawdown
For External Stability			
Resisting Moment / kNm/m	1,519.79	1,404.06	1,467.36
Disturbing Moment / kNm/m	615.79	471.20	1,020.36
Force causing sliding / kN/m	216.96	152.01	204.51
Sliding Resistance / kN/m	277.5	261.88	261.88
Allowable bearing pressure / kPa	258	258	258
Minimum bearing pressure / kPa	52.66	68.61	-
Maximum bearing pressure / kPa	111.9	86.69	225
For Internal Stability			
Allowable vertical stress / kNm^2	510	510	510
Maximum vertical stress / kNm^2	93.5	80.79	222.6
Allowable shear stress / kNm^2	63.16	60.44	60.44
Average shear stress / kNm^2	43.4	30.4	40.9

Based on the results at Location 1, the selected dimensions of the gabion for the external and internal stability under different water table conditions, such as low water level at the back, high water level at the back, high groundwater level on the retained side, and low water level in the river as sudden drawdown cases, are satisfactory. Additionally, a boulder pack was placed on the riverbed after excavation and a slope was packed after gabion wall construction to enhance structural bearing capacity, protect the Peaty Clay layer from erosion, ensure environmental friendliness, maintain permeability, and promote sustainability. This setup also helps control flow dynamics and increases passive resistance during a sudden drawdown scenario, which is considered the worst-case scenario. At Location 1, the proposed stabilization to protect the Kelani River bank includes an 8m x 5m gabion wall with a boulder packing slope of 1:1.5.

3.4.1.1 Stability calculation for Anchored sheet pile wall in Drained and Undrained conditions

This study explored the use of steel sheet pile walls as an alternative solution. In addressing the specific conditions at location 1, where weak subsoil and bedrock constraints limit embedment depth, sheet piles need to be anchored. With the limited embedment in a relatively weak Peaty Clay layer the sheet piles need to be anchored to the bedrock. The free earth support method is used to analyze the sheet pile wall. A Hot-rolled NS-SP-II U type sheet steel pile was chosen for the application. Tie rods utilizing Pre-stress bar anchors (ASTM A722) are applied at 8.0m intervals, corresponding to every twenty piles, as depicted in Figure 3.12.

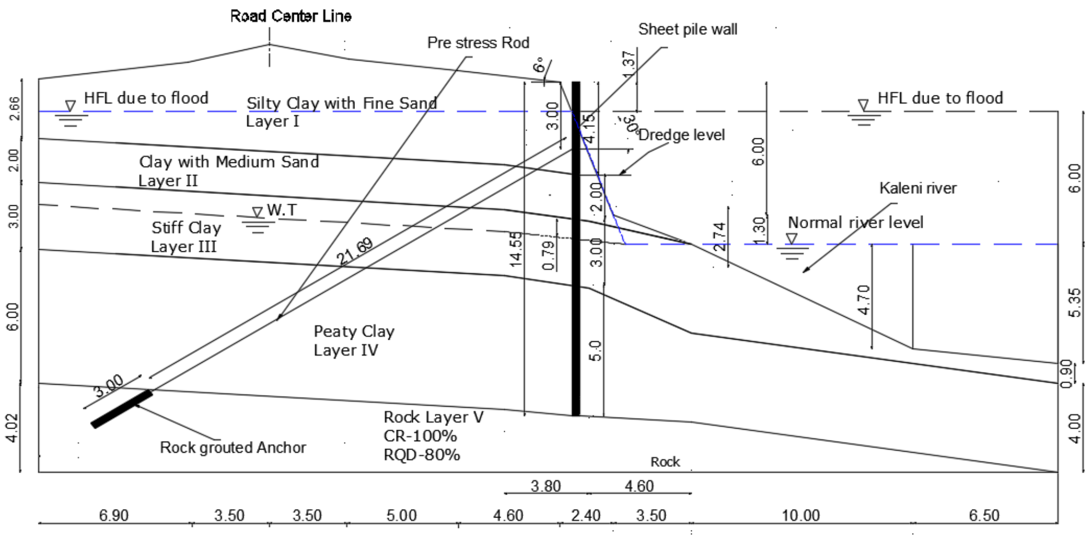

Figure 3.12: Proposed Anchored sheet pile wall

Figure 3.13 shows the diagrams for active and passive earth pressure and other forces acting on the sheet pile wall for low water level at the back case, considering Undrained conditions. Similarly, Figure B2.1 and Figure B3.1 show the diagrams for all forces acting on the sheet pile wall for the high water level at the back and sudden drawdown cases, are given in Appendix B, Section: B.2 and Section: B.3.

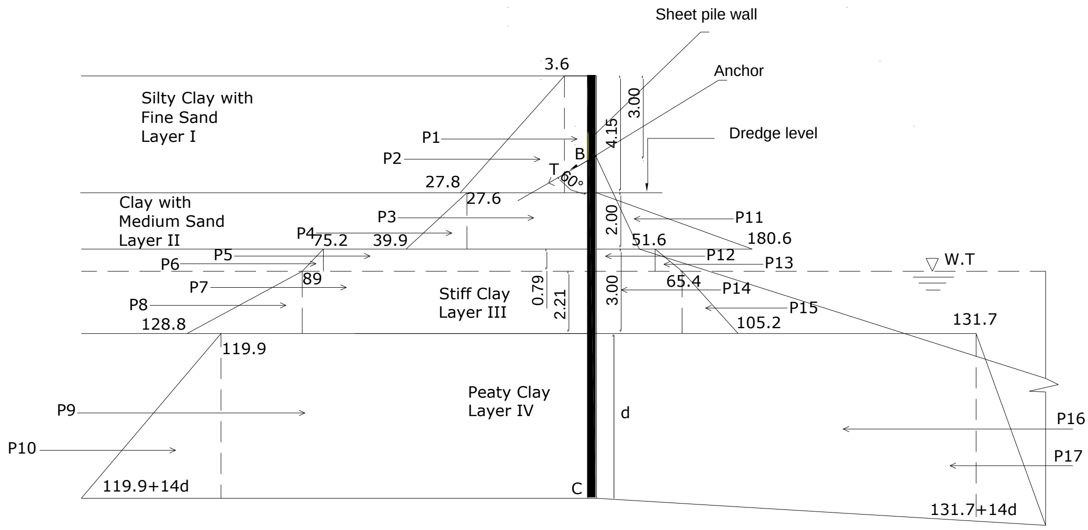

Figure 3.13: Active & passive earth pressures and forces acting on the Sheet pile wall

The stability calculations using drained shear strength parameters for different water table conditions, such as low water level at the back, high water level at the back, high groundwater level on the retained side, and low water level in the river as sudden drawdown cases, are given in Appendix B, Section: B.1, Section: B.2 and Section: B.3. The Summary of analysis results for the sheet pile wall under different water table conditions is presented below in Table 3.10.

Table 3.10 Summary of analysis results for the Sheet pile wall

Structural Parameters and Forces for Sheet Pile Wall Design	Low water level at the back	High water level at the back (drained)	Sudden Drawdown (drained)
Depth of embedment / m	0.25	0.85	1.35
Required length of Sheet pile / m	9.4	10	10.5
Allowable Pre stressing force / kN	341	341	341
Allowable skin friction for rock grout interface / kN	339	339	339
Force on the tie rod / kN	184.8	290.4	328
Allowable shear force on the tie rod / kN/m	308	308	308
Maximum shear force on the tie rod / kN/m	92.4	145.2	164
Allowable BM / kNm/m	155	155	155
Maximum BM / kNm/m	127.6	84.8	136.8
Allowable section module / cm3/m	874	874	874
Required section module / cm3/m	719	478	771

Based on the results at Location 1, the selected structural parameters of the anchored sheet pile wall for stability under different water table conditions, such as low water level at the back, high water level at the back, high groundwater level on the retained side, and low water level in the river as sudden drawdown cases, are satisfactory. At Location 1, an alternative solution to protect the Kelani river bank is a 14.55 m sheet pile wall with tie rods utilizing Pre-stresses bar anchors, applied at 8.0m intervals, corresponding to every twenty piles.

3.4.1.2 Analysis for deep-seated failure at location 1

A large boulder pack covering the gabion wall is essential for robust riverbank protection against erosion. The boulders provide an additional layer of defense, absorbing and dissipating the energy of flowing water, which reduces the direct impact on the gabion wall. This dual-layered approach enhances the overall stability and longevity of the structure. The boulders also prevent undercutting and scouring at the base of the gabion wall, which is crucial during high-flow events. Moreover, the natural appearance of the boulders helps integrate the structure into the surrounding environment, promoting ecological balance and aesthetic appeal.

It is necessary to check for deep-seated failure for the two different alternative rectification proposals. Figure 3.14 illustrates the stabilizing technique applied at Location 1. Global stability was evaluated under various water table conditions using the Morgenstern-Price limit equilibrium approach through Slope/W software. A summary of the results is presented in Figure 3.15 and Table 3.11.

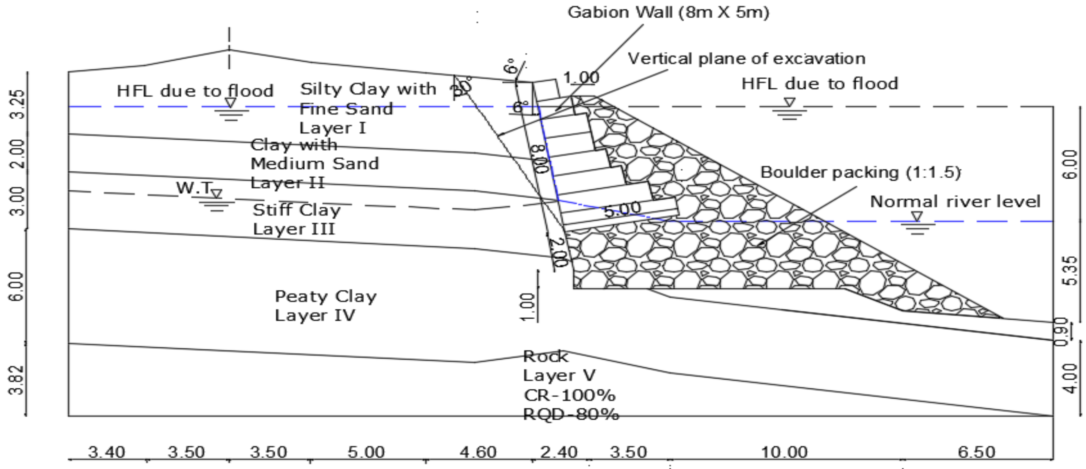

Figure 3.14 Proposed Gabion wall section (8 m X 5 m) at Location 1

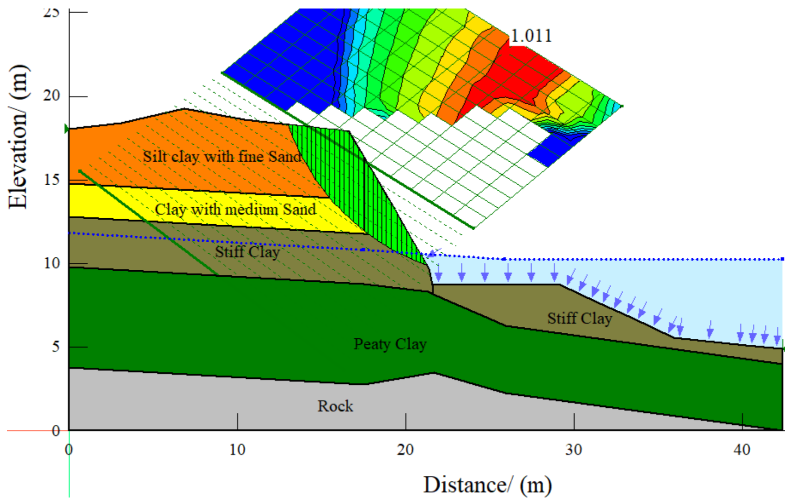

a) After excavation for the construction (during the dry period)

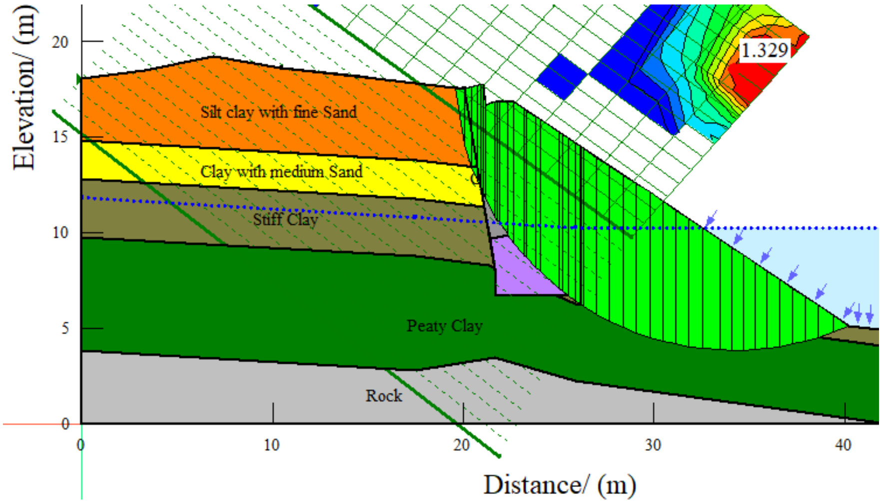

b) Normal River water level

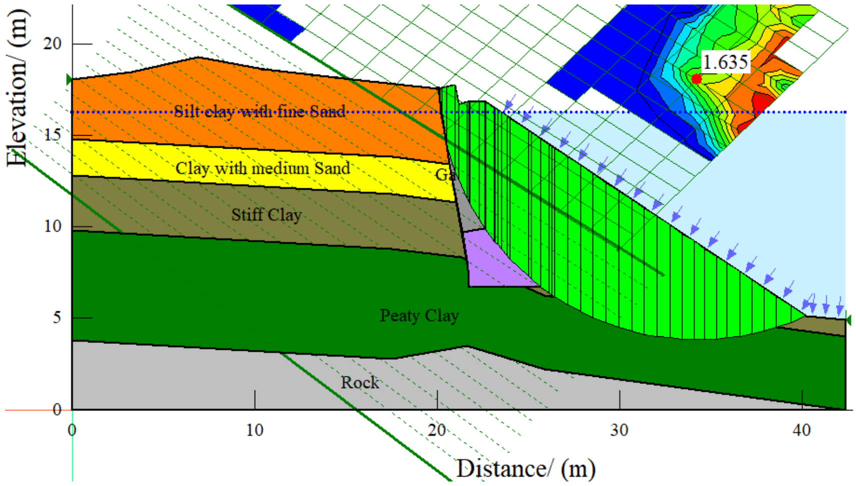

c) High flood level

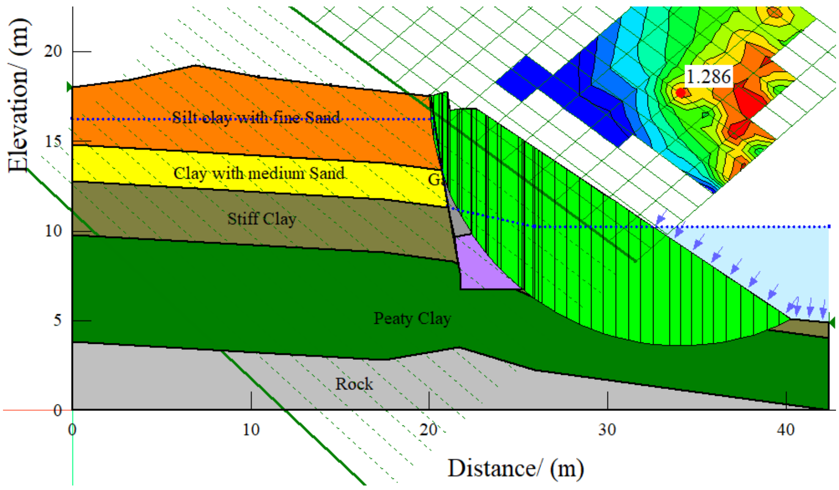

d) Sudden drawdown after Flood has receded

Figure 3.15 Assessment of stability at Location 1 with different water table conditions

Table 3.11: Summary of Analysis Results for Global Stability at Location 1

TYPE OF RECTIFICATION PROPOSAL	WATER TABLE CONDITION	MINIMUM F.O.S.
		EFFECTIVE STRESS ANALYSIS
		GRID & RADIUS
Gabion wall (8 m X 5 m) Retaining structure with Boulder packing	After excavation for the construction (during the dry period)	1.011
	Normal River water level	1.329
	High Flood level (above 6m from RWL)	1.635
	Sudden drawdown after Flood has receded	1.286

The above results show that reasonable FoS values were achieved with the proposed rectification. The FoS when the slope is excavated for the construction of the gabion wall is low. Hence the excavation should be done in small segments during a period of dry weather.

Considering different situations under various water table conditions is essential for protecting large river banks with gabion walls and boulder packing at the base and bank slope. Water table fluctuations can significantly affect stability and performance. High water levels increase hydrostatic pressure, potentially leading to wall failure, while low levels or sudden drawdowns can cause erosion and destabilization. Proper design must account for these variations to ensure long-term effectiveness and structural integrity. Addressing these conditions helps prevent failures, reduces maintenance costs, and ensures the sustained protection of the river bank against erosion and other water-induced damages.

In addressing the specific conditions at location 1, where weak subsoil and bedrock constraints limit embedment depth, sheet piles need to be anchored. With the limited embedment in a relatively weak Peaty Clay layer the sheet piles need to be anchored to the bedrock. A Hot-rolled NS-SP-II U type sheet steel pile was chosen for the application. Tie rods utilizing Pre-stress bar anchors (ASTM A722) are applied at 8.0m intervals, corresponding to every twenty piles, as depicted in Figure 3.16.

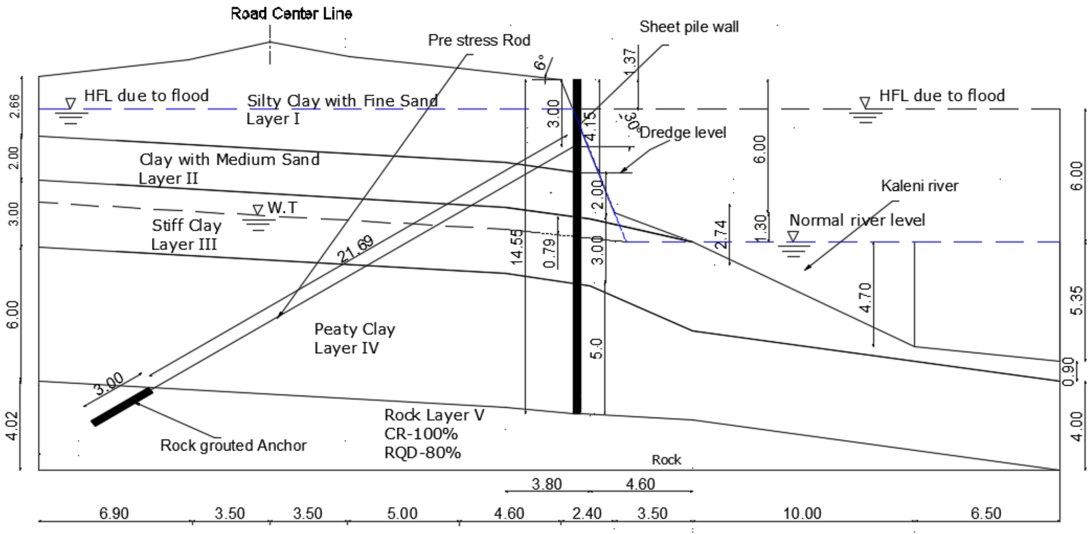

Figure 3.16 Proposed Anchored sheet pile wall

The global stability analysis was conducted under the worst-case scenario of sudden drawdown conditions, as depicted in Figure 3.17. Analysis results indicate that the sheet pile wall without lateral support will not withstand the conditions adequately (FOS = 0.867). With the provision of lateral support, the sheet pile wall was marginally stable (FOS = 1.005) in the worst-case scenario. Hence this solution was not implemented.

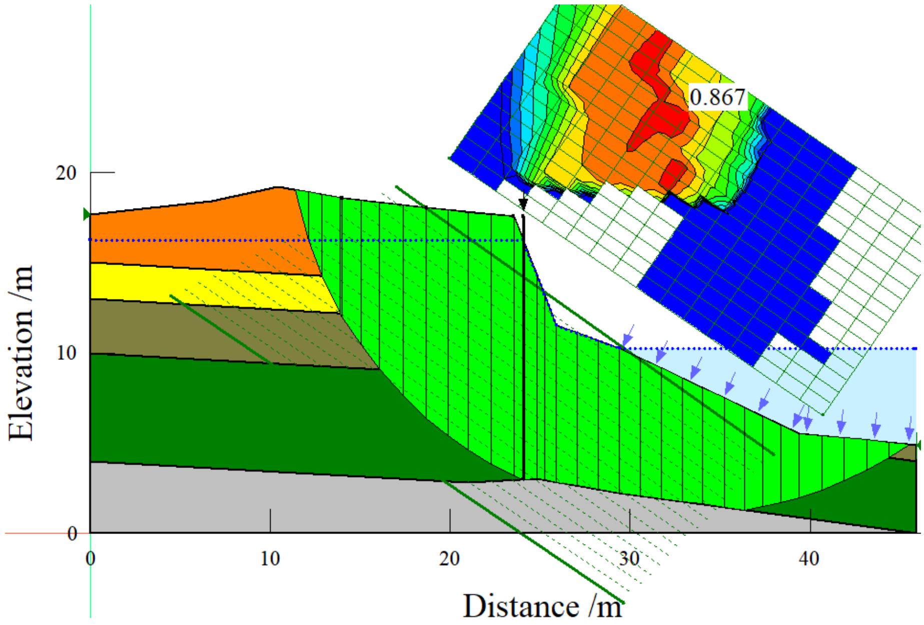

a) Sheet pile wall without lateral support

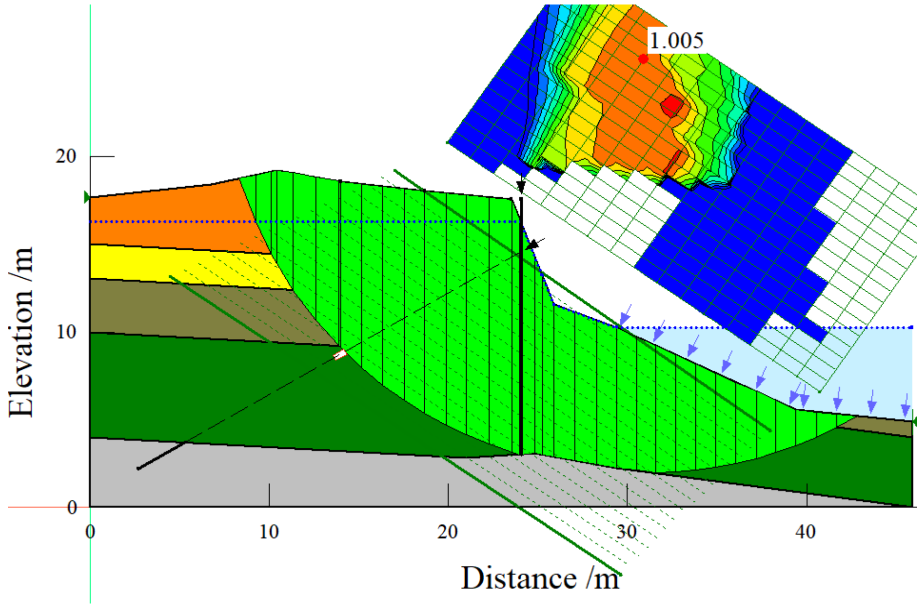

b) Sheet pile wall with the provision of lateral support

Figure 3.17 Assessment of Stability for sheet pile wall (without and with the provision of lateral support) with sudden drawdown after the flood has receded

3.4.2 Establishment of the most appropriate technique at location 2

At the 2nd location, two alternate rectification measures were considered to protect the 1.5m height. The alternative solutions are;

a) Vegetated live bamboo crib wall with Gabion at the toe (Bio-engineering wall)

b) Traditional Gabion wall

The Eco-engineering wall represented in Figure 3.18, comprises a Gabion wall at the base with a height of 1.5m, followed by a Bamboo Crib Wall with a height of 0.7m. The Bamboo Crib Wall incorporates horizontally placed live stakes spaced at 200mm intervals (utilizing Erythrina subumbrans) and is filled with a combination of stone and excavated soil.

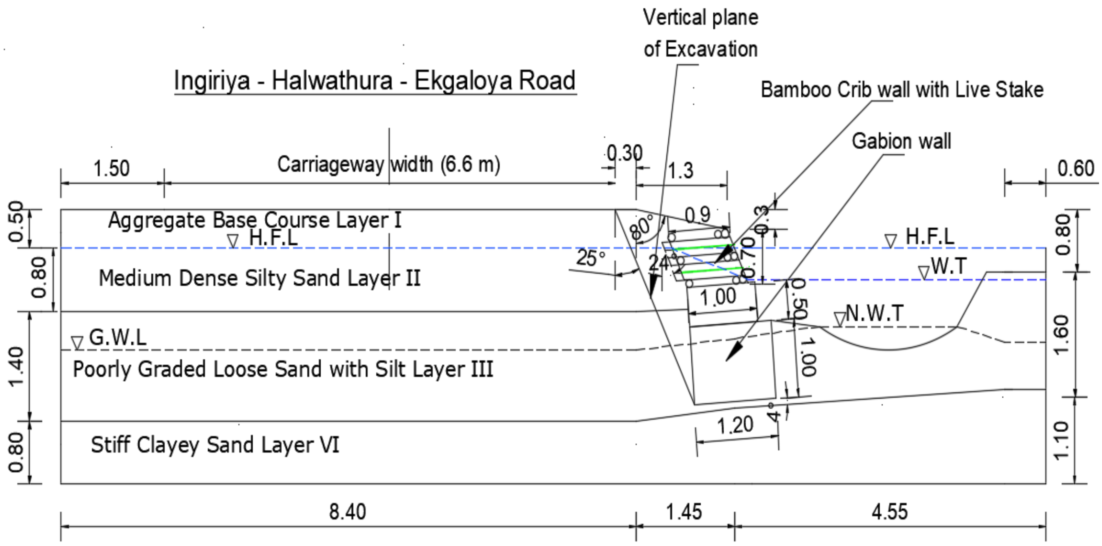

Figure 3.18: Proposed bioengineered retaining wall with Gabion at the toe

3.4.2.1 Stability calculation for Bamboo Crib wall in Drained conditions

A crib wall with a height of 0.7 m and a length of 7 m, made of bamboo elements, is analyzed here. It has an average layer thickness of 0.2 m and a uniformly distributed surcharge of 10 kN/m². Due to the small diameter of the bamboo (Ø = 100 mm), bundles of 3 bamboos are typically used as either header or stretcher elements in the bamboo crib wall. In this design, bundles of 3 bamboos are assumed for the stretcher bamboo crib wall. Figures 3.19 shows the proposed actual section of the bamboo crib wall.

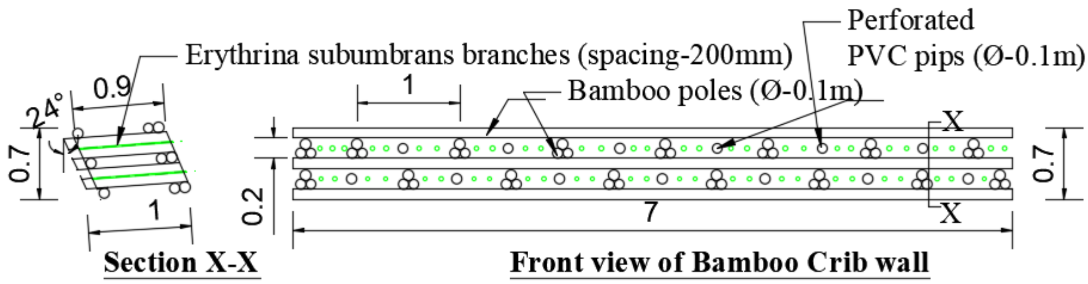

Figure 3.19: Proposed actual section of Bamboo Crib wall

The stability calculations using drained shear strength parameters for different water table conditions, such as low water level at the back, high water level at the back, high groundwater level on the retained side, and low water level in the stream as sudden drawdown cases, are given in Appendix D, Section: D.1, Section: D.2 and Section: D.3. The Summary of results for external stability of the Bamboo crib wall under different water table conditions is presented below in Table 3.12.

Table 3.12 Summary of results for external stability of the Bamboo crib wall

Structural Parameters	Low water level at the back	High water level at the back	Sudden Drawdown
Resisting Moment / kNm	1.741	1.741	1.741
Disturbing Moment / kNm	1.027	0.48	0.79
Force causing sliding / kN/m	2.6	1.2	2
Sliding Resistance / kN/m	7.34	7.34	7.34
Allowable bearing pressure / kPa	150	150	150
Minimum bearing pressure / kPa	11.1	1.57	4.2
Maximum bearing pressure / kPa	13.1	22.6	20
Maximum bearing pressure due to displaced horizontal joints / kPa	36	36	36

Based on the results at Location 2, the selected dimensions of the Bamboo crib wall for the external stability under different water table conditions, such as low water level at the back, high water level at the back, high groundwater level on the retained side, and low water level in the river as sudden drawdown cases, are satisfactory. In addition, the base layer of the crib should be secured against sliding by using steel pegs (ϕ-16 mm) that are 0.8 m long, spaced 1.5 m apart, and inserted into the top of the gabion wall (0.6 m).

3.4.2.2 Stability calculation for Traditional Gabion wall in Drained conditions

This study explored the use of gabion wall as an alternative solution at location 2. The stability analysis design was conducted by the Bridge Design Division of the RDA. A gabion wall with dimensions 2 m x 1.2 m is assumed to have a vertical back and conforms to the geometry outlined in Kerisel and Absi's (1990) charts, in BS 8002:1994. The gabion basket is filled with rubble material assumed to have a shear strength friction angle of 45°, a rubble specific gravity of 2.7 at a porosity of 0.4. During the Gabion construction it should be spread and compacted by Aggregate Base Course thickness of 300mm below the base of gabion.

3.4.2.3 Analysis for deep-seated failure at location 2

It is necessary to check against deep seated failure for the two alternate rectification measures. Global stability was evaluated for Both rectification measures under various water table conditions using the Equilibrium Approach through Slope/W software. The geotechnical model and a summary of the results corresponding to the two stabilization techniques are presented in Figure 3.20, Figure 3.21, and Table 3.13.

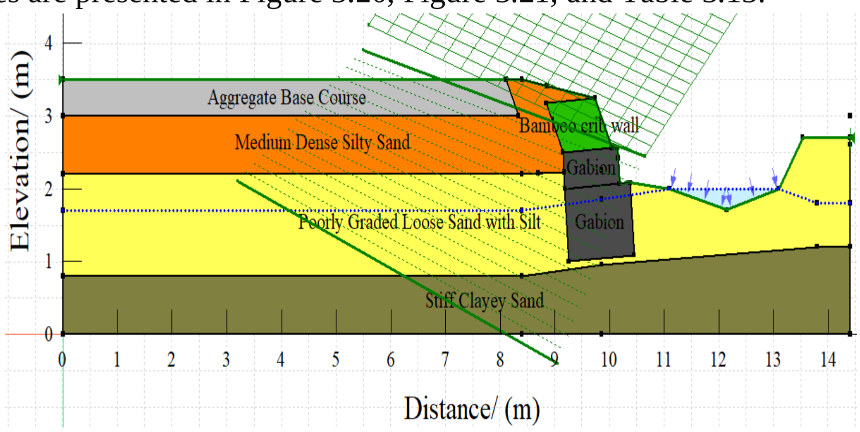

a) Bamboo crib wall with Gabion

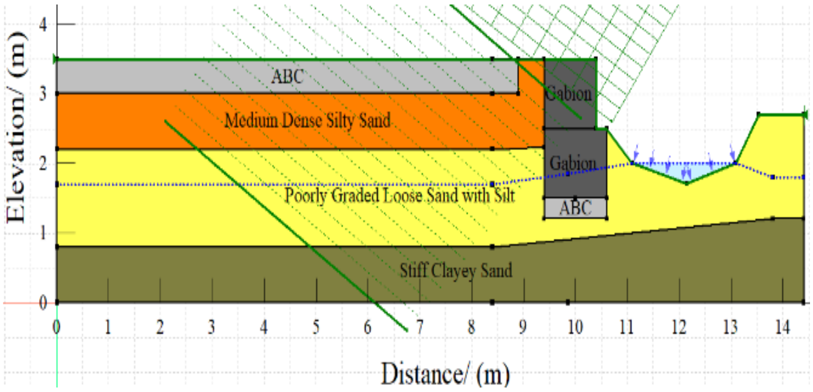

b) Traditional Gabion wall

Figure 3.20 Models of Bioengineered retaining wall and Gabion wall

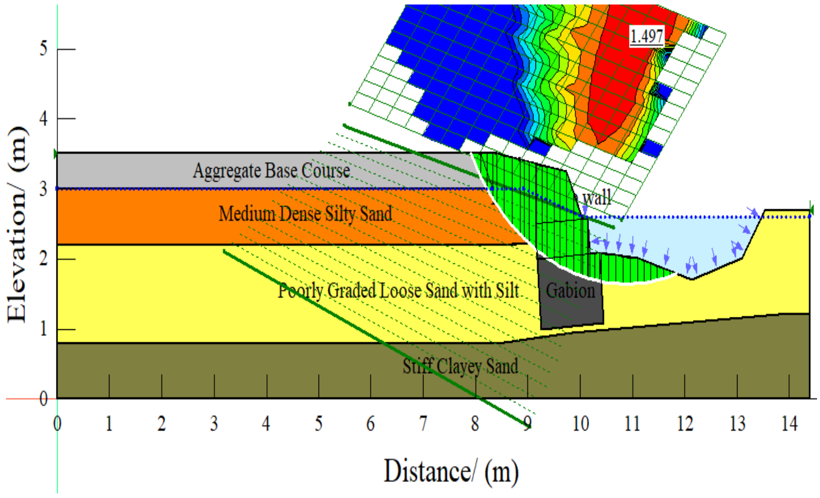

a) Sudden drawdown case for Bamboo crib wall

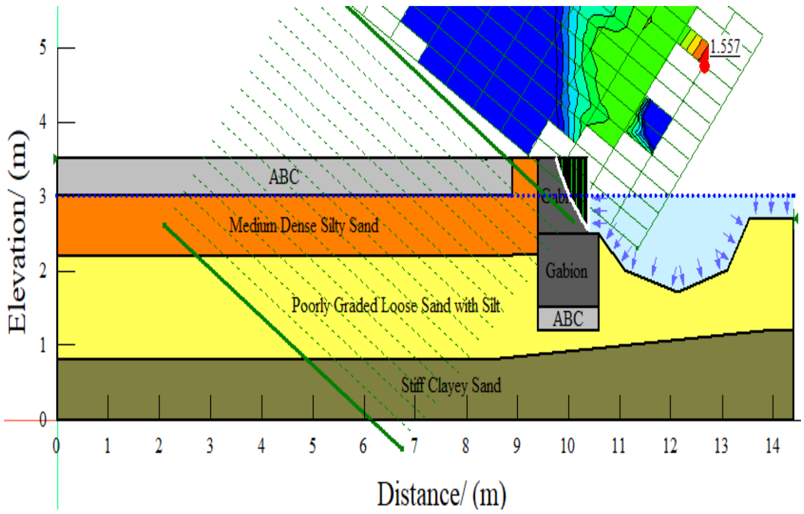

b) HFL case for Gabion wall

Figure 3.21 Assessment of Stability for Bamboo crib wall and Gabion wall

Table 3.13. Summary of analysis results for Global Stability at Location 2

TYPE OF RECTIFICATION PROPOSAL	WATER TABLE CONDITION	MINIMUM F.O.S. (Grid & Radius)
		DRAINED CONDITION
Bioengineered retaining wall # I (Gabion wall at the base, overlain by Bamboo Crib Wall with horizontally placed live stakes)	After excavation for construction during the Dry period	1.049
	Normal stream water level	1.505
	High flood level (HFL)	1.616
	Sudden drawdown after Flood has receded	1.497
Traditional Gabion wall with compacted Aggregate Base Course layer underneath # II	After excavation for construction during the Dry period	1.007
	Normal stream water level	1.393
	High flood level (HFL)	1.537
	Sudden drawdown after Flood has receded	1.481

The above results show that the calculated Factor of Safety (FOS) satisfies the design criteria (i.e., FOS = 1.5). The photo of the Bioengineered wall the selected option, immediately after construction is shown in Figure 3.22.

Figure 3.22 Photographs taken at Location 2 on 21.03.2024 after the stabilization technique

3.4.3 Establishment of the most appropriate technique at location 3

At the 3rd location, two alternate rectification measures were considered to protect the 2 m height. The alternative solutions are;

I. Vegetated flapped soil bag with a Gabion at the toe
II. Vegetated Gabion wall with Rubble packing at the toe

Live stakes, in conjunction with flapped soil bags, have been effectively utilized in Thailand to enhance soil retention, as studied by Jotisankasa (2019). He reported satisfactory survival rates for live stakes when horizontally positioned between the soil bags, demonstrating the beneficial effects of this method over time. His study investigates the performance of flapped soil bags with gabion toe walls used to stabilize a 5 m high stream bank with a 45° gradient.

Modified gabions with live staking and container plants were utilized in Manchester, New Hampshire, as studied by Brunet (2005). These structures are designed to resist erosion from the river and were used to stabilize a 2m high river bank with a 45° gradient. Stability analysis was conducted using the characteristics of the modified gabions with incorporated vegetation, both at the initial stage and after full establishment, employing standard engineering methods for slope stability and threshold resistance.

In this study, two similar types of eco-engineering walls proposed for the location are illustrated in Fig. 3.23 and Fig. 3.24.

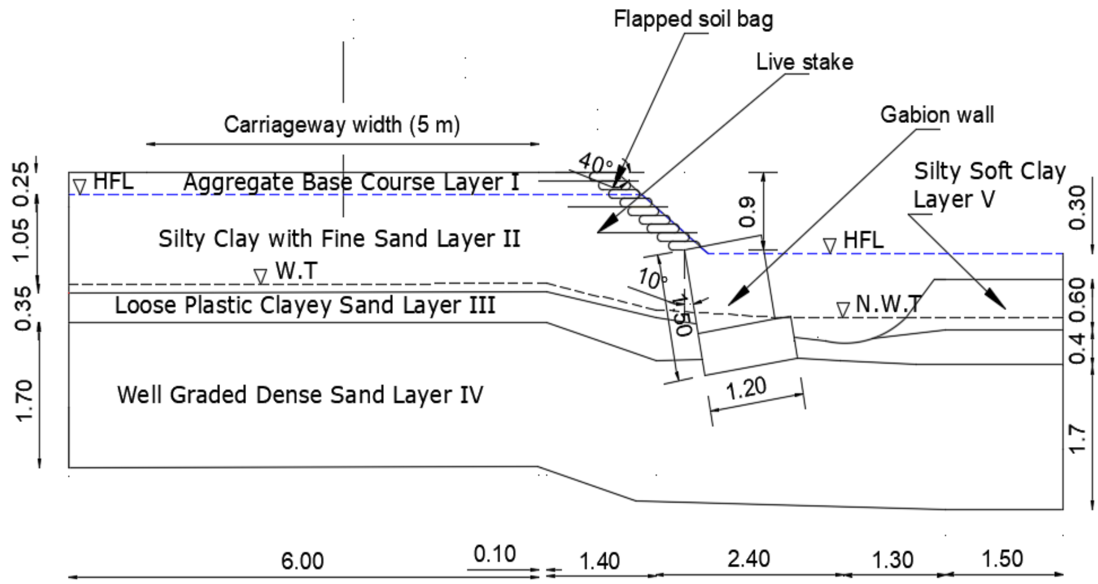

Figure 3.23 Proposed Gabion wall, overlain by flapped soil bags with nailed live stakes (1 m long and 20 cm in diameter) at a spacing of 0.5m

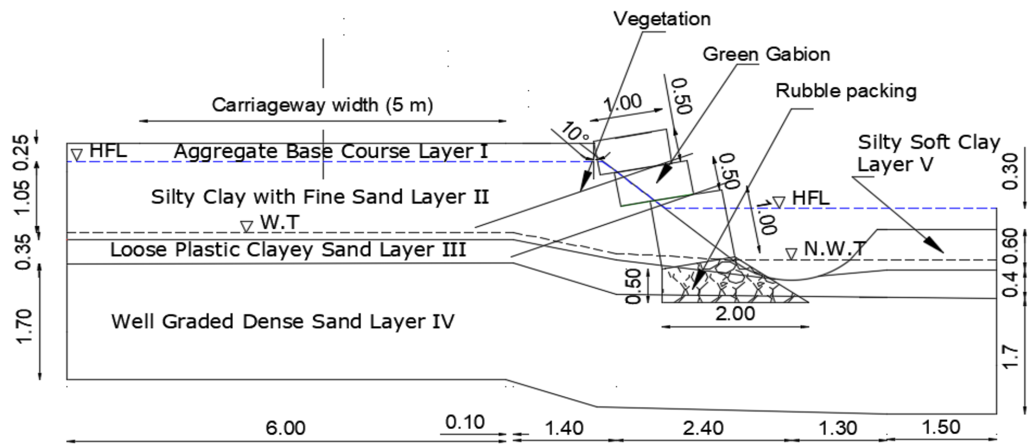

Figure 3.24 Proposed Vegetated Gabion wall (Gunny bags filled with pebble) with Rubble (Willow cuttings with a spacing of 0.3m & a length of 2m

3.4.3.1 Analysis for deep-seated failure at location 3

The geotechnical model and a summary of the results corresponding to the two stabilization techniques are presented in Fig. 3.25, Fig. 3.26, and Table 3.14.

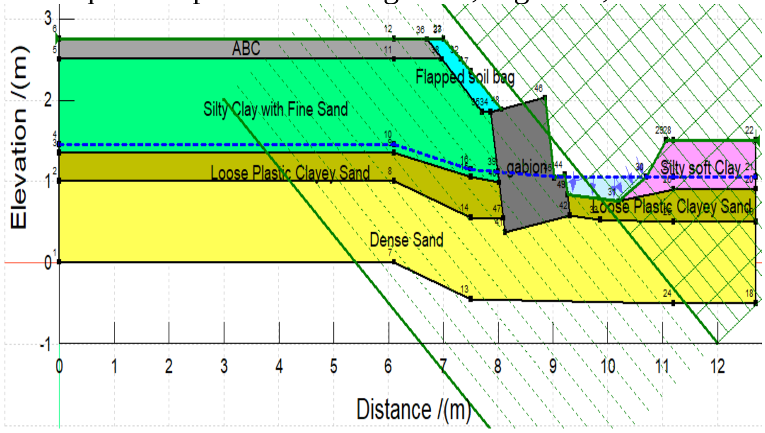

a) Vegetated flapped soil bag with a Gabion

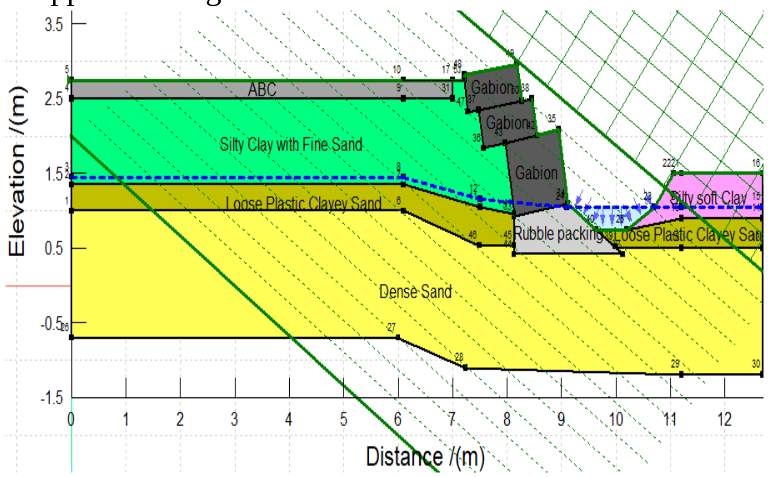

b) Vegetated Gabion wall with Rubble packing

Figure 3.25 Models of Vegetated flapped soil-bag with Gabion and Vegetated Gabion

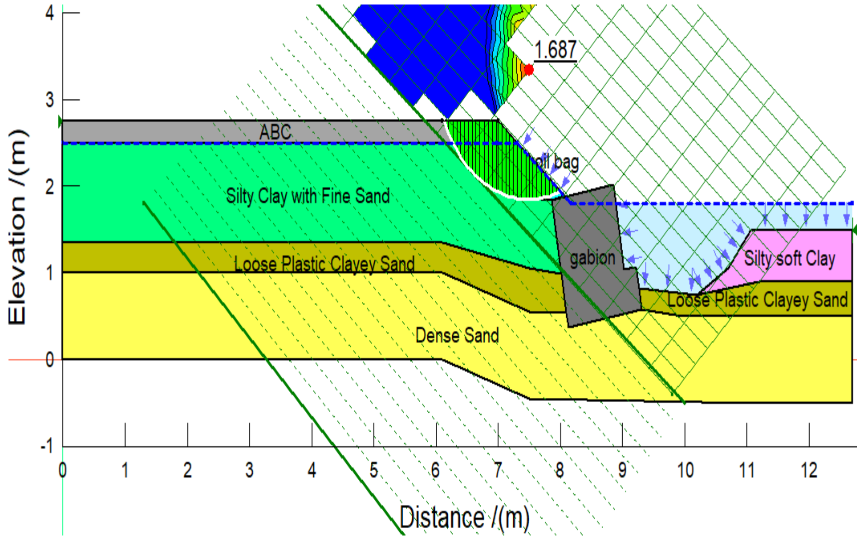

a) Sudden drawdown case for Vegetated flapped soil bag with a Gabion

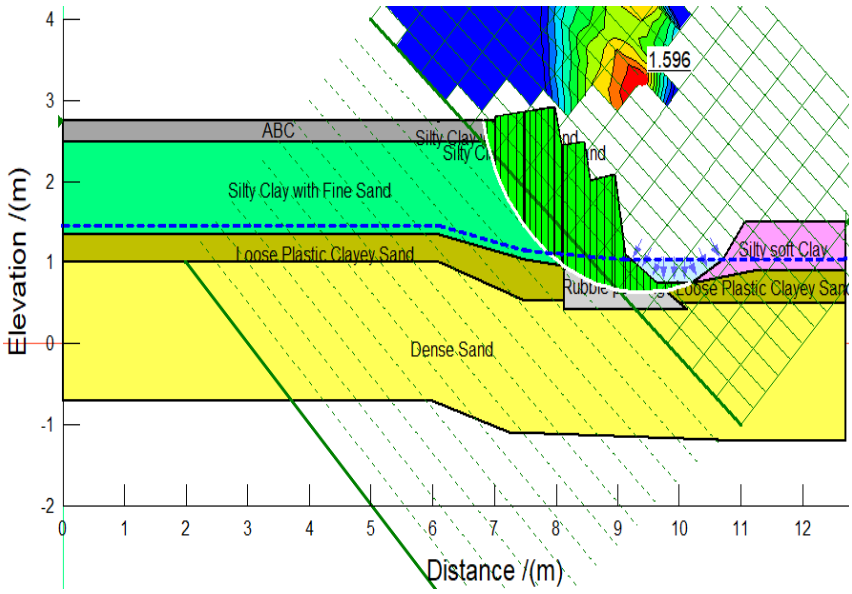

b) Normal stream water level case for Vegetated Gabion wall

Figure 3.26 Assessment of Stability for bio engineered and vegetated Gabion walls

Table 3.14. Summary of analysis results for Global Stability at Location 3

TYPE OF RECTIFICATION PROPOSAL	WATER TABLE CONDITION	MINIMUM F.O.S. (Grid & Radius)
		DRAINED CONDITION
Bioengineered retaining wall structure # I	After excavation for construction during the Dry period	1.000
	Normal stream water level	2.386
	High flood level (HFL)	1.687
Vegetated Gabion wall structure # II	After excavation for construction during the Dry period	1.027
	Normal stream water level	1.596
	High flood level (HFL)	1.341

The above results show that the calculated Factor of Safety satisfies the design criteria. As the FoS after excavation for the construction is low it should be done in short segments during a period of dry weather.

3.4.4 Establishment of the most appropriate technique at location 4

At the 4th location, two alternate rectification measures were considered to protect the 3 m height. The alternative solutions proposed are;

I. Gabion wall with Rubble packing at the toe
II. Gabion Wall with Vetiver Grass

The stability analysis design was conducted by the Bridge Design Division of the RDA. A gabion wall with dimensions 2 m x 1.5 m is assumed to have a vertical back and conforms to the geometry outlined in Kerisel and Absi's (1990) charts, in BS 8002:1994. The gabion wall cross-section is designed to place the gabion wall with a 10° batter leaning towards the retained slope and it has to be kept above the graded and compacted rubble layer.

3.4.4.1 Analysis for deep-seated failure at location 4

The two alternates proposed, considering the water flow conditions are represented in Fig. 3.27 and Fig. 3.28. The analysis results are presented in Figure 3.29 and Table 3.15.

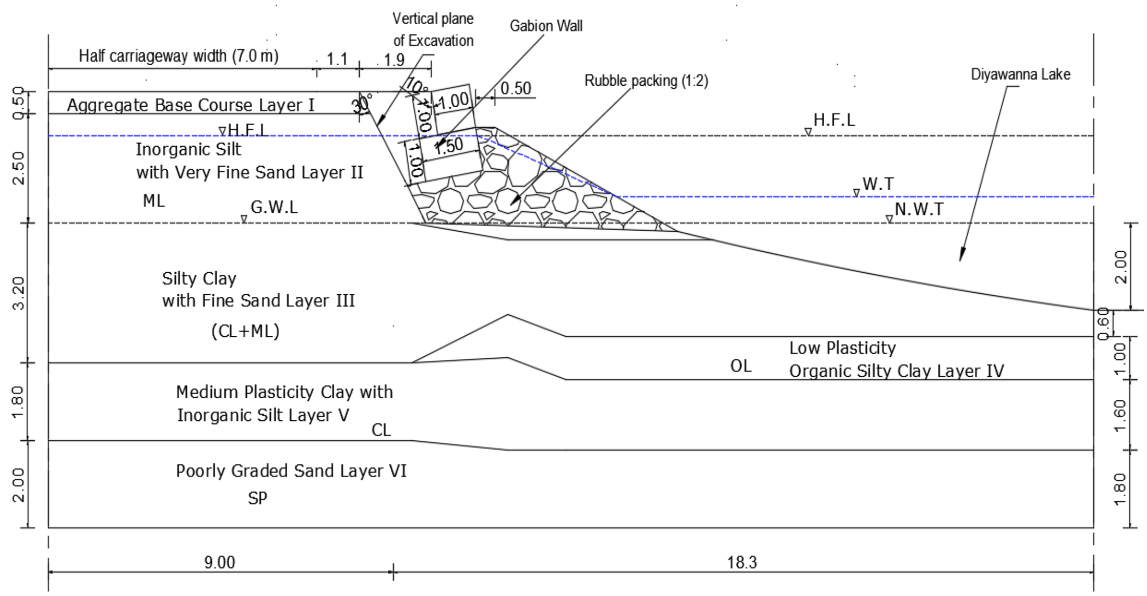

Figure 3.27 Proposed Gabion Wall section with Rubble packing at the toe

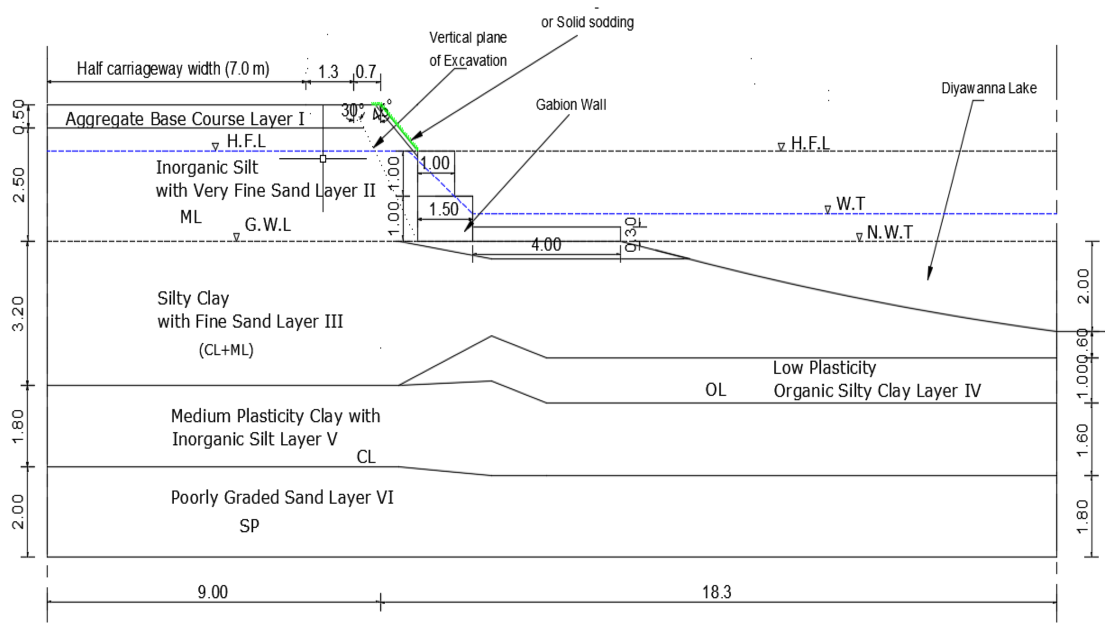

Figure 3.28 Proposed Gabion Wall at the toe, Reinforced with Solid Sodding

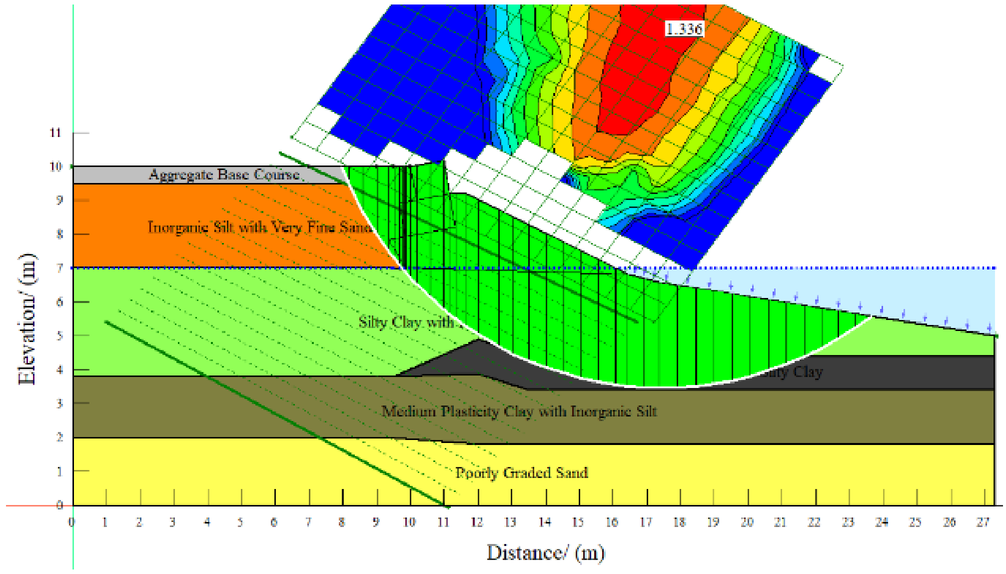

a) Normal Lake water level case for Gabion wall with Rubble packing

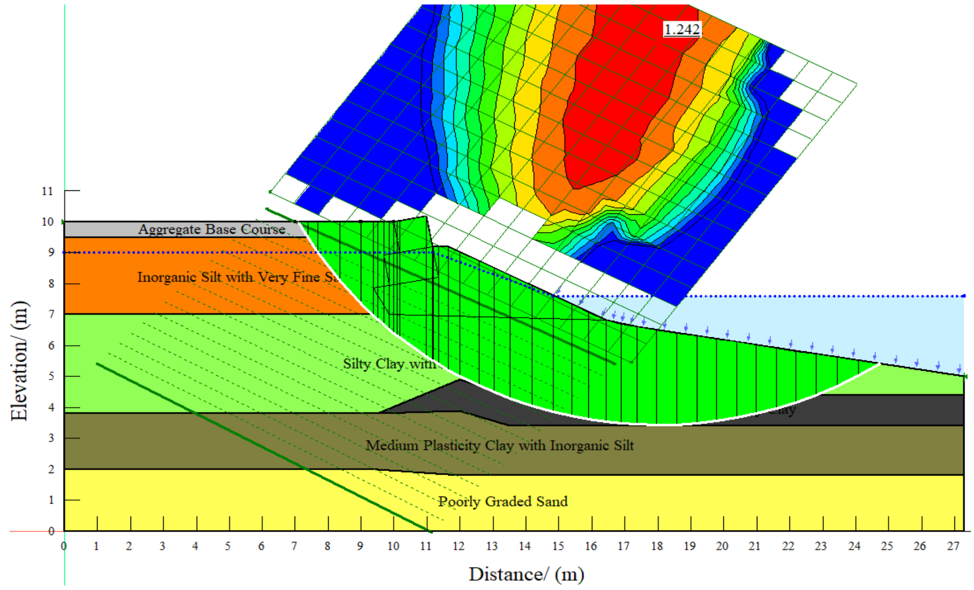

b) Sudden drawdown after Flood has receded for Gabion wall with Rubble packing

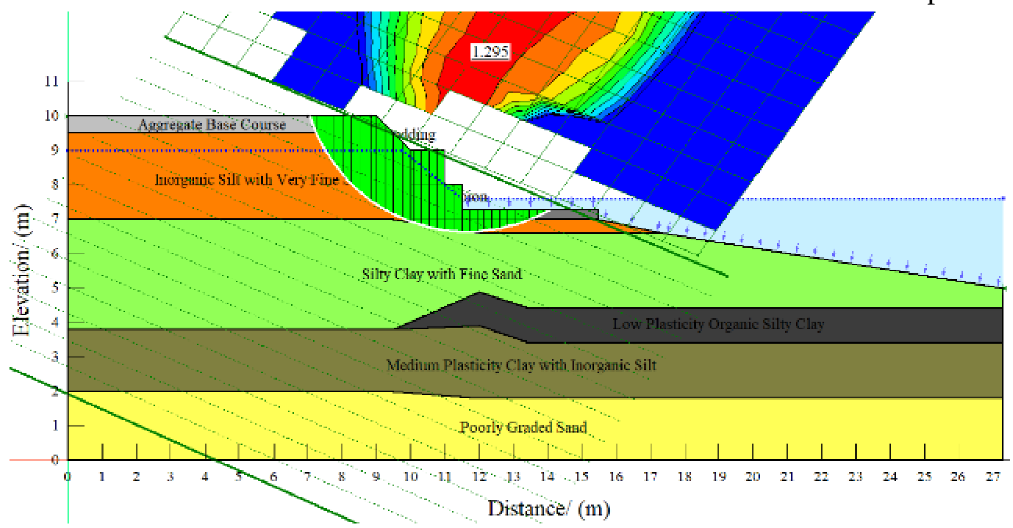

c) Sudden drawdown after Flood has receded for Gabion Wall with Vetiver Grass

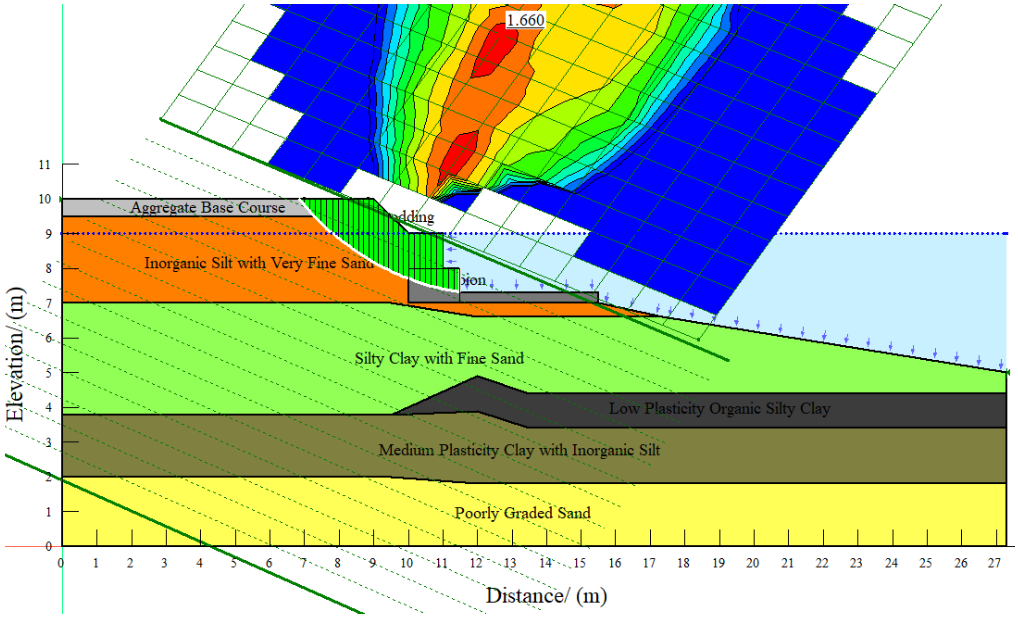

d) HFL case for Gabion Wall with Vetiver Grass

Figure 3.29 Assessment of Stability for proposals with various water table conditions

Table 3.15. Summary of analysis results for Global Stability at Location 4

TYPE OF RECTIFICATION PROPOSAL	WATER TABLE CONDITION	MINIMUM F.O.S. (Grid & Radius)
		DRAINED CONDITION
Gabion wall (2 m X 1.5 m) Retaining structure with Rubble packing as slope of 1:2 # I	After excavation for construction during the Dry period	1.057
	Normal Lake water level	1.336
	High flood level (HFL)	1.570
	Sudden drawdown after Flood has receded	1.242
Gabion Wall at toe, Reinforced with Vetiver Grass Overlay or Solid Sodding at a 45° angle # II	After excavation for construction during the Dry period	1.110
	Normal Lake water level	1.544
	High flood level (HFL)	1.660
	Sudden drawdown after Flood has receded	1.295

The above results show that the calculated FOS values are adequate with a value greater than 1.2 in the most critical sudden drawdown condition. As the FoS after excavation for the construction is low it should be done in short segments during a period of dry weather.

CHAPTER 4

4.0 SUMMARY OF THE ADOPTED SOLUTIONS AND PERFORMANCE

The adopted rectification measures classified according to the height of the slope in the summary presented in Table 4.1.

Table 4.1. Summary of adopted solutions based on height to be supported

VERTICAL HEIGHT OF SLOPE PROTECTION / m	TYPE OF WATERBODY	APPROPRIATE STABILIZING TECHNIQUE
0.5 to 1.5	Stream	Bio-engineering retaining wall (Vegetated live bamboo crib wall with Gabion at the toe)
1.5 to 2.5	Stream	Vegetated flapped soil bag with live stake retaining structure with Gabion at the toe
2.5 to 4.5	Lake	Gabion wall with Rubble packing at the toe
4.5 to 7.0	River	Gabion wall with Boulder packing

Achrya (2018 & 2020), assessed the potential use of bamboo crib walls in Nepal, emphasizing their ability to support plant growth. Their findings, affirm the suitability of the Vegetated live bamboo crib wall approach for stabilizing road embankments near small streams, with a maximum height of 1.5 meters presented in this study. This approach utilizes renewable, cost-effective materials and relies on labour-intensive techniques, enhancing its accessibility and affordability.

Live stakes, in conjunction with flapped soil bags, have been effectively utilized in Thailand to enhance soil retention, as studied by Jotisankasa (2019). He reported satisfactory survival rates for live stakes when horizontally positioned between the soil bags, demonstrating the beneficial effects of this method over time. The results, outlined in Table 4.1 by the author, validate the efficacy of the Vegetated flapped soil-bag method for stabilizing road embankments adjacent to streams, with a maximum height of 2.5 meters and 40°gradient.

The two eco-engineering approaches proposed in this study typically involve a combination of various vegetation covers, such as vetiver grass and live stakes, along with certain forms of gabion retaining structures. These combinations are aimed at enhancing soil stability and erosion control in stream bank restoration projects.

In developing nations like Sri Lanka, eco-friendly construction is crucial for economic progress and poverty reduction. Environmentally conscious practices balance development with preservation, and there's growing interest in these methods despite higher costs, due to the emphasis on sustainability and safety.

Ensuring the durability and safety of vegetative crib walls and Vegetated flapped soil-bag with live stakes could lead to their widespread adoption, potentially replacing conventional civil engineering methods within their practical limitations.

The findings, illustrated in Table 4.1, highlight the effectiveness of the Gabion wall with Boulder packing at the toe in stabilizing road embankments near large rivers or lakes. Suitable for structures up to 8 meters high with a 1:1.5 boulder packing slope, this method offers ease of construction, environmental friendliness, permeability, sustainability, erosion protection, enhanced structural capacity, and flow control. This approach provides a reliable solution for erosion mitigation and durability of riverbank infrastructure, safeguarding the highways road network.

The implemented solutions have been performing very satisfactorily over the past 10 years. Fig.4.1 illustrates the post-construction performance of the adopted stabilization techniques at location 1 after 10 years of construction, at location 2 after 3 months of construction and at location 4 after 5 years of construction.

(a) Location 1 (after 10 yrs)   (b) Location 2 (after 3 mth)   (c) Location 4 (after 5 yrs)

Figure 4.1 Photographs taken at Location 1,2 and 4 showing the post-construction performance of the adopted stabilization techniques

CHAPTER 5

5.0 CONCLUSION

The rectification solutions proven to be satisfactory for the selected four locations include both conventional hard engineering solutions and bio-engineering solutions coupled with hard engineering solutions. For each location, most appropriate option was selected after a rigorous assessment of the different design options. The conditions that lead to the failure were evaluated closely to ensure that those conditions are overcome by the selected rectification option. The proven success is an encouragement for future applications.

The satisfactory performance of vegetated bamboo crib walls highlights their potential as composite gravity walls, similar to concrete crib walls. Vegetative log crib walls, typically inclined at 20° to 30° from vertical, facilitate plant growth, with the wall base inclined at 5° to 15° to enhance sliding resistance. The success of these eco-engineering walls underscores their viability as a cost-effective slope management alternative, seamlessly integrating with other geotechnical measures even in large-scale slope failure scenarios. Soil bioengineering techniques, when conducive to plant growth, yield comparable or superior economic and environmental outcomes.

Incorporating plants into flapped soil bags prolongs their lifespan and enhances slope stability over time. However, blind replication without adherence to engineering principles is cautioned; thorough site investigation and assessment are paramount. Vegetative crib and vegetated flapped soil-bag techniques should be part of a comprehensive soil bioengineering system, emphasizing meticulous site assessment throughout.

In conclusion, the analysis suggests that for embankments higher than 4 meters with high water velocity, the Gabion wall with boulder packing is a viable stabilization technique. This method offers enduring environmental benefits and presents a sustainable solution to geotechnical challenges, ensuring effective slope management and protection against erosion while promoting environmental preservation. This integrated approach aligns with sustainable development goals, offering a reliable and eco-friendly alternative to traditional engineering methods.

REFERENCES

Acharya, M. S. (2018), “*Analytical approach to design vegetative crib walls*”. Geotechnical and Geological Engineering 36. 483–496. https://doi.org/10.1007/s10706-017-0342-5.

Acharya, M. S. (2020), “*Bamboo Crib Wall: A Sustainable Soil Bioengineering Method to Stabilize Slopes in Nepal*”. Journal of Development Innovations, Vol 4, No.1, 2020, 99-118.

Apiniti Jotisankasa. et al. (2019), “*Field performance of vegetated flapped soil-bag retaining structure along a stream bank*”. Procds. Of the 16th Asian Regional Conference on Soil Mechanics and Geotechnical Engineering, October 14-18,2019, Taipei, Taiwan.

British Standard Institution 8002:1994 “*Code of practice for Earth retaining structures*”, pp.9-10, 27-30, 39-40, 52-57 and 114-121.

Burt G. Look, “*Handbook of Geotechnical Investigation and Design Tables*” fifth edition, pp. 54,55,58 and 79-82.

A. Fakher, M. Khodaparast & C.J.F.P. Jones (2006),” The use of the Mackintosh Probe for site investigation in soft soils”, Article in Quarterly Journal of Engineering Geology and Hydrogeology.

Ghislan Brunet, Randall Shuey (2007), “*A case study on Streambank Stabilization with Vegetated Gabions”*, Intervale Country Club Golf Course Manchester, New Hampshire.

Guillermo Tardio, Slobodan B. Mickovski, “*Implementation of eco-engineering design into existing slope stability design practices”*, Journal of Ecological Engineering 92 (2016) 138-147 in ELSEVIER.

Gilbert Gedeon, P.E. (1994), “*Design of sheet pile walls*” Engineering manual, EM 1110-2-2504, pp. 1-2 to 6-8.

Joseph E. Bowles, P.E., S.E. “*Foundation analysis and design*” fifth edition, pp. 158-165,221-227 and 591-598.

Modular Gabion systems, a division of C.E.Shepherd company, 2221 Canada Dry Street, Houston TX 77023,"Gabion wall design", pp.1-5.

Santos-Ferreira, A and Ribeiro, L. (2014), "*Instability of Natural Slopes and the Reconstruction of Sabrosa Quay, in Douro River"*. International Conference on Geotechnical Engineering, Sri Lankan Geotechnical Society, August 10-11, 2015, Colombo, Sri Lanka.

S.De Baets, D. Torri, J. Poesen, M.P. Salvador and J. Meersmans, "*Modelling increased soil cohesion due to roots with EUROSEM*", November 19,2007.

Shamima Nasrin (2013), "*Erosion control and slope stabilization of embankments using Vetiver system*", M.Sc. study at Bangladesh University of Engineering and Technology, pp.16-23.

Siti Norazela Binti Hasan (2010), "*Simulation of River embankment stability: A case study on failure and remedial method at Muar River, Panchor, and Johor*", M.Eng study at University Technology Malaysia, pp.12-35.

"*Stability Modelling with SLOPE/W 2018 Version*", an Engineering Methodology Fifth Edition, March 2015, GEO-SLOPE International Ltd, Calgary, Alberta, Canada T2P 2Y5.

Steel sheet piles, Nippon Steel & Sumitomo Metal Corporation, Chiyoda-ku, Tokyo 100-8071 Japan, pp.5-30.

Tanmoy Mondal, Dr. Biplab Tripathy (2020), "*River Bank Erosion and Environmental Degradation*", International Journal of Research, Arunachal University of Studies.

U C sari, M N Sholeh, and I Hermanto (2020), "*The stability analysis study of conventional retaining walls variation design in vertical slope*". IOP Publishing at 8th Engineering International Conference in 2019.

Appendix A

Section: A.1 The stability calculations for Gabion wall using drained shear strength parameters for low water level at the back

Selected Gabion wall section parameters are,

Height of Gabion wall, H = $8\ m$

Width of Gabion base, B = $5\ m$

Fill slope angle above wall, β = 6^o

Surcharge load, q = $10kN/m^2$

<u>For layer – I</u>

Drained Internal friction angle, $\emptyset'$ = 30^0

Design internal friction angle, $\emptyset'_{des.}$ $= \tan^{-1}\frac{\tan 30^0}{1.2}$

$\emptyset'_{des.}$ $= 25.7^0$

Wall friction , δ $= \tan^{-1}(0.75\ \times\ \tan 25.7^0)$

$= 19.8^0$

So, $\frac{\beta}{\emptyset'des.} = 0.233$

$\frac{\delta}{\emptyset'des.} = 0.770$

From Kerisel and Absi's (1990) charts in BS 8002:1994,

Horizontal component k_a $= 0.364$

Use code of expression to compute active earth pressure,

Active horizontal earth pressure, P_{AN} $= б_V k_a - 2C\sqrt{ka}$

But, γ_{wet} $= 16kN/m^3$

But, vertical Stress $б_V$ $= (\gamma z + q)$

$= (16Z + 10)$

So, $P_{AN} = (16Z + 10)k_a$

$P_{AN} = 5.82Z + 3.64$

Z=0, $P_{AN} = 3.6\ kN/m^2$

Z=4.07m, $P_{AN} = 27.3\ kN/m^2$

For layer – II

Design internal friction angle, $\emptyset'_{des.} = \tan^{-1}\frac{\tan 32^0}{1.2}$

$\emptyset'_{des.} = 27.5^0$

Wall friction , $\delta = \tan^{-1}(0.75 \times \tan 27.5^0)$

$= 21.3^0$

So, $\frac{\beta}{\emptyset'des.} = 0.218$

$\frac{\delta}{\emptyset'des.} = 0.774$

From Kerisel and Absi's (1990) charts in BS 8002:1994,

Horizontal component $k_a = 0.361$

Active horizontal earth pressure, $P_{AN} = б_V k_a - 2C\sqrt{ka}$

But, $\gamma_{wet} = 17kN/m^3$

But, vertical Stress $б_V = (4.07X16 + \gamma z + 10)$

$= (17Z + 75.12)$

So, $P_{AN} = (17Z + 75.12)k_a$

$P_{AN} = 6.14Z + 27.12$

Z=0, $P_{AN} = 27.1\ kN/m^2$

Z=2.0m, $P_{AN} = 39.4\ kN/m^2$

For layer – III

Design internal friction angle, $\emptyset'_{des.}$ $= \tan^{-1} \frac{\tan 28^0}{1.2}$

$\emptyset'_{des.}$ $= 23.9^0$

Wall friction , δ $= \tan^{-1}(0.75 \times \tan 23.9^0)$

$= 18.4^0$

Hence, $\frac{\beta}{\emptyset'des.} = 0.251$

$\frac{\delta}{\emptyset'des.} = 0.770$

From Kerisel and Absi's (1990) charts in BS 8002:1994,

Horizontal component k_a $= 0.368$

Use code of expression to compute active earth pressure,

Active horizontal earth pressure, P_{AN} $= б_V k_a - 2C\sqrt{ka}$

But, γ_{wet} $= 17.5 kN/m^3$

γ_{sat} $= 18.0 kN/m^3$

But, vertical Stress (above W.T) $б_V$ $= (4.07X16 + 2X17 + \gamma z + 10)$

$= (17.5Z + 109.12)$

So, P_{AN} $= (17.5Z + 109.12)k_a$

So, P_{AN} $= 6.44Z + 40.16$

Z=0, P_{AN} $= 40.2\ kN/m^2$

Z=0.83m, P_{AN} $= 45.5\ kN/m^2$

Vertical effective Stress (below W.T), $б_V$ $= (4.07X16 + 2X17 + 0.83X17.5 + (18 - 9.81)z + 10)$

$= (8.19Z + 123.65)$

So, P_{AN} $= 3.01Z + 45.5$

Z=0, P_{AN} = 45.5 kN/m^2

Z=1.1m, P_{AN} = 48.8 kN/m^2

The ground water table on either side of the wall at the toe (point A) is assumed to be equal, considering no head loss and no net water pressure. For a conservative design, the passive earth pressure was ignored.

Gabion density, γ_g = $2700 \times 0.6 \times \frac{9.81}{1000}$

= 15.89 kN/m^3

Weight of gabion, W_g = (1x1+1x1.5+2x2+1x2.5+1x3+1x4 +1x5) x15.89

= 333.69 kN/m

Center of gravity from toe point, Xg = 3.39m

Yg = 2.95m

From the Auto CAD drawing

<u>Active forces and respective lever arms for Layer I specimen calculation</u>

Active force, P_1 = 3.64 × 4.07

= 14.81 kN/m

Respective lever arm (distance from point of rotation at A),

L_1 = 1.1+0.83+2+4.07/2

= 5.965 m

Active force, P_2 = 0.5× (27.33 −3.64) × 4.07

= 48.21 kN/m

Respective lever arm (distance from point of rotation at A),

L_2 = 1.1+0.83+2+4.07/3

= 5.287 m

Vertical component of active force, P_9 = (14.81 +48.21) × tan19.8^0

= 22.69 kN/m

Respective lever arm (distance from point of rotation at A),

$$L_9 = 5 \text{ m}$$

Active forces, Respective lever arms and resisting & overturning moments acting on the Gabion wall are presented in Table A1.1.

Table A1.1 Summary of forces, lever arms and moments acting on the Gabion wall

	Force/(kN/m)		Distance from point of rotation at A-Lever arm/(m)	Moment/(kNm/m)	
				Overturning	Resisting
P_1	14.81	L_1	5.965	88.34	
P_2	48.21	L_2	5.287	254.89	
P_3	54.24	L_3	2.930	158.92	
P_4	12.28	L_4	2.597	31.89	
P_5	33.33	L_5	1.515	50.49	
P_6	2.22	L_6	1.377	3.06	
P_7	50.05	L_7	0.550	27.53	
P_8	1.82	L_8	0.367	0.67	
P_9	22.69	L_9	5.000		113.45
P_{10}	25.94	L_{10}	5.000		129.70
P_{11}	11.83	L_{11}	5.000		59.15
P_{12}	17.26	L_{12}	5.000		86.28
W_g	333.69	L_{13}	3.390		1,131.21
				615.79	1,519.79

For external Stability Consideration,

a) Check for Overturning failure,

Overturning moment, $M_o = 615.79\ kNm/m$

Resisting moment, $M_r = 1{,}519.79\ kNm/m$

Restoring moment > Disturbing moment

It is satisfied according to BS8002.

b) Check for translational failure,

Disturbing forces, P_{ha} = $216.96\ kN/m$

Total vertical weight, $\sum W$ = W_g + P_{AV} (P_9+P_{10}+P_{11}+P_{12})

= $411.41\ kN/m$

The foundation soils for the gabion wall must be graded and compacted to accommodate the specified wall batter. During the Gabion construction it should be spread and compacted by Aggregate Base Course thickness of 300mm below the base of gabion.

A study on the friction angles of open-graded aggregates, conducted through large scale direct shear testing by Jennifer Nicks et al. (2017)

So, Base friction angle, $\delta_b = 34^o$

Sliding Resistance, F = $\sum W\ \tan \delta_b$

= $411.41 \times \tan 34^o$

= $277.5\ kN/m$

Restoring forces > Disturbing forces

It is satisfied according to BS8002.

a) Check for Bearing failure

Eccentricity, e = $\frac{B}{2} - \left(\frac{M_r - M_o}{\sum W}\right)$

= $\frac{5}{2} - \left(\frac{1519.8 - 615.8}{411.41}\right)$

e = 0.3 m ≤ ($B/6$ = 0.833 m)

Therefore, no tension at the gabion base.

Maximum stress at bottom, $бv_{max}$ = $\frac{W}{B}\left[1 + \frac{6e}{B}\right]$

= $\frac{411.41}{5}\left[1 + \frac{6 \times 0.3}{5}\right]$

= $111.9\ kPa$

Minimum stress at bottom, $бv_{min}$ = $\frac{W}{B}\left[1-\frac{6e}{B}\right]$

= $52.66\ kPa$

<u>Allowable bearing capacity below the gabion base (with in Stiff Clay)</u>

Hansen (1970) proposed Ultimate bearing capacity equation,

$$qult = CN_cS_cD_ci_cg_cb_c + \overline{q}N_qS_qD_qi_qg_qb_q + \frac{1}{2}\gamma B'N_rS_rD_ri_rg_rb_r$$

But, drained internal friction angle, $\emptyset'$ = 28^0

Drained Cohesion, C' = 0 kpa

So, $$qult = \overline{q}N_qS_qD_qi_qg_qb_q + \frac{1}{2}\gamma B'N_rS_rD_ri_rg_rb_r$$

From Foundation analysis and design by Bowles (1997), Table 4-4,

N_q = 14.7

N_r = 10.9

Shape factors in Foundation analysis and design by Bowles (1997), Table 4-5a,

S_q = 1 + (B/L) × sin Ø'

= 3.347

S_r = 1 - (B/L) × 0.4

= -1.0

Depth factors in Foundation analysis and design by Bowles (1997), Table 4-5a,

k = D/B for D/B ≤ 1

D_q = 1 + 2tan Ø' (1- sin Ø')^{2}k

= 1.066

D_r = 1

Inclination factors in Foundation analysis and design by Bowles (1997),Table 4-5b,

$$I_q = \left[1 + \frac{0.5H}{V + A_f C_a \cot \emptyset'}\right]^{2.5}$$

$$= 1.795$$

$$I_r = \left[1 - \frac{(0.7 - \frac{\eta°}{450°})H}{V + A_f C_a \cot \emptyset'}\right]^{3.5}$$

$$= 0.199$$

Factors for base on slope and tilted base in Foundation analysis & design by Bowles (1997), Table 4-5b,

$$g_q = g_r = (1 - 0.5 \tan ß)^5$$

$$= 0.763$$

$$b_q = b_r = 1$$

So, q_{ult} $=1.1x$ (18-9.81) $x14.7x3.347x1.066x1.795x0.763x1$ $+\frac{1}{2}(18-9.81)x(5-2x0.3)x10.9x(-1)x1x0.199x0.763x1$

$$= 645\ kPa$$

Allowable maximum stress at bottom,

$$бv_{all} = \frac{qulti}{FoS}$$

$$= \frac{[645]}{2.5}$$

$$= 258 \text{ kPa}$$

Hence, $бv_{all}$ $\geq$ Maximum stress induced at gabion bottom of base

Therefore, bearing capacity is satisfactory.

I) For Internal Stability Consideration,

Maximum vertical stress, $\sigma_{max} = \frac{N}{B-2e}$

$= 411.41/(5-2x0.3)$

$= 93.5\ kN/m^2$

Allowable stress, $\sigma_{max} = 100(5\gamma_g - 3)\ (\gamma_g = 1.62\frac{t}{m^3})$

$= 100(5 \times 1.62 - 3)$

$= 510\ kN/m^2$

It is satisfied

Average shear stress, $\zeta = \frac{T}{B}$

$= \frac{217}{5.0}$

$= 43.4\ kN/m^2$

Allowable stress, $\zeta am = \frac{N \tan \emptyset^x}{B} + C_g$

But, $\emptyset^x = 25\,\gamma_g - 10$

$= 25 \times 1.62 - 10$

$= 30.5^o$

C_g varies from 0.15 to 0.4 kg/cm^2, Hence take, Cg = 0.15 kg/cm^2

Allowable stress, $\zeta am = \frac{411.41 \times \tan 30.5^o}{5.0} + 0.15 \times 9.81 \times 10$

$= 48.46+14.7$

$= 63.16\ kN/m^2$

It is satisfactory.

Based on the above calculations, the selected dimensions of the gabion for external and internal stability are satisfactory.

Section: A.2 The stability calculations for Gabion wall using drained shear strength parameters for high water level at the back

<u>For layer – I</u>

Design internal friction angle, $\emptyset'_{des.}$ $= 25.7^0$

Wall friction , δ $= 19.8^0$

From Kerisel and Absi's (1990) charts in BS 8002:1994,

Horizontal component k_a $= 0.364$

Use code of expression to compute active earth pressure,

Active horizontal earth pressure, P_{AN} $= б_V k_a - 2C\sqrt{ka}$

But, γ_{wet} $= 16kN/m^3$

But, vertical Stress $б_V$ $= (\gamma z + q)$

$= (16Z + 10)$

So, P_{AN} $= (16Z\ +\ 10)k_a$

P_{AN} $= 5.82Z + 3.64$

Z=0, P_{AN} $= 3.6\ kN/m^2$

Z=1.29m, P_{AN} $= 11.15\ kN/m^2$

Vertical effective Stress (below W.T), $б_V$ $= (1.29X16 + (18 - 9.81)z + 10)$

$= (8.19Z + 30.64)$

So, P_{AN} $= 2.98Z + 11.15$

Z=0, P_{AN} $= 11.15\ kN/m^2$

Z=2.77m, P_{AN} $= 19.4\ kN/m^2$

<u>For layer – II</u>

Design internal friction angle, $\emptyset'_{des.}$ $= 27.5^0$

Wall friction , δ $= 21.3^0$

From Kerisel and Absi's (1990) charts in BS 8002:1994,

Horizontal component k_a = 0.361

Active horizontal earth pressure, $P_{AN} = б_V k_a - 2C\sqrt{ka}$

But, $\gamma_{sat} = 18kN/m^3$

But, vertical effective Stress $б_V = (8.19Z + 53.33)$

So, $P_{AN} = 2.96Z + 19.4$

Z=0, $P_{AN} = 19.4\ kN/m^2$

Z=2.0m, $P_{AN} = 25.5\ kN/m^2$

<u>For layer – III</u>

Design internal friction angle, $\emptyset'_{des.} = 23.9^0$

Wall friction , $\delta = 18.4^0$

From Kerisel and Absi's (1990) charts in BS 8002:1994,

Horizontal component, k_a = 0.368

Use code of expression to compute active earth pressure,

But, $\gamma_{sat} = 18.0kN/m^3$

Vertical effective Stress, $б_V = (8.19Z + 69.71)$

So, $P_{AN} = 3.014Z + 25.5$

Z=0, $P_{AN} = 25.5\ kN/m^2$

Z=1.94m, $P_{AN} = 31.35\ kN/m^2$

The ground water table on either side of the wall at the toe (point A) is assumed to be equal, considering no head loss and no net water pressure. For a conservative design, the passive earth pressure was ignored. Figure A2.1 shows the diagram for active earth pressure and other forces acting on the gabion wall for high water level at the back case, considering drained conditions.

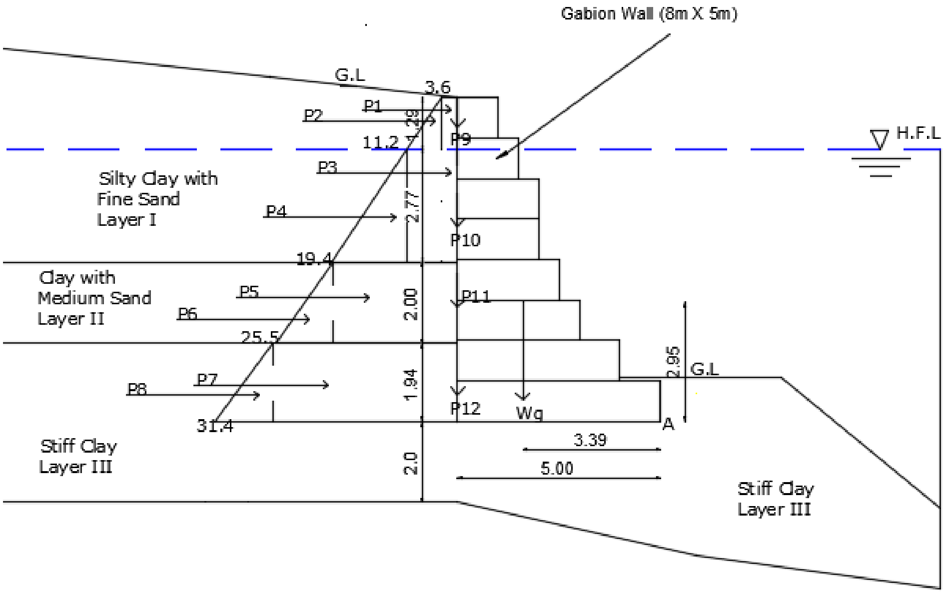

Figure A2.1 Active earth pressure and forces acting on the gabion wall

Weight of gabion, W_g = 333.69 kN/m

<u>Specimen calculation for Layer I</u>

Active force, P_1 = 3.6×1.29

= 4.64 kN/m

Respective lever arm (distance from point of rotation at A),

L_1 = 1.94+2+2.77+1.29/2

= 7.355 m

Active force, P_2 = $0.5\times (11.2 - 3.6) \times 1.29$

= 4.9 kN/m

Respective lever arm (distance from point of rotation at A),

L_2 = 1.94+2+2.77+1.29/3

= 7.14 m

Vertical component of active force, P_9 = $(4.64 + 4.9) \times \tan 19.8^0$

= 3.44 kN/m

Respective lever arm (distance from point of rotation at A),

L_9 = 5 m

Active forces, Respective lever arms and resisting & overturning moments acting on the Gabion wall are presented in Table A2.1

Table A2.1 Summary of forces, lever arms and moments acting on the Gabion wall

	Force/(kN/m)		Distance from point of rotation at A-Lever arm/(m)	Moment/(kNm/m)	
				Overturning	Resisting
P_1	4.64	L_1	7.355	34.13	
P_2	4.90	L_2	7.14	34.99	
P_3	31.02	L_3	5.325	165.18	
P_4	11.36	L_4	4.863	55.24	
P_5	38.80	L_5	2.94	114.07	
P_6	6.10	L_6	2.607	15.90	
P_7	49.47	L_7	0.970	47.99	
P_8	5.72	L_8	0.647	3.70	
P_9	3.44	L_9	5.000		17.20
P_{10}	15.26	L_{10}	5.000		76.30
P_{11}	17.51	L_{11}	5.000		87.55
P_{12}	18.36	L_{12}	5.000		91.80
W_g	333.69	L_{13}	3.390		1,131.21
				471.20	1,404.06

For external Stability Consideration,

c) Check for Overturning failure,

Overturning moment, M_o = 471.20 kNm/m

Resisting moment, M_r = 1,404.06 kNm/m

Restoring moment > Disturbing moment

It is satisfied according to BS8002.

d) Check for translational failure,

Disturbing forces, P_{ha} = 152.01 kN/m

Total vertical weight, $\sum W$ = 388.26 kN/m

Base friction angle, $\delta_b = 34^o$

Sliding Resistance, F = $388.26 \times \tan 34^o$

= $261.88\ kN/m$

Restoring forces > Disturbing forces

b) Check for Bearing failure

Eccentricity, e = 0.097 m

e $\leq$ ($^B/_6$ = 0.833 m)

Therefore, no tension at the gabion base.

Maximum stress at bottom, σv_{max} = $86.69\ kPa$

Minimum stress at bottom, σv_{min} = $68.61\ kPa$

According to the previous calculation, σv_{all} = 258 kPa

Hence, σv_{all} $\geq$ Maximum stress induced at gabion bottom of base

II) For Internal Stability Consideration,

Maximum vertical stress, σ_{max} = $\frac{N}{B-2e}$

= 80.79 kN/m^2

Average shear stress, ζ = $\frac{T}{B}$

= $30.4\ kN/m^2$

Allowable stress, ζam = $\frac{388.26 \times \tan 30.5^o}{5.0} + 0.15 \times 9.81 \times 10$

= $60.44\ kN/m^2$

It is satisfactory.

Based on the above calculations, the selected dimensions of the gabion for external and internal stability are satisfactory.

Section: A.3 The stability calculations for Gabion wall using drained shear strength parameters for high groundwater level on the retained side, and low water level in the river as sudden drawdown case

For layers I, II and III, the active earth pressure values are the same as the computations in the previous for high water level at the back.

<u>Calculation of Passive Side resistance for layer III</u>,

But (from previous calculations), $\frac{\beta}{\text{ø'des.}} = 0.251$

$\frac{\delta}{\text{ø'des.}} = 0.770$

From in Kerisel and Absi's (1990) charts in BS 8002:1994,

Horizontal component, $k_p = 5.447$

Use code of expression to compute active earth pressure,

Passive Side resistance, $P_P = б_V k_p + 2C\sqrt{kp}$

But, $\gamma_{sat} = 18.0 kN/m^3$

An average height of 2m of boulder packing is considered as a surcharge load on the passive side.

Vertical effective Stress (below W.T), $б_V = (2X16 + (18 - 9.81)z)$

$= (8.19Z + 32)$

So, $P_P = 44.61Z + 174.3$

Z=0, $P_P = 174.3\ kN/m^2$

Z=1.11 m, $P_P = 223.8\ kN/m^2$

Figure A3.1 shows the diagram for active earth pressure and other forces acting on the gabion wall for high groundwater level on the retained side, and low water level in the river as sudden drawdown case.

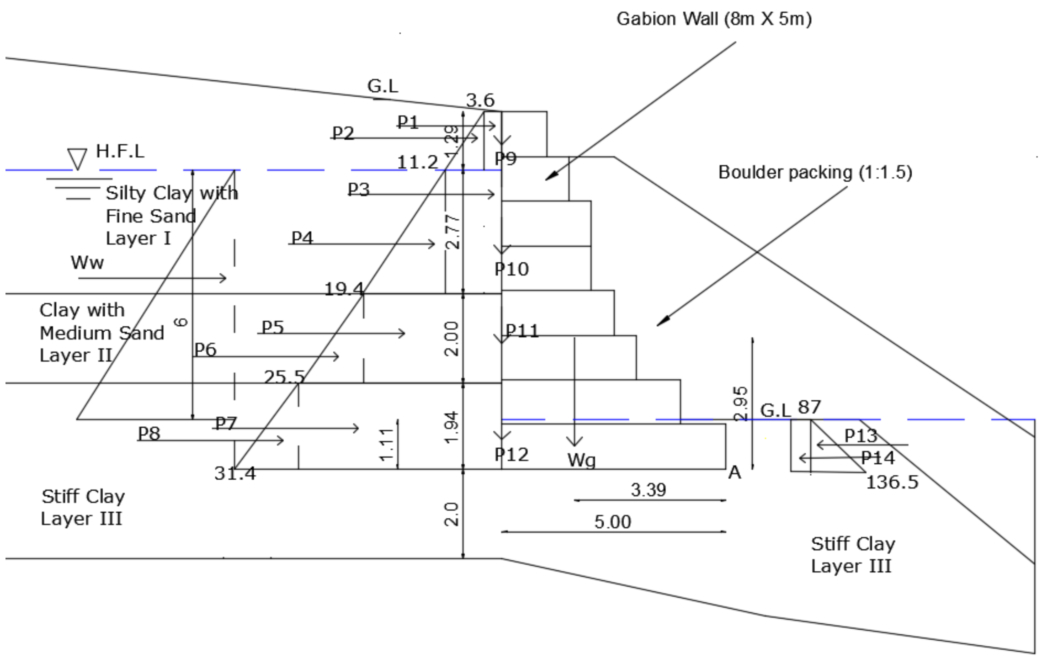

Figure A3.1 Active earth pressure and forces acting on the gabion wall

Weight of gabion, W_g = 333.69 kN/m

The Specimen calculation for Layer I is the same as the computations in the previously done for the high water level at the back.

Force exerted by the water, W_w = $0.5 \times 9.81 \times 6 \times 6$

= 176.58 kN/m

Respective lever arm (distance from point of rotation at A),

L_w = $1.11 + 6/3$

= 3.11 m

Active forces, Respective lever arms and resisting & overturning moments acting on the Gabion wall are presented in Table A3.1

Table A3.1 Summary of forces, lever arms and moments acting on the Gabion wall

	Force/(kN/m)		Distance from point of rotation at A-Lever arm/(m)	Moment/(kNm/m)	
				Overturning	Resisting
P_1	4.64	L_1	7.355	34.13	
P_2	4.90	L_2	7.14	34.99	
P_3	31.02	L_3	5.325	165.18	
P_4	11.36	L_4	4.863	55.24	
P_5	38.80	L_5	2.94	114.07	
P_6	6.10	L_6	2.607	15.90	
P_7	49.47	L_7	0.970	47.99	
P_8	5.72	L_8	0.647	3.70	
W_w	176.58	L_w	3.110	549.16	
P_9	3.44	L_9	5.000		17.20
P_{10}	15.26	L_{10}	5.000		76.30
P_{11}	17.51	L_{11}	5.000		87.55
P_{12}	18.36	L_{12}	5.000		91.80
P_{13}	27.48	L_{12}	0.370		10.17
P_{14}	96.60	L_{12}	0.550		53.13
W_g	333.69	L_{13}	3.390		1,131.21
				1,020.36	1,467.36

<u>For external Stability Consideration</u>,

e) Check for Overturning failure,

Overturning moment, M_o = 1,020.36 kNm/m

Resisting moment, M_r = 1,467.36 kNm/m

Restoring moment > Disturbing moment

f) Check for translational failure,

Disturbing forces, P_{ha} = 204.51 kN/m

Total vertical weight, $\sum W$ = 388.26 kN/m

Sliding Resistance, F = $388.26 \times \tan 34^o$

= $261.88\ kN/m$

Restoring forces > Disturbing forces

c) Check for Bearing failure

Eccentricity, e = 1.35 m

e $\gg$ (${}^{B}/_{6}$ = 0.833 m)

Therefore, tension at the gabion base.

e' = $\left(\frac{M_r - M_o}{\sum W}\right)$

= 1.15 m

Equating the soil reaction under the Gabion wall base in actual stress distribution with axial force,

W = $\frac{1}{2} \times б_{red} \times 3 \times e'$

$б_{red}$ = $225\ kPa$

Maximum stress at bottom, $бv_{max}$ = $225\ kPa$

According to the previous calculation, $бv_{all}$ = 258 kPa

III) For Internal Stability Consideration,

Maximum vertical stress, $б_{max}$ = $\frac{N}{B-2e}$

= 222.6 kN/m^2

Average shear stress, ζ = $\frac{T}{B}$

= $40.9\ kN/m^2$

Allowable stress, ζam = $60.44\ kN/m^2$

It is satisfactory.

Based on the above calculations, the selected dimensions of the gabion for external and internal stability are satisfactory.

Appendix B

Section: B.1 The stability calculations for Anchored sheet pile wall using Undrained (worse scenario) shear strength parameters for low water level at the back

<u>For layer I</u>

Drained Internal friction angle, $\emptyset'$ = 30^0

Design internal friction angle, $\emptyset'_{des.}$ = $\tan^{-1}\frac{\tan 30^0}{1.2}$

$\emptyset'_{des.}$ = 25.7^0

k_a = 0.364 (from Kerisel and Absi, 1990)

Active horizontal earth pressure, P_{AN} = $б_V k_a - 2C\sqrt{ka}$

But, γ_{wet} = $16kN/m^3$

So, P_{AN} = $(16Z + 10)k_a$

P_{AN} = $5.82Z + 3.64$

Z=0, P_{AN} = $3.64\ kN/m^2$

Z=4.15m, P_{AN} = $27.8\ kN/m^2$

<u>For layer II</u>

Drained Internal friction angle, $\emptyset'$ = 32^0

Design internal friction angle, $\emptyset'_{des.}$ = $\tan^{-1}\frac{\tan 32^0}{1.2}$

$\emptyset'_{des.}$ = 27.5^0

k_a = 0.361 (from Kerisel and Absi, 1990)

Use code of expression to compute active earth pressure,

Active horizontal earth pressure, P_{AN} = $б_V k_a - 2C\sqrt{ka}$

But, γ_{wet} = $17kN/m^3$

So, P_{AN} $= (17Z + 16x4.15 + 10)k_a$

P_{AN} $= 6.14Z + 27.58$

Z=0, P_{AN} $= 27.58\ kN/m^2$

Z=2.0m, P_{AN} $= 39.86\ kN/m^2$

Calculation of Passive Side resistance for layer II,

As per the previous calculation Horizontal component,

k_p = 5.313 (from B58002, 1994, Annex A)

Passive Side resistance, P_P $= б_V k_p + 2C\sqrt{kp}$

But, γ_{wet} $= 17kN/m^3$

So, P_P $= (17Z)\ k_p$

Z=2.0m, P_P = 180.64 kPa

For Layer III

Undrained cohesion, C_u = 20Kpa

Design Undrained cohesion, Cu_{desi} $= \frac{20}{1.5}$

= 13.3 kPa

Design adhesion, C_w $= 0.75 \times 13.3$

= 10 kPa

Active horizontal earth pressure computation in terms of Total Stress,

P_{AN} $= б_V - 2\ Cu\left[1 + \frac{C_w}{C_u}\right]^{\frac{1}{2}}$

But, γ_{wet} $= 17.5kN/m^3$

γ_{sat} $= 18kN/m^3$

But, vertical Stress σ_V $= (4.15X16 + 2X17 + \gamma z + 10)$

$= (\gamma Z + 110.4)$

$P_{AN} = [110.4 + \gamma Z] - 2 \times 13.3 \times \left[1 + \frac{10}{13.3}\right]^{1/2}$

$P_{AN} = [75.2 + \gamma Z]$

Z=0, $P_{AN} = 75.2\ kPa$

Z=0.79m, $P_{AN} = 89\ kPa$

Z=2.21m, $P_{AN} = [89 + 18 \times 2.21]$

$= 128.8\ kPa$

Passive Side resistance computation in terms of Total Stress,

$$P_p = \sigma_V + 2C_u \left[\frac{C_w}{C_u}\right]^{1/2}$$

$$P_p = (2 \times 17 + \gamma Z) + 2 \times 13.3 \times \left[1 + \frac{10}{13.3}\right]^{1/2}$$

$P_p = 51.6 + \gamma Z$

Z=0, $P_p = 51.6\ kPa$

Z=0.79m, $P_p = 51.6 + 17.5\ X0.79$

$= 65.4\ kPa$

Z=2.21m, $P_p = 65.4 + 18\ X2.21$

$= 105.2\ kPa$

<u>For layer IV</u>

Undrained cohesion, C_u $= 25Kpa$

Design Undrained cohesion, Cu_{desi} $= \frac{25}{1.5}$

$= 16.67\ kPa$

Design adhesion, C_w = 0.75×13.3

= $12.5\ kPa$

Active horizontal earth pressure computation in terms of Total Stress,

$$P_{AN} = б_V - 2\,Cu\left[1 + \frac{C_w}{C_u}\right]^{\frac{1}{2}}$$

But, γ_{sat} = $14 kN/m^3$

But, vertical Stress $б_V$ = $(4.15X16 + 2X17 + 0.79X17.5 + 2.21X18 + \gamma z + 10)$

= $(14Z + 164)$

$$P_{AN} = [164 + 14Z] - 2 \times 16.67 \times \left[1 + \frac{12.5}{16.67}\right]^{1/2}$$

$$P_{AN} = [119.9 + 14Z]$$

Z=0, P_{AN} = $119.9\ kPa$

Z=d m, P_{AN} = $(119 + 14d\ )kPa$

Passive Side resistance computation in terms of Total Stress,

$$P_p = б_V + 2C_u\left[\frac{C_w}{C_u}\right]^{1/2}$$

$$P_p = (2 \times 17 + 0.79 \times 17.5 + 2.21 \times 18\ + 14Z) + 2\ \times 16.67\ \times \left[1 + \frac{12.5}{16.67}\right]^{1/2}$$

$$P_p = 131.7+14Z$$

Z=0, P_p = $131.7\ kPa$

Z=dm, P_p = $131.7+14d\ kPa$

<u>Active forces and respective lever arms for Layer I specimen calculation</u>

Active force, P_1 = 15.11 kN/m

Respective lever arm (distance from rigid of rotation at B),

L_1 = 0.925 m

Active force, P_2 = $0.5\times(27.8-3.64)\times 4.15$

= 50.13 kN/m

Respective lever arm (distance from rigid of rotation at B),

L_2 = 0.233 m

Active forces, passive forces, respective lever arms, and resisting and overturning moments acting on the anchored sheet pile wall are summarized in Table B1.1.

Table B1.1: Summary of forces, lever arms and moments acting on the sheet pile wall.

	Force/(kN/m)		Distance from rigid of rotation at B-Lever arm/(m)	Moment/(kNm/m)	
				Overturning	Resisting
P_1	15.11	L_1	0.925		13.98
P_2	50.13	L_2	0.233		11.68
P_3	55.20	L_3	2.15	118.68	
P_4	12.30	L_4	2.483	30.54	
P_5	59.40	L_5	3.545	210.57	
P_6	5.45	L_6	3.677	20.04	
P_7	196.69	L_7	5.045	992.3	
P_8	43.98	L_8	5.413	238.06	
P_9	119.9d	L_9	6.15+d/2	$737.4d+60d^2$	
P_{10}	$7d^2$	L_{10}	6.15+2d/3	$43d^2+4.67d^3$	
P_{11}	180.60	L_{11}	2.483		448.43
P_{12}	40.76	L_{12}	3.545		144.49
P_{13}	5.45	L_{13}	3.677		20.04
P_{14}	144.53	L_{14}	5.045		729.15
P_{15}	43.98	L_{15}	5.413		238.06
P_{16}	131.7d	L_{16}	6.15+d/2		$810d+87.8d^2$
P_{17}	$7d^2$	L_{17}	6.15+2d/3		$43d^2+4.67d^3$

Sheet pile wall is subject to a rigid rotation at B, No reaction at bottom end and considering the moment equilibrium at B, $\sum M = 0$

$$60d^2+737.4d+1620.19 \quad = 87.8d^2+810d+1605.83$$

By solving the above equation,

$$D_1 = 0.21 \text{ m} \;\&\; D2 = -2.79 \text{ m (This is not possible)}$$

The embedment depth is increased by 20% to reduce lateral deflection at the base of the sheeting.

D = 0.25 m

Required height of sheet pile wall, = 9.4 m

To determine the anchor force T consider the horizontal equilibrium,

$$438.26 = 415.32 + 2.95 + \mathrm{T}\cos 30°$$

T = 23.1 kN/m

Required tensile strength for pre stressing rod,

T = 23.1 kN/m

Figure B1.1 Shear force diagram for determining zero shear force and maximum bending moment on sheet pile.

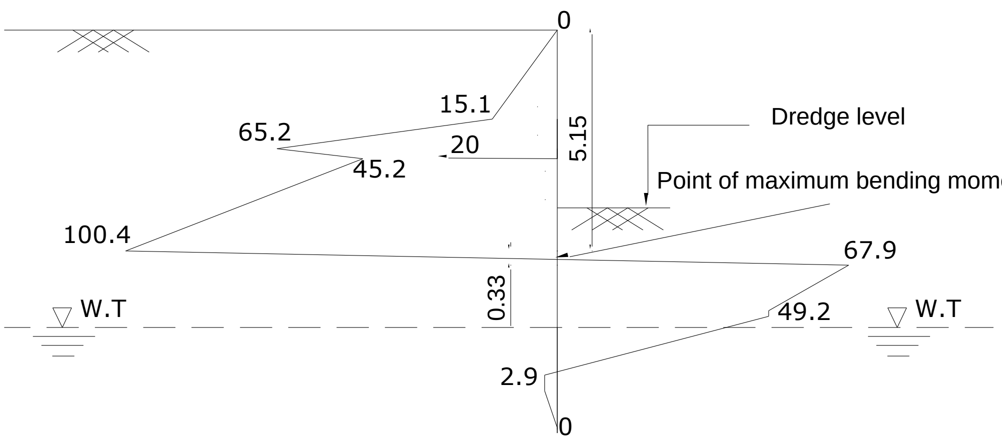

Figure B1.1: Shear forces acting on the Sheet pile wall

Depth of maximum Bending moment $= 5.15 + \frac{100.4 \times 0.33}{(100.4+67.9)}$

= 5.35 m below top of Sheet pile

Take moment about and above the level of zero shear,

Maximum bending moment, $(M)_{max}$ $= 15.11 \times 3.275 + 50.13 \times 2.583 - 20 \times 2.35 + 33.1 \times 0.6 + 4.4 \times 0.4 - 65.04 \times 0.4$

= 127.6 kNm/m Run of wall

Design of a Steel sheet pile

A hot-rolled NS-SP-II U-type steel sheet pile, manufactured by Nippon Steel & Sumitomo Metal Corporation in Tokyo, Japan, was selected. The sectional properties of the steel sheet pile (BS EN 10248-1:1996, S355GP) is given in Appendix C.

Available maximum length = 25 m

Proposed sheet pile length = 14.55 m

Characteristic yield strength of Sheet pile,

= 355 N/mm^2

Characteristic Tensile strength of Sheet pile,

= 480 N/mm^2

Allowable bending stress in mild steel (American Institute of Steel Construction),

f_b = Yield strength X 0.5

= 177.5 N/mm^2

Using bending formula theory, $\frac{M}{I} = \frac{b}{y}$

Maximum allowable bending moment, M_{all} = 155 kNm/m ≥ 127.6 kNm/m

The selected section of the sheet pile wall satisfies the flexural strength requirements. The shear area for U-shaped sections may be taken as,

$A v$ = $t_w\, h / w$

= 2,625 mm^2/m

Allowable Shear force in steel sheet pile,

V_{max} = Yield strength X 0.33 X Area (AISC)

= 308 kN/m

The minimum section modulus, Z_{min} $= M_{max} / fb$

$= 719\ cm^3/m < 874\ cm3/m$

The selected section of the sheet pile wall meets the requirements.

<u>Design of Pre stress bar Anchors</u>

The properties of Prestressing steel bars (ASTM A722) is given in Appendix C.

Steel grade = 150 ksi

Nominal diameter = 26 mm

Pre stressing force = $341kN$

Tie rods utilizing Pre-stress bar anchors (ASTM A722) are applied at 8.0m intervals, corresponding to every twenty piles.

Required tie rod force at bottom = 23.1 kN/m (previously calculated)

Hence, Design load in tie rod, $= 23.1 \times 8$

$= 184.8kN \leq 341kN$

Maximum shear load of tie rod $= 23.1 \times 8 \times 0.5$

= 92.4 kN

The selection of prestressing bar anchor sizes is satisfactory.

<u>Design of Rock grouted anchor</u>

The average ultimate bond stress for rock grout interface (after PTI, 1996) is given in Appendix C.

Allowable bond stress for rock grout interface,

= 360 kPa

But, rock socket diameter = 100 mm

Assumed rock socket length = 3 m

Allowable skin friction = 339 kN > 184.8 kN

Hence, the rock socket anchor length is sufficient to withstand the prestressing force.

Section: B.2 The stability calculations for Anchored sheet pile wall using drained shear strength parameters for high water level at the back

<u>For layer – I</u>

Design internal friction angle, $\emptyset'_{des.}$ $= 25.7^0$

From Kerisel and Absi's (1990) charts in BS 8002:1994,

Horizontal component k_a $= 0.364$

Use code of expression to compute active earth pressure,

Active horizontal earth pressure, P_{AN} $= б_V k_a - 2C\sqrt{ka}$

But, γ_{wet} $= 16kN/m^3$

But, vertical Stress $б_V$ $= (\gamma z + q)$

$= (16Z + 10)$

So, P_{AN} $= (16Z\ +\ 10)k_a$

P_{AN} $= 5.82Z + 3.64$

Z=0, P_{AN} $= 3.6\ kN/m^2$

Z=1.3m, P_{AN} $= 11.2\ kN/m^2$

Vertical effective Stress (below W.T), $б_V$ $= (8.19Z + 30.64)$

So, P_{AN} $= 2.98Z + 11.2$

Z=0, P_{AN} $= 11.2\ kN/m^2$

Z=2.85m, P_{AN} $= 19.6\ kN/m^2$

<u>For layer – II</u>

Design internal friction angle, $\emptyset'_{des.}$ $= 27.5^0$

Wall friction , δ $= 21.3^0$

From Kerisel and Absi's (1990) charts in BS 8002:1994,

Horizontal component k_a $= 0.361$

Active horizontal earth pressure, P_{AN} $= б_V k_a - 2C\sqrt{ka}$

But, γ_{sat} $= 18kN/m^3$

But, vertical effective Stress $б_V$ $= (8.19Z + 54)$

So, P_{AN} $= 2.96Z + 19.6$

Z=0, P_{AN} $= 19.6\ kN/m^2$

Z=2.0m, P_{AN} $= 25.7\ kN/m^2$

<u>Calculation of Passive Side resistance for layer II</u>,

k_p = 5.313 (from B58002, 1994, Annex A)

Passive Side resistance, P_P $= б_V k_p + 2C\sqrt{kp}$

But, γ_{sat} $= 18kN/m^3$

So, P_P $= ((18 - 9.81)Z)\ k_p$

Z=2.0m, P_P $= 87\ kPa$

<u>For Layer III</u>

Drained Internal friction angle, $\emptyset'$ = 28^0

Design internal friction angle, $\emptyset'_{des.}$ $= \tan^{-1}\frac{\tan 28^0}{1.2}$

$\emptyset'_{des.}$ $= 23.9^0$

But, Horizontal component from previous calculation,

k_a = 0.368 (from Kerisel and Absi, 1990)

γ_{sat} $= 18.0kN/m^3$

Vertical effective Stress, $б_V$ $= (8.19Z + 70.38)$

So, P_{AN} $= 3.01Z + 25.7$

Z=0, P_{AN} $= 25.7\ kN/m^2$

Z=3.0m, P_{AN} $= 35\ kN/m^2$

Calculation of Passive Side resistance for layer III,

From in Kerisel and Absi's (1990) charts in BS 8002:1994,

Horizontal component, k_p = 5.447

Use code of expression to compute active earth pressure,

Passive Side resistance, P_P $= б_V k_p + 2C\sqrt{kp}$

γ_{sat} $= 18.0 kN/m^3$

Vertical effective Stress , $б_V$ $= (8.19Z + 16.38)$

So, P_P $= 44.6Z + 87$

Z=0, P_P $= 87\ kN/m^2$

Z=3.0m, P_P $= 227.8\ kN/m^2$

For layer IV

Design internal friction angle, $\emptyset'_{des.}$ $= 21.2^0$

From in Kerisel and Absi's (1990) charts in BS 8002:1994,

Horizontal component, k_a = 0.374

Use code of expression to compute active earth pressure,

Active horizontal earth pressure, P_{AN} $= б_V k_a - 2C\sqrt{ka}$

But, γ_{Sat} $= 14 kN/m^3$

But, vertical Stress $б_V$ $= \left((14 - 9.81)z + 94.95\right)$

So, P_{AN} $= (4.19Z\ +\ 94.95)k_a$

Z=0, P_{AN} $= 35\ kN/m^2$

Z=d, P_{AN} $= 1.57d + 35\ kN/m^2$

Calculation of Passive Side resistance for layer IV,

From in Kerisel and Absi's (1990) charts in BS 8002:1994,

Horizontal component, k_p = 5.572

But, γ_{sat} $= 14 kN/m^3$

Vertical effective Stress, $б_V$ $= (4.19Z + 40.95)$

So, Passive Side resistance, P_P $= 23.35Z + 227.8$

Z=0, P_P $= 227.8\ kN/m^2$

Z=d, P_P $= 23.35d + 227.8\ kN/m^2$

The ground water table on either side of the wall at B is assumed to be equal, considering no head loss and no net water pressure. Figure B2.1 shows the diagram for active and passive earth pressure and other forces acting on the sheet pile wall for high water level at the back case, considering drained conditions.

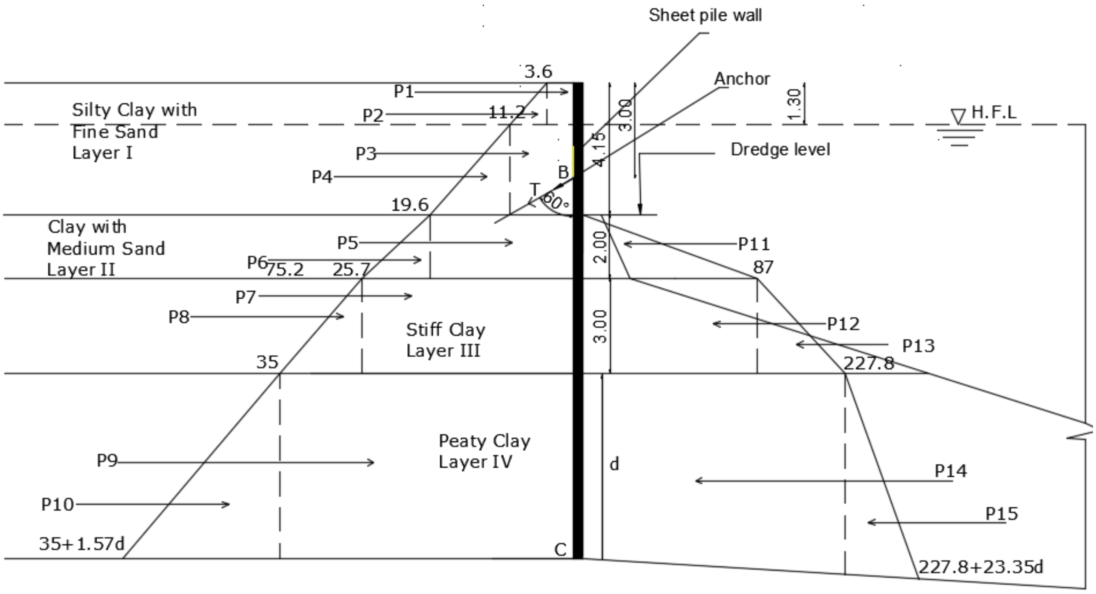

Figure B2.1 shows the diagrams for active and passive earth pressure and other forces acting on the sheet pile wall

<u>Active forces and respective lever arms for Layer I specimen calculation</u>

Active force, P_1 $=$ 3.6×1.3

$=$ 4.7 kN/m

Respective lever arm (distance from rigid of rotation at B),

L_1 $=$ 2.35 m

Active force, P_2 $=$ $0.5\times (11.2 - 3.6) \times 1.3$

$=$ 4.9 kN/m

Respective lever arm (distance from rigid of rotation at B),

$$L_2 \quad = \quad 4.133 \text{ m}$$

Active forces, passive forces, respective lever arms, and resisting and overturning moments acting on the anchored sheet pile wall are presented in Table B2.1.

Table B2.1: Summary of forces, lever arms and moments acting on the sheet pile wall.

	Force/(kN/m)		Distance from rigid of rotation at B-Lever arm/(m)	Moment/(kNm/m)	
				Overturning	Resisting
P_1	4.68	L_1	2.35		11
P_2	4.94	L_2	2.133		10.54
P_3	31.92	L_3	0.275		8.78
P_4	11.97	L_4	0.2	2.39	
P_5	39.20	L_5	2.15	84.28	
P_6	6.10	L_6	2.483	15.15	
P_7	77.10	L_7	4.65	358.52	
P_8	13.95	L_8	5.15	71.84	
P_9	35d	L_9	6.15+d/2	$215.25d+17.5d^2$	
P_{10}	$0.8d^2$	L_{10}	6.15+2d/3	$4.92d^2+0.53d^3$	
P_{11}	87.00	L_{11}	2.483		-
P_{12}	261.00	L_{12}	4.65		-
P_{13}	211.80	L_{13}	5.15		-
P_{14}	137d	L_{16}	6.15+d/2		$842.55d+68.5d^2$
P_{15}	$11.68d^2$	L_{17}	6.15+2d/3		$71.83d^2+7.787d^3$

For the conservative design, the passive resistance from layer II and layer III is omitted. Sheet pile wall is subject to a rigid rotation at B, No reaction at bottom end and considering the moment equilibrium at B, $\sum M = 0$

$$7.257d^3 + 117.91d^2 + 627.3d - 501.86 \quad = 0$$

By solving the above equation,

$$D_1 = 0.7 \text{ m}, \; D2 \text{ and } D3 = -8.5 \text{ m (This is not possible)}$$

Design depth.

$$D \quad = 0.85 \text{ m}$$

Required height of sheet pile wall, = 10 m

To determine the anchor force T consider the horizontal equilibrium,

$$189.86 = 124.89 + 33.5 + T \cos 30°$$

$$T = 36.3 \text{ kN/m}$$

Maximum bending moment, $(M)_{max}$ $= 4.68 \times 4.85 + 4.94 \times 4.633 - 36.3 \times 2.5 + 31.92 \times 2.775 + 11.97 \times 2.3 + 39.2 \times 0.35 + 6.1 \times 0.02$

$= 84.8$ kNm/m Run of wall

Maximum allowable bending moment, M_{all} $= 155$ kNm/m ≥ 84.8 kNm/m

The minimum section modulus, Z_{min} $= M_{max} / fb$

$= 478 \text{ cm}^3/\text{m} < 874$ cm3/m

The selected section of the sheet pile wall meets the requirements.

<u>Design of Pre stress bar Anchors</u>

Tie rods utilizing Pre-stress bar anchors (ASTM A722) are applied at 8.0m intervals, corresponding to every twenty piles.

Design load in tie rod, $= 36.3 \times 8$

$= 290.4kN \leq 341kN$

Maximum shear load of tie rod $= 36.3 \times 8 \times 0.5$

$= 145.2$ kN

The selection of prestressing bar anchor sizes is satisfactory.

The average ultimate bond stress for rock grout interface (after PTI, 1996) is given in Appendix C.

Allowable bond stress for rock grout interface,

$= 360$ kPa

Allowable skin friction $= (22/7) \times 0.1 \times 3 \times 360$

$= 339$ kN > 290.4 kN

Hence, the rock socket anchor length is sufficient to withstand the prestressing force.

Section: B.3 The stability calculations for Sheet pile wall using drained shear strength parameters for high groundwater level on the retained side, and low water level in the river as sudden drawdown case

For layers I, II, III and IV the active and passive earth pressure values are the same as the computations in the previous for high water level at the back.

Figure B3.1 shows the diagram for active earth pressure and other forces acting on the sheet pile wall for sudden drawdown case, considering drained conditions.

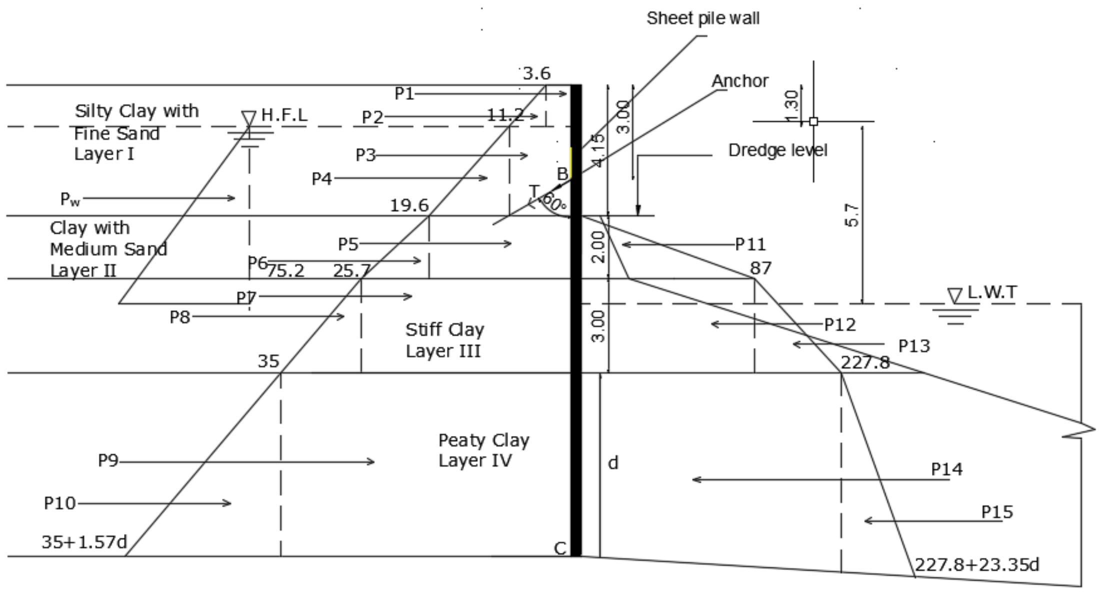

Figure B3.1 shows the diagrams for active and passive earth pressure and other forces acting on the sheet pile wall

The Specimen calculation for Layer I is the same as the computations in the previously done for the high water level at the back.

Force exerted by the water, $P_w = 0.5 \times 9.81 \times 5.7 \times 5.7$

$= 159.4$ kN/m

Respective lever arm (distance from rigid of rotation at B),

$L_w = 2\times5.7/3 - 1.7$

$= 2.1$ m

Active forces, passive forces, Respective lever arms and resisting & overturning moments acting on the Gabion wall are presented in Table B3.1

Table B3.1: Summary of forces, lever arms and moments acting on the sheet pile wall.

	Force/(kN/m)		Distance from rigid of rotation at B-Lever arm/(m)	Moment/(kNm/m)	
				Overturning	Resisting
P_1	4.68	L_1	2.35		11
P_2	4.94	L_2	2.133		10.54
P_3	31.92	L_3	0.275		8.78
P_4	11.97	L_4	0.2	2.39	
P_5	39.20	L_5	2.15	84.28	
P_6	6.10	L_6	2.483	15.15	
P_7	77.10	L_7	4.65	358.52	
P_8	13.95	L_8	5.15	71.84	
P_w	159.4	L_w	2.1	334.74	
P_9	35d	L_9	6.15+d/2	$215.25d+17.5d^2$	
P_{10}	$0.8d^2$	L_{10}	6.15+2d/3	$4.92d^2+0.53d^3$	
P_{11}	87.00	L_{11}	2.483		-
P_{12}	261.00	L_{12}	4.65		-
P_{13}	211.80	L_{13}	5.15		-
P_{14}	137d	L_{16}	6.15+d/2		$842.55d+68.5d^2$
P_{15}	$11.68d^2$	L_{17}	6.15+2d/3		$71.83d^2+7.787d^3$

For the conservative design, the passive resistance from layer II and layer III is omitted. Sheet pile wall is subject to a rigid rotation at B, No reaction at bottom end and considering the moment equilibrium at B, $\sum M = 0$

$$7.257d^3 + 117.91d^2 + 627.3d - 836.6 = 0$$

By solving the above equation,

$D_1 = 1.1$ m , D2 and D3 = -8.67 m (This is not possible)

Design depth,.

D = 1.35 m

Required height of sheet pile wall, = 10.5 m

To determine the anchor force T consider the horizontal equilibrium,

$$355.3 = 232.8 + 87 + T \cos 30°$$

$$T = 41 \text{ kN/m}$$

Maximum bending moment, $(M)_{max}$ = $4.68 \times 4.85 + 4.94 \times 4.633 - 41 \times 2.5 + 31.92 \times 2.775 + 11.97 \times 2.3 + 39.2 \times 0.35 + 6.1 \times 0.02 + 159.4 \times 0.4$

= 136.8 kNm/m Run of wall

Maximum allowable bending moment, M_{all} = 155 kNm/m ≥ 136.8 kNm/m

The minimum section modulus, Z_{min} = M_{max} / fb

= 771 cm^3/m < 874 cm3/m

The selected section of the sheet pile wall meets the requirements.

<u>Design of Pre stress bar Anchors</u>

Tie rods utilizing Pre-stress bar anchors (ASTM A722) are applied at 8.0m intervals, corresponding to every twenty piles.

Design load in tie rod, = 41×8

= $328kN \leq 341kN$

Maximum shear load of tie rod = 41×8×0.5

= 164 kN

The selection of prestressing bar anchor sizes is satisfactory.

The average ultimate bond stress for rock grout interface (after PTI, 1996) is given in Appendix C.

Allowable bond stress for rock grout interface,

= 360 kPa

But, rock socket diameter = 100 mm

Assumed rock socket length = 3 m

Allowable skin friction = (22/7) ×0.1× 3×360

= 339 kN > 328 kN

Hence, the rock socket anchor length is sufficient to withstand the prestressing force.

Appendix C

Some references shown in Appendix C were used in the design and construction of the gabion wall and continuous sheet pile wall with a rock anchor system. People should be able to find them based on the information given.

Table C1.1: Estimated Average Ultimate Bond Stress for Grout Interface in the Anchor Bond Zone (after PTI,1996).

Rock		Cohesive Soil		Cohesionless Soil	
Rock type	Average ultimate bond stress (MPa)	Anchor type	Average ultimate bond stress (MPa)	Anchor type	Average ultimate bond stress (MPa)
Granite and basalt	1.7 - 3.1	Gravity-grouted anchors (straight shaft)	0.03 - 0.07	Gravity-grouted anchors (straight shaft)	0.07 - 0.14
Dolomitic limestone	1.4 - 2.1	Pressure-grouted anchors (straight shaft)		Pressure-grouted anchors (straight shaft)	
Soft limestone	1.0 - 1.4	• Soft silty clay	0.03 - 0.07	• Fine-med. sand, med. dense – dense	0.08 - 0.38
Slates and hard shales	0.8 - 1.4	• Silty clay	0.03 - 0.07	• Med.–coarse sand (w/gravel), med. dense	0.11 - 0.66
Soft shales	0.2 - 0.8	• Stiff clay, med. to high plasticity	0.03 - 0.10	• Med.–coarse sand (w/gravel), dense - very dense	0.25 - 0.97
Sandstones	0.8 - 1.7	• Very stiff clay, med. to high plasticity	0.07 - 0.17	• Silty sands	0.17 - 0.41
Weathered Sandstones	0.7 - 0.8	• Stiff clay, med. plasticity	0.10 - 0.25	• Dense glacial till	0.30 - 0.52
Chalk	0.2 - 1.1	• Very stiff clay, med. plasticity	0.14 - 0.35	• Sandy gravel, med. dense-dense	0.21 - 1.38
Weathered Marl	0.15 - 0.25	• Very stiff sandy silt, med. plasticity	0.28 - 0.38	• Sandy gravel, dense-very dense	0.28 - 1.38
Concrete	1.4 - 2.8				

Table C1.2: Show the standard dimensions of the Gabion structures units from Maccaferri, product standard specification.

Characteristics	Galvanized	PVC Coated	Galvanized	PVC Coated	Galvanized	PVC Coated
Mesh Hole	80 x 100mm		60 x 80mm		100x120mm	
Wire Dia	2.7mm	3.7mm	2.2mm	3.2mm	2.7mm	3.7mm
Selvedge Wire	3.4mm	4.4mm	2.7mm	3.7mm	3.4mm	4.4mm
Binding Wire	2.2mm	3.2mm	2.2mm	3.2mm	2.2mm	3.2mm
Whole Size	2m x 1m x 1m 3m x 1m x 1m 4m x 1m x 1m			2m x 1m x 0.5m 3m x 1m x 0.5m 4m x 1m x 0.5m		

Table C1.3: Properties of Prestressing steel bars (ASTM A722)

Steel grade	Nominal diameter	Ultimate stress f_{pu}	Nominal cross section area A_{ps}	Ultimate strength $f_{pu}\,A_{ps}$	Prestressing force		
					$0.8\ f_{pu}\,A_{ps}$	$0.7\ f_{pu}\,A_{ps}$	$0.6\ f_{pu}\,A_{ps}$
(ksi)	(in.)	(ksi)	(in.^{2})	(kips)	(kips)	(kips)	(kips)
150	1	150	0.85	127.5	102.0	89.3	76.5
	1-1/4	150	1.25	187.5	150.0	131.3	112.5
	1-3/8	150	1.58	237.0	189.6	165.9	142.2
	1-3/4	150	2.66	400.0	320.0	280.0	240.0
	2-1/2	150	5.19	778.0	622.4	435.7	466.8
160	1	160	0.85	136.0	108.8	95.2	81.6
	1-1/4	160	1.25	200.0	160.0	140.0	120.0
	1-3/8	160	1.58	252.8	202.3	177.0	151.7
(ksi)	(mm)	(N/mm^2)	(mm^2)	(kN)	(kN)	(kN)	(kN)
150	26	1035	548	568	454	398	341
	32	1035	806	835	668	585	501
	36	1035	1019	1055	844	739	633
	45	1035	1716	1779	1423	1246	1068
	64	1035	3348	3461	2769	2423	2077
160	26	1104	548	605	484	424	363
	32	1104	806	890	712	623	534
	36	1104	1019	1125	900	788	675

Table C1.4: Sectional properties of Hot-rolled NS-SP-II U type sheet steel pile ((BS EN 10248-1:1996, S355GP) manufactured from Nippon steel & sumitomo metal Corporation, Tokyo in Japan.

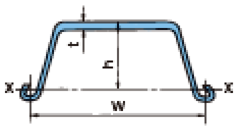

Sectional properties

Type	Dimension			Per pile				Per 1 m of pile wall width			
	Effective width W mm	Effective height h mm	Thickness t mm	Sectional area cm²	Moment of inertia cm⁴	Section modulus cm³	Unit mass kg/m	Sectional area cm²/m	Moment of inertia cm⁴/m	Section modulus cm³/m	Unit mass kg/m²
NS-SP-II	400	100	10.5	61.18	1,240	152	48.0	153.0	8,740	874	120
NS-SP-III	400	125	13.0	76.42	2,220	223	60.0	191.0	16,800	1,340	150
NS-SP-IIIA	400	150	13.1	74.40	2,790	250	58.4	186.0	22,800	1,520	146
NS-SP-IV	400	170	15.5	96.99	4,670	362	76.1	242.5	38,600	2,270	190
NS-SP-VL	500	200	24.3	133.8	7,960	520	105	267.6	63,000	3,150	210
NS-SP-VIL	500	225	27.6	153.0	11,400	680	120	306.0	86,000	3,820	240
NS-SP-IIw	600	130	10.3	78.70	2,110	203	61.8	131.2	13,000	1,000	103
NS-SP-IIIw	600	180	13.4	103.9	5,220	376	81.6	173.2	32,400	1,800	136
NS-SP-IVw	600	210	18.0	135.3	8,630	539	106	225.5	56,700	2,700	177

Appendix D

Section: D.1 The stability calculations for Bamboo Crib wall using drained shear strength parameters for low water level at the back

Figures D1.1 shows the proposed idealized section of the bamboo crib wall and selected Bamboo crib wall section parameters are,

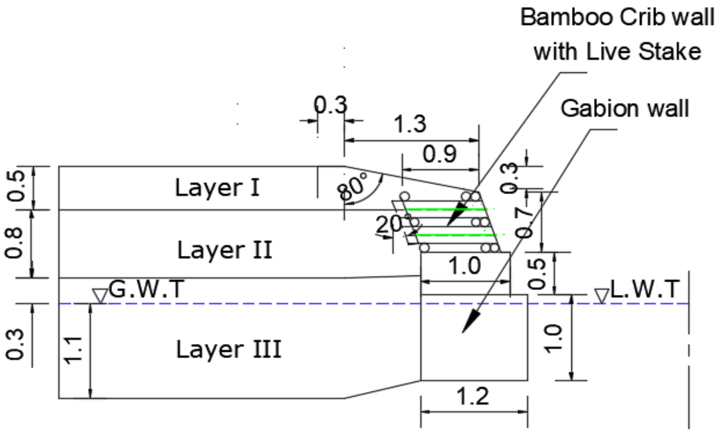

Figure D1.1: Proposed idealized section of Bamboo Crib wall

Height of slope (H_s): 1.0 m, total height of wall (H_w): 0.7 m

Slope inclination, $\beta = 10°$

Wall inclination angle, $\alpha = 20°$ from vertical

Drained cohesion, $C' = 1.5$ kN/m^2

Design internal friction angle, $\emptyset'_{des.} = 28°$

Bulk density, $\gamma_{dry} = 18$ kN/m^3

Wall friction, $\delta = 2/3\ \phi = 19°$

Uniformly distributed surface load, p= 10 kN/m^2

According to Coulomb's earth pressure theory:

$$\lambda_{ah} = \frac{Cos^2(\emptyset+\alpha)}{Cos^2\alpha\left\{1+\sqrt{\frac{Sin(\emptyset+\delta)Sin(\emptyset-\beta)}{Cos(\alpha-\delta)Cos(\alpha+\beta)}}\right\}^2}$$

$= 0.32$

And : $\lambda_a = \frac{\lambda_{ah}}{Cos(\alpha-\delta)}$

$= 0.32$

The effects of uniformly distributed surface load (p) can be represented by a fictitious height z´ based on z´ $= \frac{p}{\gamma_{dry}}$

$= 0.56$ m

So, total height from the wall base to the ground surface can be calculated as,

$$Z = 0.56 + 0.7 + 0.3$$

$$= 1.56 \text{ m}$$

The earth pressure at the base of wall,

$$e_{ah} = \gamma.Z.\ \lambda_{ah}$$

$$= 18 \times 1.56 \times 0.32$$

$$= 9 \text{ kN/m}^2$$

A reduction of the active earth pressure due to cohesion (c) of fill existing soils is given by: $\Delta_{eah} = -2C\sqrt{\lambda_{ah}} \times \sqrt{\cos(\delta-\alpha)}$

$$= -1.7 \text{ kN/m}^2$$

Then the effective earth pressure at the base of wall,

$$= 9 - 1.7$$

$$= 7.3 \text{ kN/m}^2$$

The effective earth pressure at the top of wall,

$$= 18 \times 0.3 \times 0.32 - 1.7$$

$$= 0 \text{ kN/m}^2$$

The total horizontal earth pressure applied to the wall surface,

$$E_{ah} = \frac{1}{2} \times 7.3 \times 0.7$$

$$= 2.6 \text{ kN/m}$$

But, vertical component of earth pressure,

$$E_{av} = 0 \text{ kN/m}$$

The monolithic theory suggests that external forces acting on the crib wall will be transferred to the ground similarly to gravity walls. For the calculations, the average density of the composite structure is used. The unit weight of bamboo ranges from 3.7 to 8.5 kN/m³; for this analysis, an average unit weight of 5.0 kN/m³ is assumed.

The total volume of bamboo per unit length of wall,

$$= \frac{\pi d^2}{4} \times \text{total length of crib elements}$$

$$= \frac{\pi 0.1^2}{4} \times (3 \times 3 \times 1 + 3 \times 3 \times 0.9)$$

$$= 0.134 \text{ m}^3$$

The total volume of wall, $= 0.9 \times 0.7 \times 1$

$$= 0.63 \text{ m}^3$$

The average density of wall (γ_w), $= \frac{(0.134 \times 5 + 0.496 \times 18)}{0.63}$

$$= 15.23 \text{ kN/m}^3$$

By taking into account the center of gravity of the wall and all acting forces, the point of application of the resultant earth pressure has been calculated to be 0.395 m above the wall base.

Normal force resulting from the self-weight of the soil and crib wall,

$$N = 0.9 \times 0.7 \times 15.23 + 0.5 \times 0.9 \times \tan 10° \times 18$$

$$= 10.88 \text{ kN/m}$$

Resultant, $R = \{(10.88)2 + (2.6)^2\}^{0.5}$

$= 11.2$ kN/m

Angle of inclination of the resultant, $\delta_s = \tan^{-1}(2.6/10.88)$

$= 13.4°$ to the vertical.

Taking moment at the centre of the wall base of all acting forces, neglecting the passive pressure from the front side,

Overturning moment, $M_o = 1.027\ kNm$ (Clockwise)

Resisting moment, $M_r = 1.741\ kNm$ (Anticlockwise)

$$\sum(Mr - Mo) = (0.45-0.29) \times 10.88 - 2.6 \times 0.395$$

$= 0.71$ kNm. (Anticlockwise)

Safety for overturning is satisfied according to BS8002.

The eccentricity, $e = \frac{\sum(Mr-Mo)}{\sum V}$

$= 0.065$ m

But, $e_{per} = \frac{b\prime}{4}$

$= 0.2\ \text{m} \geq e$

The resultant of the forces passes through a point located 0.065 meters inward from the center of the wall base, meaning it lies within the inner half of the base. The maximum and minimum pressures on the bottom soil are then given as follows:

$$б_{1,2} = \frac{N}{A}\left(1 \pm \frac{6e}{b\prime}\right)$$

$$б_{1,2} = \frac{10.88}{0.9}\left(1 \pm \frac{6\ x\ 0.065}{0.8}\right)$$

$б_1 = 13.1$ kN/m^2

$б_2 = 11.1$ kN/m^2

Where, A is the total area of the wall base, b' the effective width and e is the eccentricity.

In case of displaced horizontal joints situation, the maximum pressure will begiven by,

$$б_3 = \frac{2N}{C}$$

$$б_3 = 36 \text{ kN/m}^2$$

Where, C the distance of resultant from outer edge of the wall.

Based on past research (IBC, 1997), $бv_{all} = 150\ Kpa \geq$ Maximum stress induced at bamboo crib wall

Therefore, bearing capacity is satisfactory.

For sliding safety,

Disturbing forces, $E_{ah} = 2.6\ kN/m$

Total vertical weight, $N = 10.88\ kN/m$

The bamboo crib wall will need to be placed on a foundation above the gabion, with the top layer graded and compacted. During construction, an Aggregate Base Course with a thickness of 100mm should be spread and compacted below the base of the crib wall.

From Jennifer Nicks et al. (2017), base friction angle,

$$\delta_b = 34^o$$

Sliding Resistance, $F = N\ x\ \tan \delta_b$

$= 10.88 \times \tan 34^o$

$= 7.34\ kN/m$

It is satisfied according to BS8002.

Section: D.2 The stability calculations for Bamboo Crib wall using drained shear strength parameters for high water level at the back

Figures D2.1 shows the proposed idealized section of the bamboo crib wall for high water level at the back case, considering drained conditions.

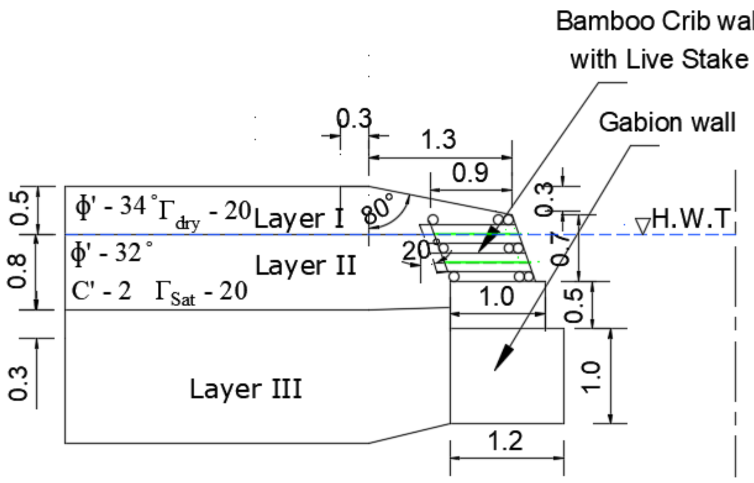

Figure D2.1: Proposed idealized section of Bamboo Crib wall

$$e_{ah} = \gamma.Z.\lambda_{ah}$$

$$= (20\text{-}9.81) \times 1.56 \times 0.32$$

$$= 5.1 \text{ kN/m}^2$$

$$e'_{ah} = 5.1 - 1.7$$

$$= 3.4 \text{ kN/m}^2$$

$$E_{ah} = \frac{1}{2} \times 3.4 \times 0.7$$

$$= 1.2 \text{ kN/m}$$

Taking moment at the centre of the wall base,

Overturning moment, M_o = 0.48 kNm (Clockwise)

Resisting moment, M_r = 1.741 kNm (Anticlockwise)

Safety for overturning is satisfied according to BS8002.

The eccentricity, e = 0.116 m

But, $e_{per} = \frac{b'}{4}$

$= 0.2 \text{ m} \geq e$

The maximum and minimum pressures on the bottom soil are as follows:

$б_1 = 22.6 \text{ kN/m}^2$

$б_2 = 1.57 \text{ kN/m}^2$

According to a previous study (IBC, 1997),

$бv_{all} = 150\ Kpa \geq$ Maximum stress induced at bamboo crib wall

Therefore, bearing capacity is satisfactory.

For sliding safety,

Disturbing forces, $E_{ah} = 1.2\ kN/m$

Total vertical weight, $N = 10.88\ kN/m$

The bamboo crib wall will need to be placed on a foundation above the gabion, with the top layer graded and compacted. During construction, an Aggregate Base Course with a thickness of 100mm should be spread and compacted below the base of the crib wall.

Sliding Resistance, $F = N\ x\ \tan\delta_b$

$= 10.88 \times \tan 34^o$

$= 7.34\ kN/m$

It is satisfied according to BS8002.

Section: D.3 The stability calculations for Bamboo crib wall using drained shear strength parameters for high groundwater level on the retained side, and low water level in the stream as sudden drawdown case.

Figures D3.1 shows the proposed idealized section of the bamboo crib wall for sudden drawdown case, considering drained conditions

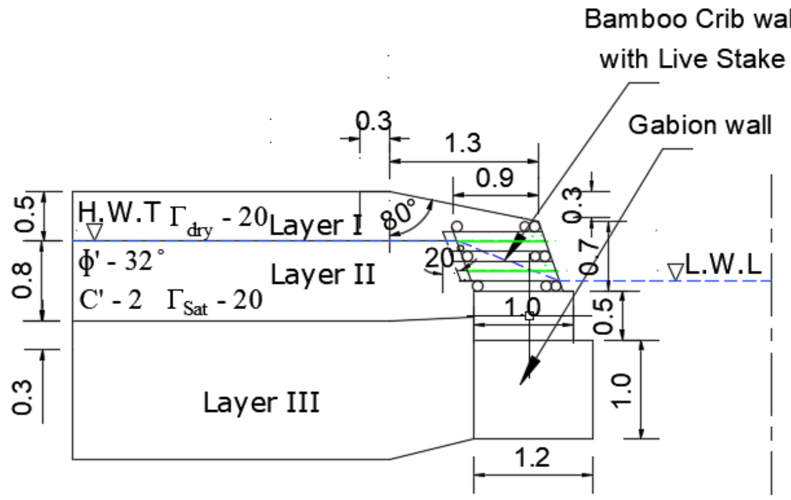

Figure D3.1: Proposed idealized section of Bamboo Crib wall

$$e_{ah} = \gamma . Z . \lambda_{ah}$$

$$= (20\text{-}9.81) \times 1.56 \times 0.32$$

$$= 5.1 \text{ kN/m}^2$$

$$e'_{ah} = 5.1 - 1.7$$

$$= 3.4 \text{ kN/m}^2$$

$$E_{ah} = \frac{1}{2} \times 3.4 \times 0.7 + \frac{1}{2} \times 9.81 \times 0.4 \times 0.4$$

$$= 2 \text{ kN/m}$$

Taking moment at the centre of the wall base,

Overturning moment, M_o = 0.79 kNm (Clockwise)

Resisting moment, M_r = 1.741 kNm (Anticlockwise)

Safety for overturning is satisfied according to BS8002.

The eccentricity, $e = 0.087$ m

But, $e_{per} = \frac{b'}{4}$

$= 0.2 \text{ m} \geq e$

The maximum and minimum pressures on the bottom soil are as follows:

$б_1 = 20 \text{ kN/m}^2$

$б_2 = 4.2 \text{ kN/m}^2$

According to a previous study (IBC, 1997)

$бv_{all} = 150\ Kpa \geq$ Maximum stress induced at bamboo crib wall

Therefore, bearing capacity is satisfactory.

For sliding safety,

Disturbing forces, $E_{ah} = 2\ kN/m$

Total vertical weight, $N = 10.88\ kN/m$

The bamboo crib wall will need to be placed on a foundation above the gabion, with the top layer graded and compacted. During construction, an Aggregate Base Course with a thickness of 100mm should be spread and compacted below the base of the crib wall.

Sliding Resistance, $F = N\ x\ \tan \delta_b$

$= 10.88 \times \tan 34^o$

$= 7.34\ kN/m$

It is satisfied according to BS8002.